論文 / 著書情報
Article / Book Information

題目(和文)	
Title(English)	Effects of Mn/Fe Ratio and Cooling Rate on Modification of Fe Intermetallic Compounds in Cast AA356 Based Aluminum Alloys with High Fe Contents
著者(和文)	ZhangZhijun
Author(English)	Zhijun Zhang
出典(和文)	学位:博士(工学), 学位授与機関:東京工業大学, 報告番号:甲第9272号, 授与年月日:2013年9月25日, 学位の種別:課程博士, 審査員:小林 郁夫,里 達雄,熊井 真次,史 蹟,木村 好里
Citation(English)	Degree:Doctor (Engineering), Conferring organization: Tokyo Institute of Technology, Report number:甲第9272号, Conferred date:2013/9/25, Degree Type:Course doctor, Examiner:,,,,
学位種別(和文)	博士論文
Type(English)	Doctoral Thesis

Effects of Mn/Fe Ratio and Cooling Rate on Modification of Fe Intermetallic Compounds in Cast AA356 Based Aluminum Alloys with High Fe Contents

Doctoral Dissertation

2013

Department of Metallurgy and Ceramics Science

Tokyo Institute of Technology

Zhang Zhijun

Contents

Chapter 1

General introduction

Iron is the most common and detrimental impurity in cast Al-Si alloys. Due to its small solid solubility in Al matrix, it will form Fe intermetallic compounds with Al and Si during solidification. There are three main kinds of Fe compounds in cast Al-Si alloys with Fe and Mn, the platelet β-Al_5FeSi type Fe compound, the Chinese script α-$Al_{15}(Fe,Mn)_3Si_2$ type Fe compound and the star-like and/or polyhedral shape α-$Al_{15}(Fe,Mn)_3Si_2$ type Fe compound. Among them, the platelet β type Fe compound has been accepted as the most harmful compound to the mechanical properties of cast Al-Si alloys, especially the ductility. When the Fe is inevitable, to improve the mechanical properties, the platelet β type Fe compound should be modified to the more desired Chinese script α type Fe compound.

This thesis investigated the influence of three main factors, Fe content, Mn/Fe ratio and cooling rate on this modification process systematically. The mechanisms behind the modification by these three factors were discussed as well. The effects of different kinds of Fe compounds on tensile properties of cast alloys were evaluated finally.

In this chapter, some background will be given about application of Al-Si cast alloys and detailed information about the Fe intermetallic compounds firstly. Subsequently, the objective of this thesis is described. Finally the outline of this thesis is presented, explaining briefly the contents and conclusions of each separate chapter.

1.1 Cast Al-Si alloys and secondary aluminum alloys

Aluminum alloys have been acquiring increasing significance for the past few decades due to its excellent properties. They are extensively used to manufacture a large number of components for automotive, construction, aerospace, etc. Among them, aluminum-silicon (Al-Si) cast alloys are fast becoming the most universal and popular commercial materials. Comprising 85% to 90% of the aluminum cast parts produced for the automotive industry, due to their high strength-to-weight ratio, excellent castability, high corrosion resistant and chemical stability, good mechanical properties and wear resistance. The phase diagram of Al-Si system is shown in Fig. 1.1[1]. The cast microstructure of the hypoeutectic Al-Si alloys consists of the primary Al phase and a eutectic phase of Al and Si.

The increasing demand for aluminum-based products and further globalization of the aluminum industry have contributed significantly to the higher consumption of aluminum scrap for re-production of aluminum alloys [2]. Hence, recycled aluminum alloys (secondary aluminum alloys) are made out of aluminum scrap and workable aluminum garbage by recycling become more and more important nowadays. Care of environment in industry of aluminum connects with the decreasing consumption resource as energy, materials, waters and soil with increase recycling [3]. The energy consumption of aluminum secondary production is only about 5% compared with the primary production [4].

However, in the secondary aluminum alloys, the impurity level especially the iron content is usually very high. For example in the automotive industries, the aluminum parts are produced and attached with other materials such as steel and rivet. The mechanical separation of aluminum part from other materials is insufficient and will lead to the increase of the impurity level during the subsequent melting. The high level of impurity, especially the high content of iron impurity will restrict the application of the primary and secondary

aluminum alloys significantly. Moreover, in the manufacturing process of primary aluminum, various amounts of impurity elements may be introduced to the final Al-Si alloys. Iron is the most common impurity in aluminum and its alloys. It is always present in aluminum as a natural and dominant impurity. It comes into aluminum during the manufacture of primary aluminum via the Bayer Process that converts bauxite (the ore) into alumina (the feedstock) and the subsequent Hall-Héroult electrolytic reduction process that converts alumina into molten aluminum (> 950˚C) [5]. Depending on the quality of the incoming ore and the control of the various processing parameters and other raw materials, molten primary aluminum metal typically contains between 0.02-0.15wt.% iron, with ~0.07-0.10 wt.% being average [6]. Iron can also enter an aluminum melt via the addition of low-purity alloying materials, e.g. silicon, as well as from the steel equipment used in melting and casting. Hence, in the recycled aluminum alloys, the level of impurity is very high. And the high impurity of Fe is very detrimental to the mechanical properties of alloys.

1.2 Iron intermetallic compounds in cast Al-Si alloys

Iron has been widely accepted as the most common and detrimental impurity in die casting Al-Si alloys. The liquid solubility limits for Fe in aluminum alloys is 1.87 wt% at 655 °C. However, its solid solubility is less than 0.05 wt% [7,8]. Therefore, during solidification and cooling, there is a strong driving force for the formation of Fe-rich intermetallic compounds (hereafter also referred to as Fe compounds) containing Al and Si in Al-Si cast alloys. Several compounds can form depending on the alloy compositions and solidification in the Al-Si-Fe system. The phase diagram of this system is shown in Fig. 1.2 [9], where θ-Al_3Fe (or $Al_{13}Fe_4$), α-Al_8Fe_2Si (τ_5) and β-Al_5FeSi (τ_6) are the most common Fe compounds in cast Al-Si commercial alloys. The structures and properties of these Fe compounds were showed in Table.1.1 [5].

θ-Al_3Fe compound is not stable when the Si concentrate is high in the alloys. In the most common foundry alloys containing Si, the dominant phases are the hexagonal α-Al_8Fe_2Si phase and the monoclinic/orthorhombic β-Al_5FeSi compound (also reported as $Al_{4.5}FeSi$ stoichiometry) [10]. Another phase that forms when Mn is present with Si is the cubic $Al_{15}(Fe,Mn)_3Si_2$, also confusingly called as α type Fe compound. This phase tends to form in preference to the hexagonal α compound whenever Mn is present. There are also less common phases which form when other elements are present, e.g. Ni, Co, Cr, but these are beyond the scope of this thesis.

The iron intermetallic compounds listed above are quite different in their morphologies within the microstructures of Al-Si alloys. They are usually identified by their dominant shape under the microscope. β-Al_5FeSi type Fe compound, which has been considered as the most detrimental one in Al-Si alloy castings [11-13], appears as the platelet, as shown in Fig. 1.3 (a). In the alloys with both Fe and Mn, another compound α-$Al_{15}(Fe,Mn)_3Si_2$ usually appears as Chinese script, as shown in Fig. 1.3 (b). When the Fe and Mn contents are high, the α-$Al_{15}(Fe,Mn)_3Si_2$ type Fe compound is also found as a more compact polyhedral shape, as shown in Fig. 1.3 (c).

The effect of iron on the mechanical properties of cast aluminum alloys has been reviewed extensively by several authors [14-16]. It is consistently reported that as Fe levels increase, the ductility of Al-Si based alloys decreases since the formation of Fe compounds. Among the Fe compounds, the platelet β type Fe compound has been widely accepted as the most damage one. Its deleterious effect on the mechanical properties, especially ductility has generally been attributed to its stress raising potential as a result of its platelet morphology, and its apparently brittle nature. In addition, the presence of the platelet compounds considerably increases tendencies and shrinkage cavities during solidification,

because of the blockage of the channels, thus hindering the flow of liquid metal to feed solidification shrinkage at a late stage of solidification [6].

Comparing to the platelet β type Fe compound, the metallurgically preferable compound is Chinese script α type Fe compound. These effects are due to its more compact shape and its more diffuse interface with the aluminum matrix. Compact forms, such as the Chinese script, present less of an internal stress concentration than do sharp platelet β type Fe compound. On the other hand, β type Fe compound is poorly bonded to the matrix, as indicated by the sharp inter phase boundary. The crack can initiate easily at boundary between the β type Fe compound and Al matrix.

Hence, in order to improve the mechanical properties of cast Al-Si alloys with impurity Fe, it is very important and necessary to modify the plate β-Al_5FeSi compound to more compact Chinese script α type Fe compound.

1.3 Modification of iron intermetallic compounds

So far, there is no known way to economically remove iron from aluminum or its alloys. Therefore, the modification of Fe compounds in cast Al-Si alloys is becoming a very popular and import research field. And a lot of the beneficial results have been reported, especially when the Fe concentration was low [10, 13, 14].

There are several methods to modify the harmful morphologies of Fe intermetallic compounds and get the more desirable α type Fe compounds. Certain alloying elements, such as Mn, Cr, Na and etc., were added to the alloy to promote the formation of α type Fe compounds during ingot solidification. Additionally, high cooling rate during solidification can restrict the nucleation and growth of Fe intermetallic compounds. The refined small size Fe compounds are beneficial to the mechanical properties. Moreover, Over-heating the

alloys to 800-900˚C can melt the nucleation site of β type Fe compound and lead to Fe compounds solidify as α type. The heat treatment by homogenization are effective to shorten the majority thin platelet β type Fe compound, which forms on solidification into the square or spherical shape α type compound [17-19].

In the previous work, Mn addition in cast Al-Si alloys played a very effective role in modifying platelet β type Fe compound to more compact Chinese script α type Fe compound, especially when the Fe content was low. Although the addition of Mn to Al-Si alloys has been widely investigated and documented, the amount of Mn needed to neutralize Fe has not been well established, especially with the change of the cooling rate [14, 15]. The previous works mainly revealed the influences of the Mn and Fe content on the type and size of different Fe compounds [20-22] or the cooling rate on the evolution of different Fe compounds during the modification process [23, 24] separately. Still very limited work has reported systematically about the influences of the Fe content, the Fe/Mn ratio and cooling rate on the modification of Fe compounds.

1.4 Originality and objective of the present thesis

This present thesis mainly investigated the combined influences of the Fe content (high Fe content, more than 1wt.%), Mn/Fe ratio (0, 0.35, 0.5 and 0.65 at each given Fe content) and cooling rate (from 0.59-17.3˚C/s) on the modification of Fe intermetallic compounds in cast AA356 (JIS, AC4C) based aluminum alloys.

1. Firstly, the influences of different kinds and size of Fe intermetallic compounds on the mechanical properties of the alloys were evaluated by changing with chemical compositions of alloys and solidification situation.

2. Three main factors, Fe content, Mn/Fe ratio and cooling rate were alerted individually

or combined to investigate their influences on the modification of Fe intermetallic compounds from platelet β type Fe compound to the less harmful Chinese script α type Fe compound systematically.

3. The evolution of Fe compounds during solidification in this modification process was investigated under low cooling rate (0.59-0.67˚C/s) by comparing quenching experiments.

4. Finally, the mechanisms behind the modification of Fe compounds by these three factors were discussed as well.

1.5 Outline of the present thesis

The flow chart of the present thesis is shown in Fig.1.4. The outlines of the present thesis are briefly summarized as follows.

Chapter 1 is **"General introduction"**. This chapter describes the application of the cast Al-Si alloys and the restriction of their application by Fe intermetallic compounds. The characteristics of different Fe compounds and the method of Fe compounds modification are introduced detailed. Based on the former introduction, the objective of the present work are summarized.

Chapter 2 describes **"Influence of Fe content, Mn/Fe ratio and cooling rate on mechanical properties of cast AA356 based alloys"**. In this chapter, the tensile properties of alloys with different composition under different cooling situation were evaluated. The type and size of Fe compounds influenced the tensile properties of alloys significantly. The small size Chinese script Fe compound is beneficial to the tensile properties of cast Al-Si alloys.

Chapter 3 describes **"Influence of Fe content, Mn/Fe ratio and cooling rate on morphology of Fe intermetallic compounds in cast AA356 based alloys"**. In this chapter,

the attempt has been proceeded to modify the platelet β type Fe compound to the Chinese script α type Fe compound by alerting three parameters, Fe content, Mn/Fe ratio and cooling rate. They performed different influences on this modification process separately and combined.

Chapter 4 describes **"Evolution of Fe intermetallic compounds during solidification in cast AA356 based alloys with different Fe content and Mn/Fe ratio"**. In this chapter, the evolution of Fe compounds during solidification was discussed. Water-quenched experiments were used to reveal the solidification sequence of Fe compounds. Fe content and Mn/Fe ratio effected the evolution of Fe compounds greatly.

Chapter 5 describes **"Mechanisms of modification of Fe intermetallic compounds by different factors: Mn addition, Fe content and cooling rate in cast AA356 based alloys"**. In this chapter, mechanisms of three factors which can influence the modification process of Fe compounds from platelet β type to Chinese script α type were discussed one by one mainly based on the data obtained in Chapter 3 and 4.

Chapter 6 is **"General conclusions"**. This chapter summarizes the conclusions of the present thesis. Ideas and suggestions are pointed out for the future improvements.

References

[1] H. Beker (edi.): *Metals handbook, 10th Edi., Vol. 3, ASM International,* (1992) 2.52.

[2] M. Mahfoud, A. K. Prasada Rao and D. Emadi: J. Therm. Anal Calorim, **100** (2010), 847-851.

[3] L. Sencakova and E. Vircikova: Acta Metallurgica Slovaca, **13**(2007), 412-419.

[4] M. E. Schlesinger: *Aluminum Recycling, CRC Press,* (2007), 25-37.

[5] N. A. Below, A. A. Aksenov and D. G. Eskin： *Iron in aluminum alloys: Impurity and* alloying elemen*t, Taylor & Francis Inc, New York,* (2002), 1-7, 24-28, 52.

[6] J. A. Taylor: Procedia Materials Science, **1**(2012), 19-33.

[7] L. Wang, D. Apelian and M. M. Makhlouf: AFS Transactions, **146**(1999), 231-238.

[8] L.F. Mondolfo: *Aluminum Alloys: Structure and Properties,* (Butterworths, London, 1976), 661-663.

[9] G. Effenberg and S. Ilyenko: *Landolt-Börnstein, Ternary Alloy Systems Phase Diagrams, Crystallographic and Thermodynamic Data, Subvol. D, Part 1, Springer-Verlag Berlin, Heidelberg,* (2008) pp.53-54.

[10] M. V. Kral: Materials Letters, 59 (2005), 2271-2276.

[11] L. Backerud, G. Chai and J. Tamminen: *Solidification Characteristics of Aluminium Alloys*, AFS/Skanaluminum, Foundry Alloys Vol. 2 (1990), 71-84.

[12] S. Shivkumar, L. Wang and D. Apelian: JOM, **43** (1991), 26-32.

[13] P. Ashtari, H. Tezuka and T. Sato: Scr. Mater. **51** (2004), 43-46.

[14] A. Couture: AFS International Cast Metals Journal, **6 (4)** (1981), 9-17.

[15] P. N. Crepeau: AFS Transactions, **103** (1996), 361-366.

[16] T. O. Mbuya, B. O. Odera, S. P. Ng'ang'a: International Journal of Cast Metals Research, **16 (5)** (2003), 451-465.

[17] S. Zajac, B. Hutchinson, A. Jphansson and L. O. Gulman: Mater. Sci. Techol., **10** (1994), 323-333.

[18] M. Ryvola and L. R. Morris: Microstruct. Sci., **5** (1977), 203-206

[19] T. Sugawara: Proceeding of ICAA-6 (1998), Aluminum Alloys, vol. 2, 715-720.

[20] S.G. Shabestari: Mater. Sci. Eng. A. 383 (2004) 289-298.

[21] J.Y. Hwang, H.W. Doty and M.J. Kaufman: Mater. Sci. Eng. A. 488 (2008) 496-504.

[22] C.M. Dinnis, J.A. Tayor and A.K. Dahle: Metall. Mater. Trans. A. 37A (2006) 3283-3291.

[23] B. Dutta and M. Rettenmayr: Mater. Sci. Eng. A. 283 (2000) 218-224.

[24] Y.H Zhang, Y.C. Liu, Y.J. Han, C.Wei and Z.M. Gao: J. Alloys Compd. 473 (2009) 442-445.

Table 1.1 Structures and properties of Fe compounds in Al-Fe-Si system [5].

Phase	Structure	Lattice parameters	Density ($g.cm^3$)
θ-Al_3Fe (or Al_7Fe_2, $Al_{13}Fe_4$)	Monoclinic with C2/m space group, orthorhombic	a= 1.549 nm b= 0.808 nm c= 1.248 nm β= 107.72°	3.896
α-Al_8Fe_2Si (or $Al_{12}Fe_3Si_2$)	hexagonal	a= 1.23-1.24 nm c= 2.62-2.63 nm	3.58
β-Al_5FeSi (or $Al_9Fe_2Si_2$)	monoclinic	a=b= 0.612 nm c= 4.148-4.150 nm β= 91°	3.3-3.6

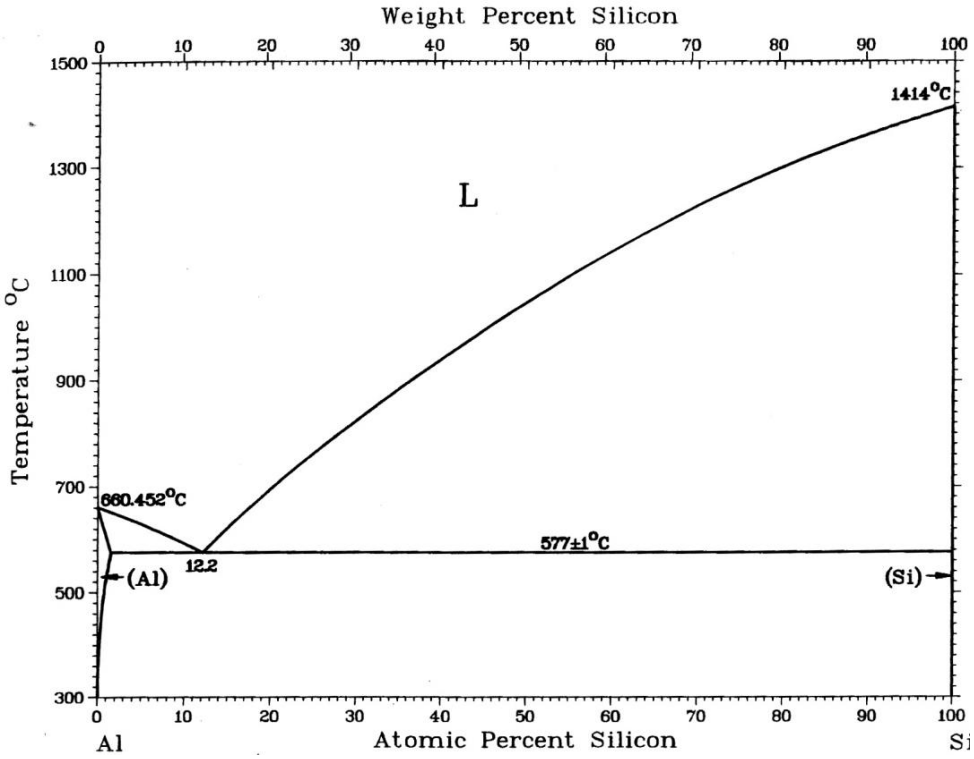

Fig. 1.1 Al-Si phase diagram [1].

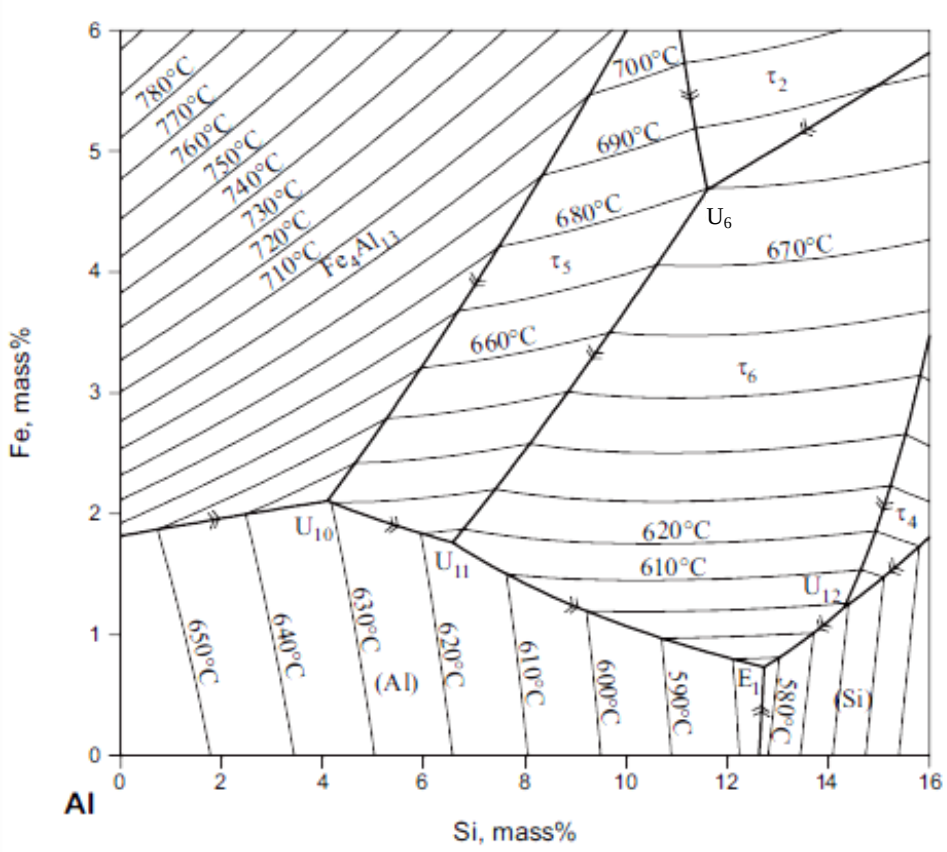

Fig. 1.2 Calculated liquidus surface of the Al-Fe-Si ternary phase diagram [9], where τ4 represents δ–Al_3FeSi_2, τ5 represents α-Al_8Fe_2Si and τ6 represents β–Al_5FeSi, respectively. Fe_4Al_3 also was confusedly named as θ–Al_3Fe.

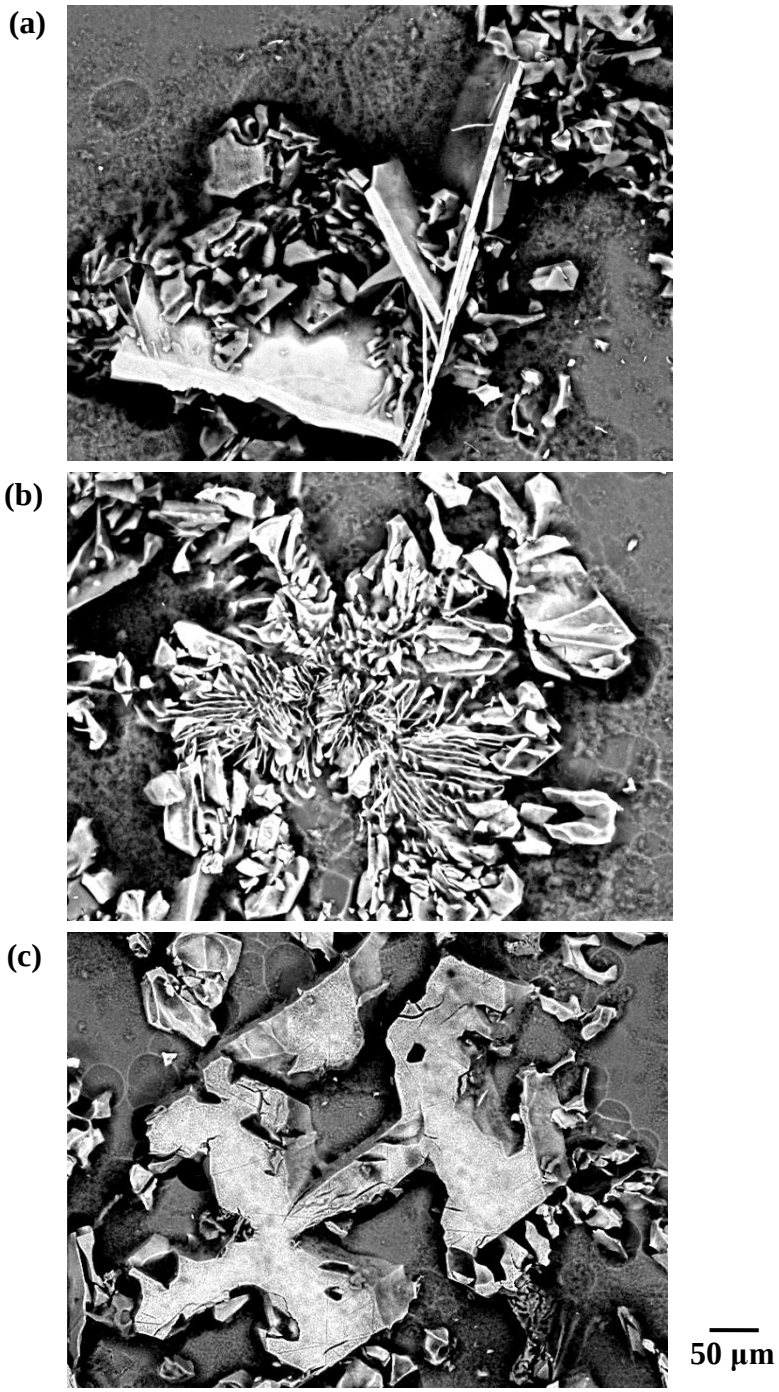

Fig. 1.3 Morphology of different Fe compounds after deep etching: (a) platelet β type Fe compound, (b) Chinese script α type Fe compound, (c) polyhedral shape α type Fe compound.

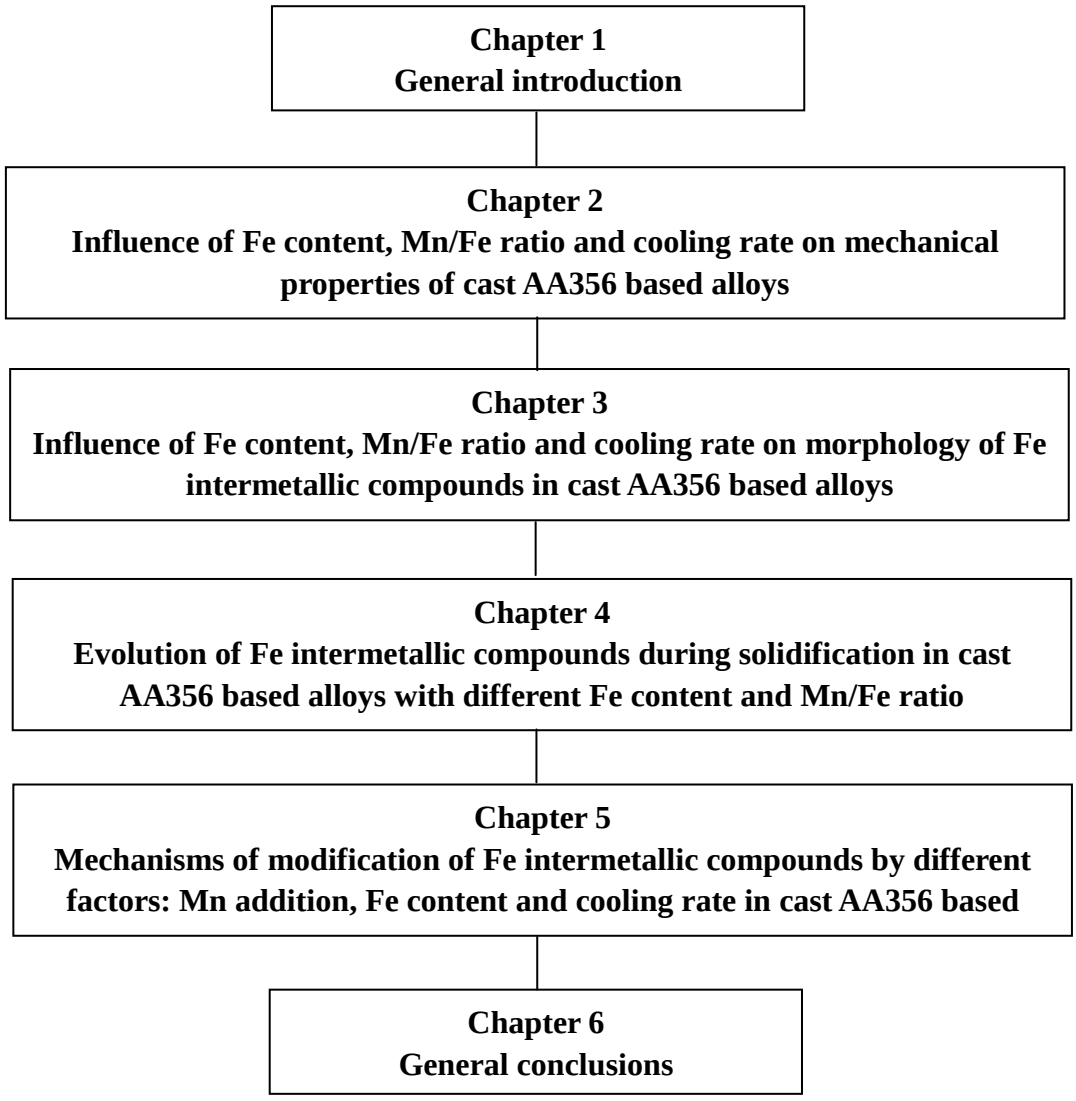

Fig. 1.4 Flow chart showing the outlines of the present thesis.

Chapter 2

Influence of Fe content, Mn/Fe ratio and cooling rate on mechanical properties of cast AA356 based alloys

The presence of the Fe impurity in cast Al-Si alloys will damage their mechanical properties significantly, especially the ductility. In this chapter, three factors, Fe content, Mn/Fe ratio and cooling rate were altered to investigate their effects on the tensile properties of cast AA356 based alloys. The results revealed that the Fe content was the main factor which could determine the final tensile properties of alloys. The high Fe content can lead to the formation of large size platelet β type Fe compound, which can easily be a crack initiation region and result in the decrease of the elongation and UTS. Mn addition can convert the platelet β type Fe compound to the Chinese script α type Fe compound and/or polyhedral shape α type Fe compound, which was expected to enhance the tensile properties of alloys. However, the increase of elongation of alloys with low Fe content by converting the Fe compound is not obvious in the present work. The branches of large size Chinese script can easily be a crack initiation region and result in the decrease of the tensile properties as well. The large size polyhedral shape Fe compound shows very detrimental influence on the tensile properties of alloys as that of large size platelet shape Fe compound. This compound can easily act as the nucleation sites for cracks under loading. In addition, the formation of large size polyhedral shape Fe compound usually accompanies the

formation of pores. High cooling rate can refine the size of all phases in the alloys and resulted in the enhancement of the tensile properties.

2.1 Introduction

Cast AA356 aluminum alloys are widely used in automotive industry due to their good properties, such as high strength/weight ratio, good castability, high corrosion resistance, low coefficient of thermal expansion, etc. The presence of the Fe impurity in the alloys damage their mechanical properties significantly, especially ductility due to the formation of Fe intermetallic compounds during solidification. The β type Fe compound with the platelet morphology is reported to bring out a serious alloy embrittlement [1,2]. This is due to the high stress concentration at the sharp edges of the platelet shape, which easily leads to a crack initiation. The Chinese script α type Fe compound presents less stress concentration than the sharp edges of the platelet β type Fe compound. Thus, the formation of Chinese script α type Fe compound is preferred and expected to enhance the ductility. To modify the Fe compounds from platelet β type to Chinese script α type well, three factors Fe content, Mn/Fe ratio and cooling rate were changed throughout the whole research work to investigate their effects on the formation of Fe compounds. In this chapter, the performance of the modification of Fe compounds will be evaluated based on microstructure analysis and mechanical properties in cast AA356 based alloys by alerting Fe content, Mn/Fe ratio and cooling rate.

2.2 Experimental procedures

Chemical compositions of the alloys used in this chapter are shown in Table 2.1.The master alloy Al-7.0wt.% Si-0.35wt.% Mg were molten in a graphite crucible under an Ar protective atmosphere by an electrical resistance furnace. The iron was added in the form of Fe wire, and Fe contents in each alloy are 1.0wt.%, 1.5wt.%, 2.0wt.% and 2.5wt.%,

respectively. Mn was added in the form of the Al-9.93 wt.% Mn. Different Mn contents were added to make sure the Mn/Fe ratio are 0, 0.35, 0.5 and 0.65, respectively. The samples are named as x Fe or x Fe+ y in the text, where the x represents the Fe content (in mass %) and y represents the Mn/Fe ratio. The schematic illustration of the casting process was showed in Fig. 2.1. To obtain various solidification conditions, each alloy was cast into a step-like stainless steel mold having sections with different thicknesses, as shown in Fig. 2.2. The thicknesses of the casts at different steps are 7 mm, 15 mm and 28 mm, respectively. Hence, during solidification, the different steps of the casts show the different cooling rates. The thermocouples were set in the center of each step during casting to monitor the cooling curves. The average cooling rate at each step was calculated from the beginning to the onset of the eutectic temperature (around 570˚C) in each cooling curve. The calculated cooling rates based on the cooling curves were showed in Fig. 2.3. The casting temperature of 720˚C was used throughout this study.

Microstructures of the alloys were studied by an optical microscope (OM). Tensile properties of the specimens were evaluated using an universal tensile testing machine at a constant crosshead speed of 0.5 mm/min. Two or four tensile test samples were prepared from each cast ingot at the same stage. The cutting position of tensile test samples from step-like cast ingot was schematically illustrated in Fig. 2.4 (a). The shape and size of the tensile test sample was showed in Fig. 2.4 (b). Samples for the microstructural analysis were prepared by standard techniques with the final polishing stage using the 0.05 μm colloidal silica.

2.3 Results

2.3.1 Effect of Fe content and cooling rate

Fig. 2.5 shows UTS and elongation of the alloy Al-7 wt.% Si- 0.35 wt.% Mg without Fe addition (less than 0.1 wt.%). Without Fe impurity, this alloy shows very good mechanical properties. Both the strength and elongation increased with increasing the cooling rate. The crack propagation under loading in this alloy mainly occurred along with the eutectic Si phase, as shown in Fig. 2.6. The high cooling rate refined both the size of α-Al and eutectic Si and improved the UTS and elongation.

The presence of Fe impurity damaged the tensile properties of alloys significantly, as shown in Fig. 2.7. In the alloys with Fe content ranging from 0 to 2.5 wt.%, the elongation of the alloys decreased greatly with increasing Fe content, as show in Fig. 2.7 (a). The UTS of alloys appeared the same tendency as well, as shown in Fig. 2.7 (b). Increasing the cooing rate at a given Fe content is beneficial to improve both the elongation and UTS. From the corss-sections of the fracture surfaces of the alloys with different Fe contents, it is clear that the cracks propagated mainly along with platelet Fe compounds, regardless of their locations, e.g. with eutectic Si or inside α-Al phase, as shown in Fig. 2.8. High cooling rate decreased the size of platelet Fe compound and made the elongation and UTS increase.

2.3.2 Effect of Mn/Fe ratio and cooling rate

In the alloys with 1.0 wt.% Fe and different Mn/Fe ratio at low cooling rate (3.2˚C/s), with increasing the Mn/Fe, the elongation of the alloys increased slightly, as shown in Fig. 2.9 (a). With increasing the Mn/Fe ratio, more Fe compounds appeared as Chinese script. The crack propagated along with large branches of Chinese script Fe compound instead of platelet Fe compound, as shown in Fig. 2.10 (a), (d), (g) and (f). However, even Fe

compounds were modified from platelet to Chinese script which was expected to enhance the ductility greatly, the elongation of the alloys showed slightly increase. Increasing the cooling rate from 3.2˚C/s to 8.1˚C/s, the elongation of the alloys showed slightly increase comparing with that of the alloys at the cooling rate of 3.2˚C/s. When the cooling rate increased to 15.5˚C/s, the elongation showed large increase. Even most of the Fe compounds appeared as platelet shape under this cooling rate in the alloys with different compositions, as shown in Fig. 2.10 (c), (f), (i) and (l). The UTS of the alloys increased with increasing the cooling rate. The Mn/Fe ratio increase showed no obvious influence on the UTS.

In the alloys with 1.5 wt.% Fe and different Mn/Fe ratio at low cooling rate (3.2˚C/s), the elongation increased with the Mn/Fe ration from 0 to 0.35, then decreased with increasing the Mn/Fe ratio, as shown in Fig. 2.11(a). From the fracture surface, with increasing the Mn/Fe ratio, the cracks propagated along with polyhedral shape Fe compound instead of platelet shape, as shown in Fig. 2.12 (a), (d), (g) and (j). The polyhedral shape Fe compounds showed detrimental influence on the elongation of alloys. Increasing the cooling rate from 3.2˚C/s to 8.1˚C/s, the elongation of the alloys increased at the same composition. From the fracture surface, the cracks propagated along with Chinese script Fe compounds instead of platelet shape Fe compounds, as shown in Fig. 2.12 (b), (e), (h) and (k). At high cooling rate of 15.5˚C/s, the elongation of the alloys decreased comparing to that of the alloys at low cooling rate of 8.1˚C/s. From the fracture surface, at this cooling rate, the cracks propagation happened along with small platelet shape Fe compounds instead of big ones, as shown in Fig. 2.12 (c), (f), (i) and (l). The UTS showed almost no change with increasing the Mn/Fe ratio. Increasing the cooling rate can increase the UTS in alloys with the same composition.

At different cooling rates, even at high cooling rate, the elongation of the alloy 2.5 Fe is very low, as shown in Fig. 2.13 (a). From the fracture surface, even at high cooling rate, large size platelet Fe compound appeared. The cracks propagated along with large size platelet Fe compounds, as shown in Fig. 2.14 (a), (b) and (c). In the alloy 2.5 Fe + 0.65, the elongation of this alloy at different cooling rates is very low, as shown in Fig. 2.13 (a). From the fracture surface, the cracks propagation happened along with large size polyhedral shape Fe compounds instead of platelet Fe compounds, as shown in Fig. 2.14 (j), (k) and (l). In the alloys 2.5 Fe + 0.35 and 2.5 Fe + 0.5, the elongation increased comparing with that of the alloys 2.5 Fe and 2.5Fe + 0.65 at different cooling rates, as shown in Fig. 2.13 (a). From the fracture surface, in the alloy 2.5 Fe + 0.35, the cracks propagation happened along with platelet, Chinese script and polyhedral shape Fe compounds at different cooling rates. In the alloy 2.5 Fe + 0.5, the cracks propagation happened along with Chinese script and polyhedral shape Fe compounds. With increasing the cooling rate, the amount of Chinese script Fe compounds increased along with decreasing the amount of polyhedral shape Fe compounds.

2.4 Discussion

The presence of Fe in cast Al-Si alloys damage their mechanical properties significantly, as shown in Fig. 2.6 and Fig. 2.7. With increasing the Fe content, the tensile properties decreased greatly. Similar results were also reported in other works [3, 4]. The detrimental effect of iron on ductility is due to the fact that, during plastic deformation, the cracks preferentially nucleate along the harmful platelet β type Fe compound, oriented perpendicularly to the load direction, where a high stress concentration is reached [5]. In addition, from the cross-section fracture surface, it is clear that the cracks usually located inside of the platelet compound, as shown in Fig. 2.15. This result is also consistent with X.

J. Cao's work [6-8]. They reported that the cracks were the typical feature of platelet β type Fe compound, which were usually located inside of the platelet compound. In addition, the increase the Fe content leads to the increase of porosity, as shown in Fig. 2.16 (a). It is due to the precipitation of large size platelet Fe compound which, in turn, prevent the liquid metal to fill the spaces between the branched platelets [9, 10]. The larger the size of platelet shape Fe compound is, their detrimental effect on tensile properties it will be. The cooling rate can refine the size of all the phases during solidification. The refined small size platelet Fe compound is beneficial to the tensile properties of alloys.

Mn addition can modify the platelet β type Fe compound to Chinese script α type compound or over-modified to polyhedral shape α type compound, which mainly depending on the Fe content, Mn/Fe ratio and cooling rate. It is widely accepted that the Chinese script α type Fe compound shows less detrimental effects on the tensile properties of alloys comparing with platelet β type Fe compound [4-10]. In this work, the increase of tensile properties by converting the platelet compound to Chinese script Fe compound is obvious when the Fe content is relative high. However, in the alloy with low Fe content (1.0 wt.%), even the platelet β type Fe compound was modified to Chinese script α type Fe compound in the alloy 1 Fe + 0.65 at low cooling rate, the elongation increase is not obvious comparing with that of the alloy 1.0 Fe. This is due to that the size of the large branches of the Chinese script Fe compound is very big, even close to the size of platelet β type Fe compound in the alloy 1.0 Fe. The large branches of the Chinese script Fe compound can also easily be a crack initiation region and result in the decrease strength and ductility, as shown in Fig. 2.10 (g) and (j) marked by arrows.

When the alloys with high Fe content and high Mn/Fe ratio under low cooling rate, such as alloys 1.5 Fe +0.65, 2.5 Fe + 0.5 and 2.5 Fe + 0.65, most of the Fe compounds solidified

as polyhedral shape. From the fracture surface of these alloys at low cooling rate, as shown in Fig. 2.12 (f), Fig. 2.14 (g) and (j), the crack propagated along with the polyhedral shape Fe compound. The cracks can easily nucleate inside the large size polyhedral shape Fe compound and result in the decrease of the tensile properties. Additionally, the formation of polyhedral shape Fe compound usually accompanies by the formation of pores, as shown in Fig. 2.16 (b), which will damage the tensile properties of alloys significantly as well.

2.5 Conclusions

In this chapter, the effects of the Fe content, Mn/Fe ratio and cooling rate on the tensile properties of cast AA356 based alloys were investigated. Three factors were changed individually and combined during casting to reveal their effects on the microstructure and tensile properties of alloys. The results can be drawn as follows:

1. Fe content is the main factor which can determine the final tensile properties of alloys. The high Fe content can lead to the formation of large size platelet β type Fe compound, which can easily be a crack initiation region and result in the decrease of the elongation and UTS. Meanwhile, during solidification, the large size platelet Fe compound which solidified earlier than α-Al will block the feeding channel of liquid and lead to the formation of pores. High porosity will damage the mechanical properties of alloys significantly.

2. Mn addition can convert platelet β type Fe compound to Chinese script α type Fe compound and/or polyhedral shape α type Fe compound, which was expected to enhance the tensile properties of alloys. However, in the alloy with low Fe content (1.0 wt.%), the increase of elongation of alloys by converting the Fe compound is not obvious in the present work. The branches of large size Chinese script can easily be a crack initiation region and result in the decrease of the tensile properties as well. The large size polyhedral shape Fe compound shows very detrimental influence on the tensile properties of alloys as that of

large size platelet shape Fe compound. Both of them can easily act as the nucleation sites for cracks under loading. In addition, the formation of large size polyhedral shape Fe compound usually accompanies by the formation of pores.

3. High cooling rate can refine the size of all phases in the alloys. The refined small size Fe compound is beneficial to the tensile properties of alloys. Simultaneously, the cooling rate influences the modification process from platelet β type Fe compound to Chinese script α type Fe compound (over-modified to polyhedral shape α type Fe compound). Hence, the influence of cooling rate on the tensile properties of alloys with Mn as a modifier should be considered carefully in both the type of Fe compound as well as the size of Fe compounds.

References

[1] J. Dornaulf, A. M. Frankfurt: Chem. Abstr., **22** (1928), 210.

[2] L. Grand: Fonderie, **217** (1964), 65.

[3] L. Ceschini, I. Boromei, L. Morri, S. Seifeddine and I. L. Svensson: J. Mater. Process. Technol., **209(15-16)** (2009), 5669-5679.

[4] G. Ran, J. Zhou and Q. G. Wang: J. Mater. Process. Technol., **207 (1-3)** (2008), 46-52.

[5] S. Seifeddine, S. Johansson and I. L. Svensson: Mater. Sci. Eng. A, **490** (2008), 385-390.

[6] X. J. Cao and J. Campbell: AFS Trans. **108** (2000), 391-400.

[7] X. J. Cao and J. Campbell: J. Metall. Mat. Trans. A, **34A** (2003), 1409-1420..

[8] X. J. Cao and J. Campbell: Materials Transaction, **47 (5)** (2006), 1303-1312.

[9] P. N. Crepeau: AFS Transactions, **95** (1996), 361-366.

[10] M. A. Moustafa: J. Mater. Process. Technol. **209** (2009), 605-610.

Table 2.1 Nominal compositions of the AA356 based alloys with different Fe and Mn contents. The samples are named as x Fe or x Fe+ y in the text, where the x represents the Fe content (in mass %) and y represents the Mn/Fe ratio.

Alloys	Elements (mass %)					Mn/Fe ratio
	Al	Si	Mg	Fe	Mn	
Set 1	Bal.	7.00	0.35	0	0	-
Set 2	Bal.	7.00	0.35	1.0	0, 0.35, 0.5, 0.65	0, 0.35, 0.5 0.65
Set 3	Bal.	7.00	0.35	1.5	0, 0.525, 0.75, 0.975	0, 0.35, 0.5, 0.65
Set 4	Bal.	7.00	0.35	2.0	0	0
Set 5	Bal.	7.00	0.35	2.5	0, 0.875, 1.25, 1.625	0, 0.35, 0.5, 0.65

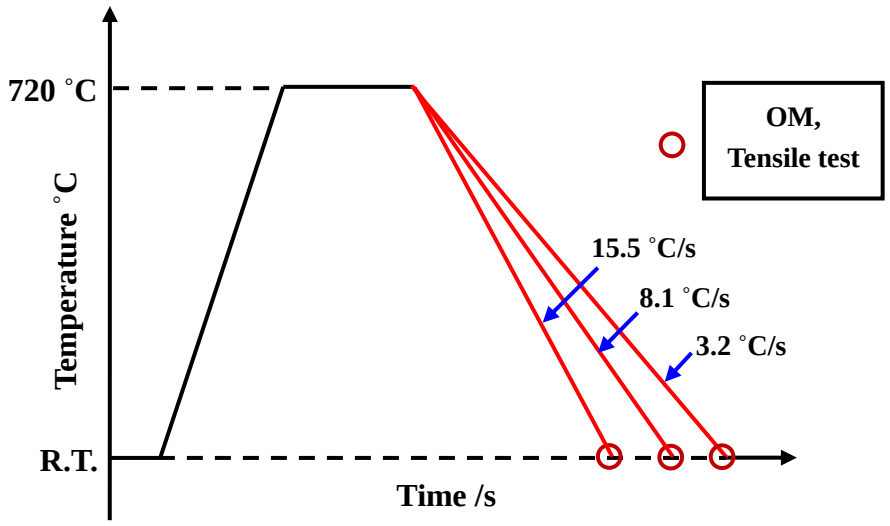

Fig. 2.1 Schematic illustration of the casting process utilized by step-like mold.

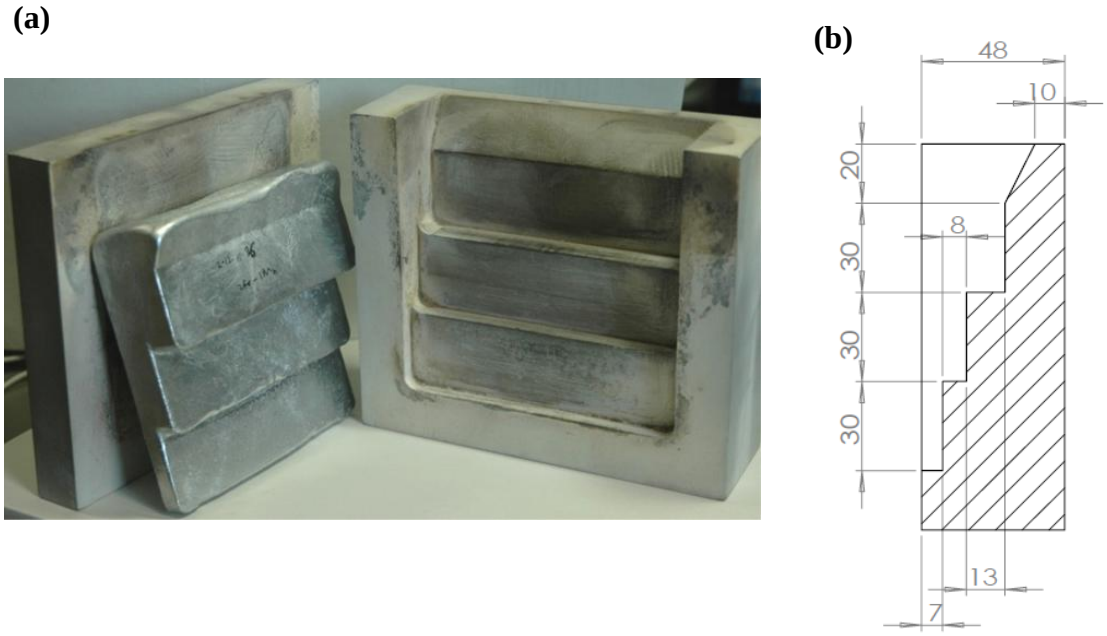

Fig. 2.2 Appearance of the step-like mold used in the present work with the cast ingot (a) and the schematic illustration of the longitudinal section of the step-like mold (b).

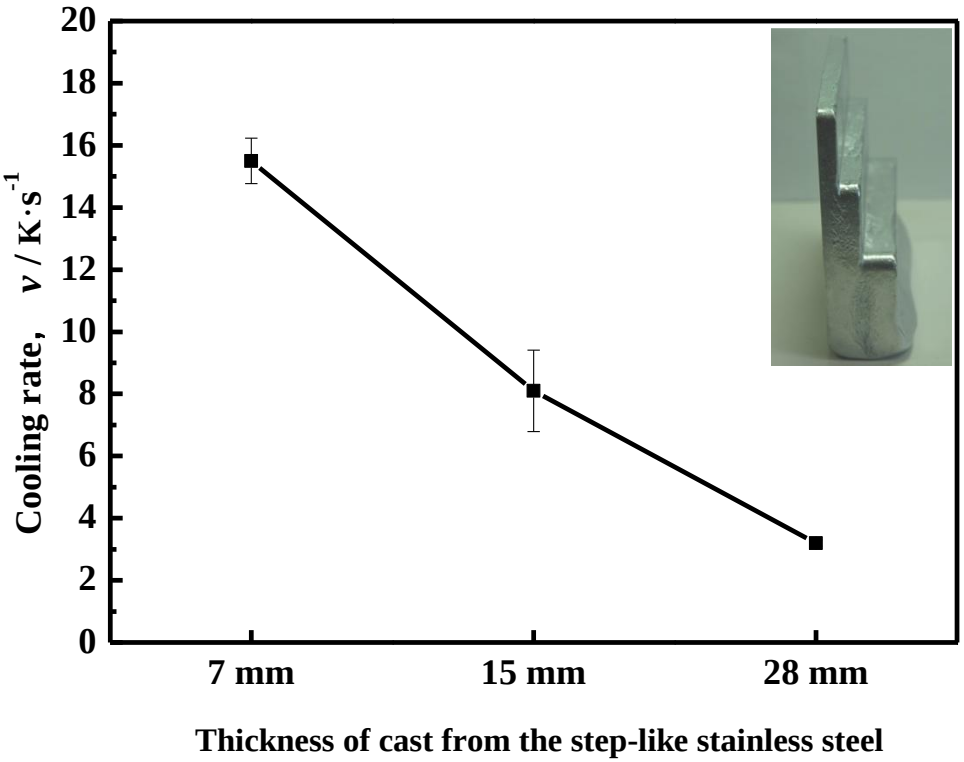

Fig. 2.3 Values of the cooling rates are averaged for the alloys with different Fe contents and no Mn addition.

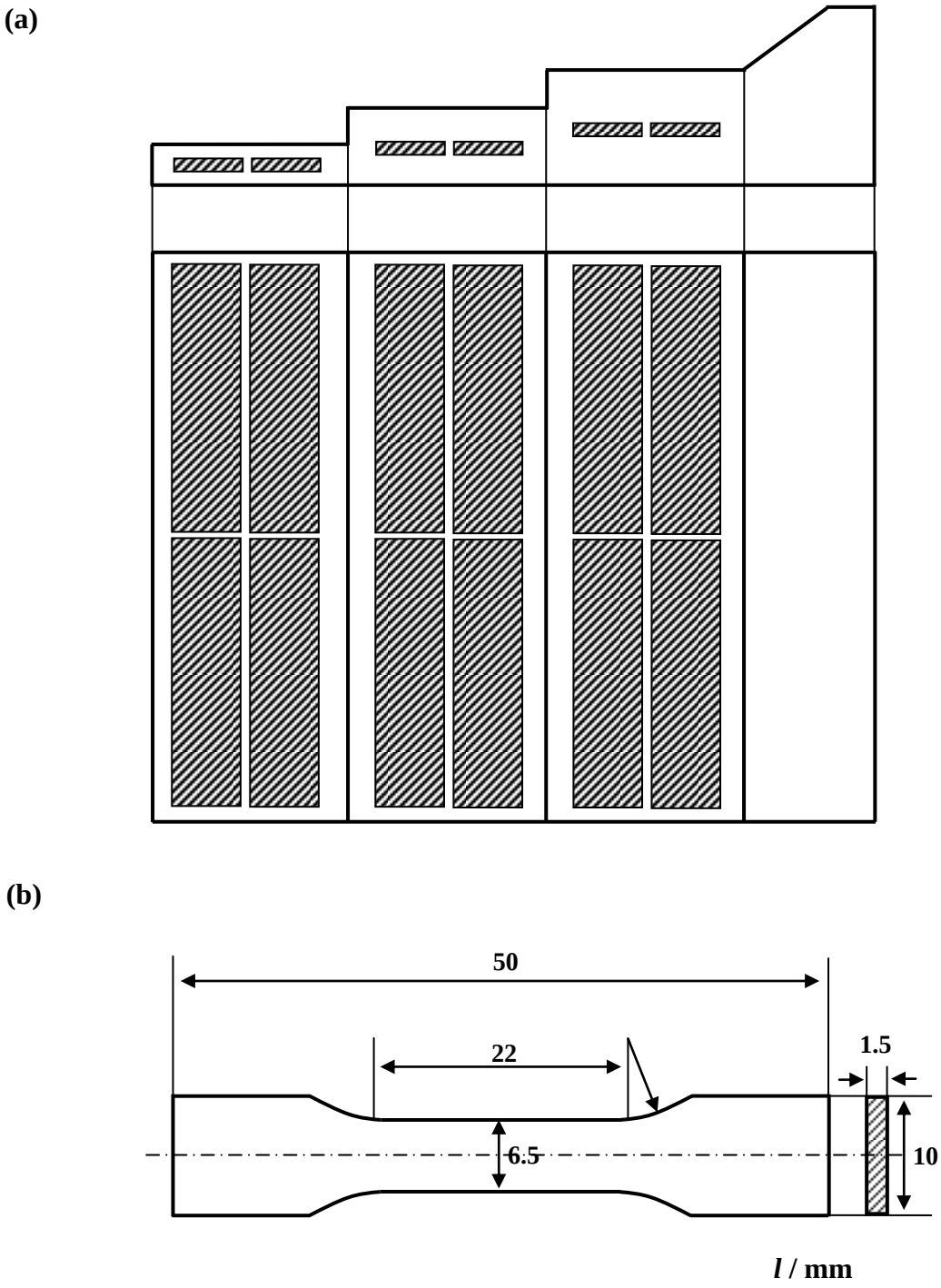

Fig. 2.4 Schematic draws illustrates the locations to get tensile test samples from the cast ingot (a) and the shape of the test samples (b).

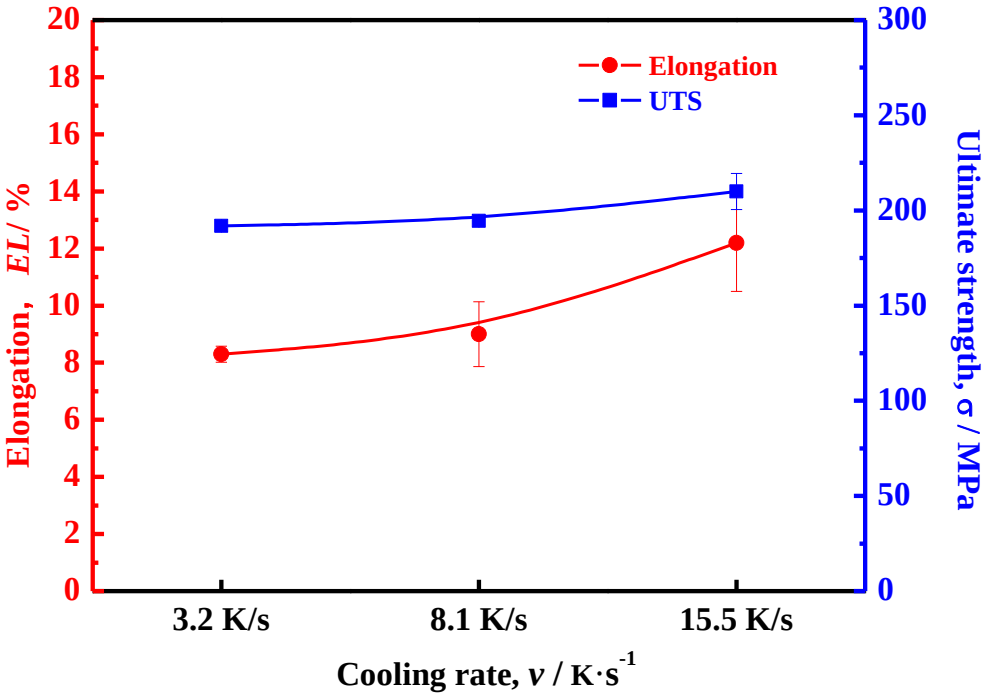

Fig. 2.5 Elongation and ultimate strength of the alloy Al-7.0 wt.% Si-0.35 wt.% Mg without Fe addition under different cooling rates.

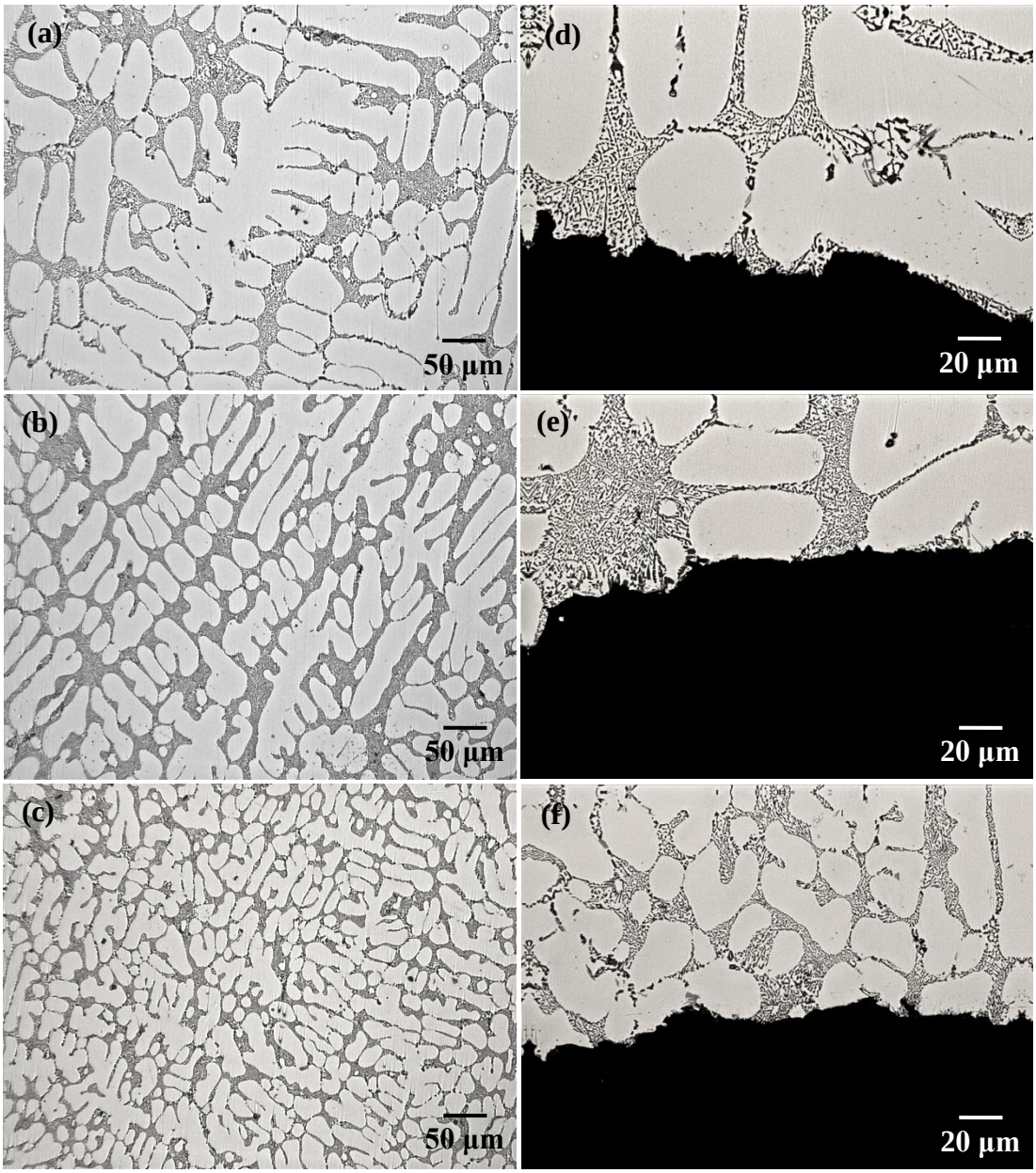

Fig.2.6 Microstructures of the alloy Al-7.0 wt.% Si-0.35 wt.% Mg without Fe addition under different cooling rates, (a) 3.2˚C/s, (b) 8.1˚C/s, (c)15.5˚C/s; The corresponding microstructures of the cross-sections of the tensile specimens under the fracture surface, (d) 3.2˚C/s, (e) 8.1˚C/s, (f) 15.5˚C/s.

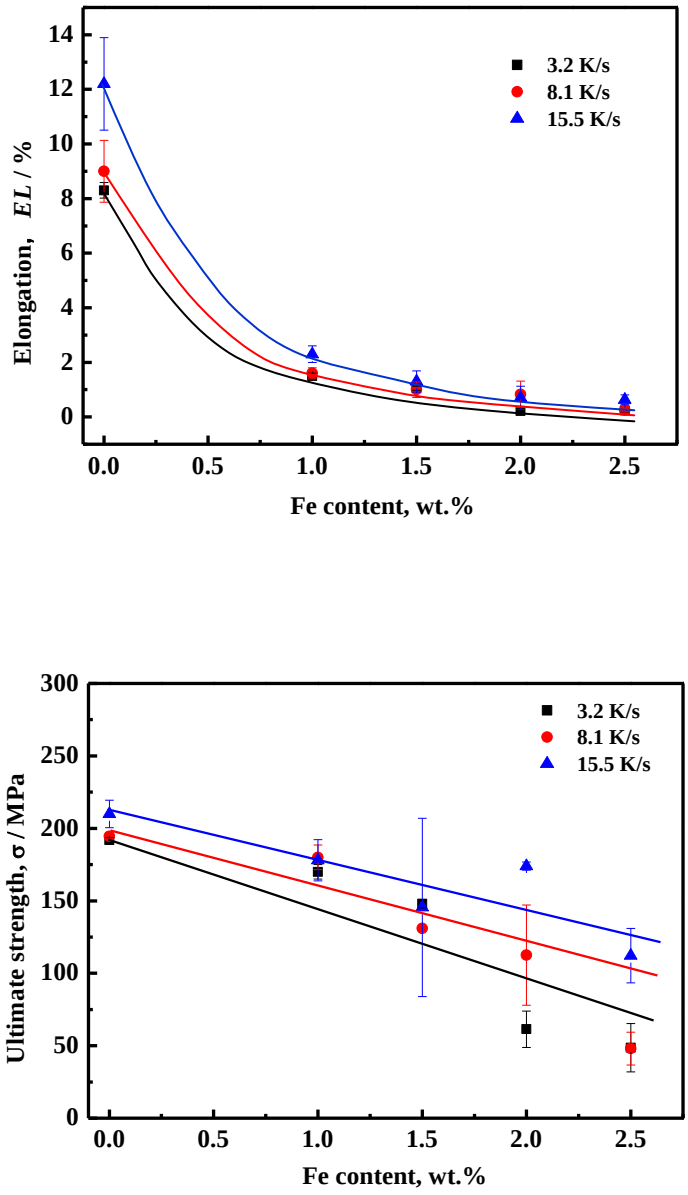

Fig.2.7 Mechanical properties of cast AA356 based alloys with different Fe contents ranging from 1.0 wt.% to 2.5 wt.% under different cooling rates: (a) elongation, (b) UTS.

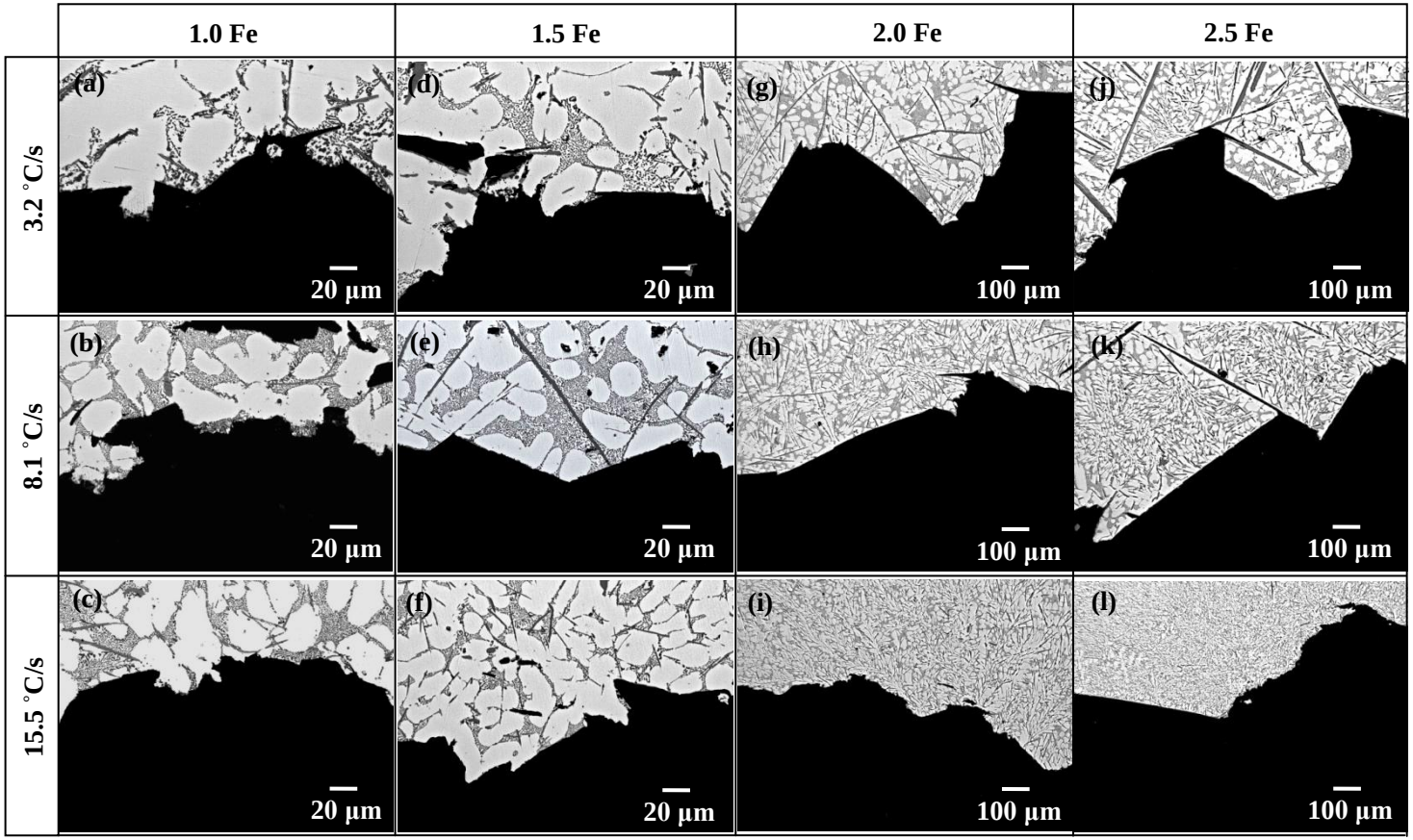

Fig.2.8 Microstructures of the cross-sections of the tensile specimens with different Fe contents under different cooling rates, 1.0 Fe: (a) 3.2˚C/s, (b) 8.1˚C/s, (c) 15.5˚C/s; 1.5 Fe: (d) 3.2˚C/s, (e) 8.1˚C/s, (f) 15.5˚C/s; 2.0 Fe: (g) 3.2˚C/s, (h) 8.1˚C/s, (i) 15.5˚C/s; 2.5 Fe: (j) 3.2˚C/s, (k) 8.1˚C/s, (l) 15.5˚C/s.

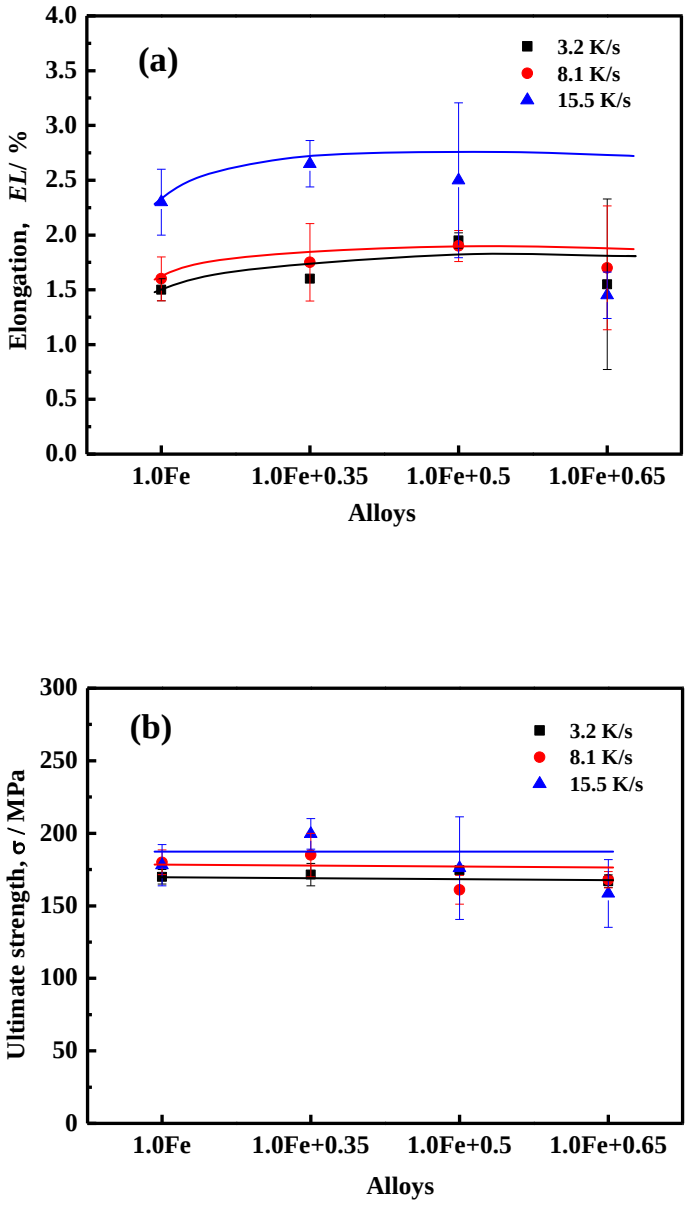

Fig.2.9 Mechanical properties of cast AA356 based alloys with 1.0 Fe and different Mn/Fe ratio under different cooling rates: (a) elongation, (b) UTS.

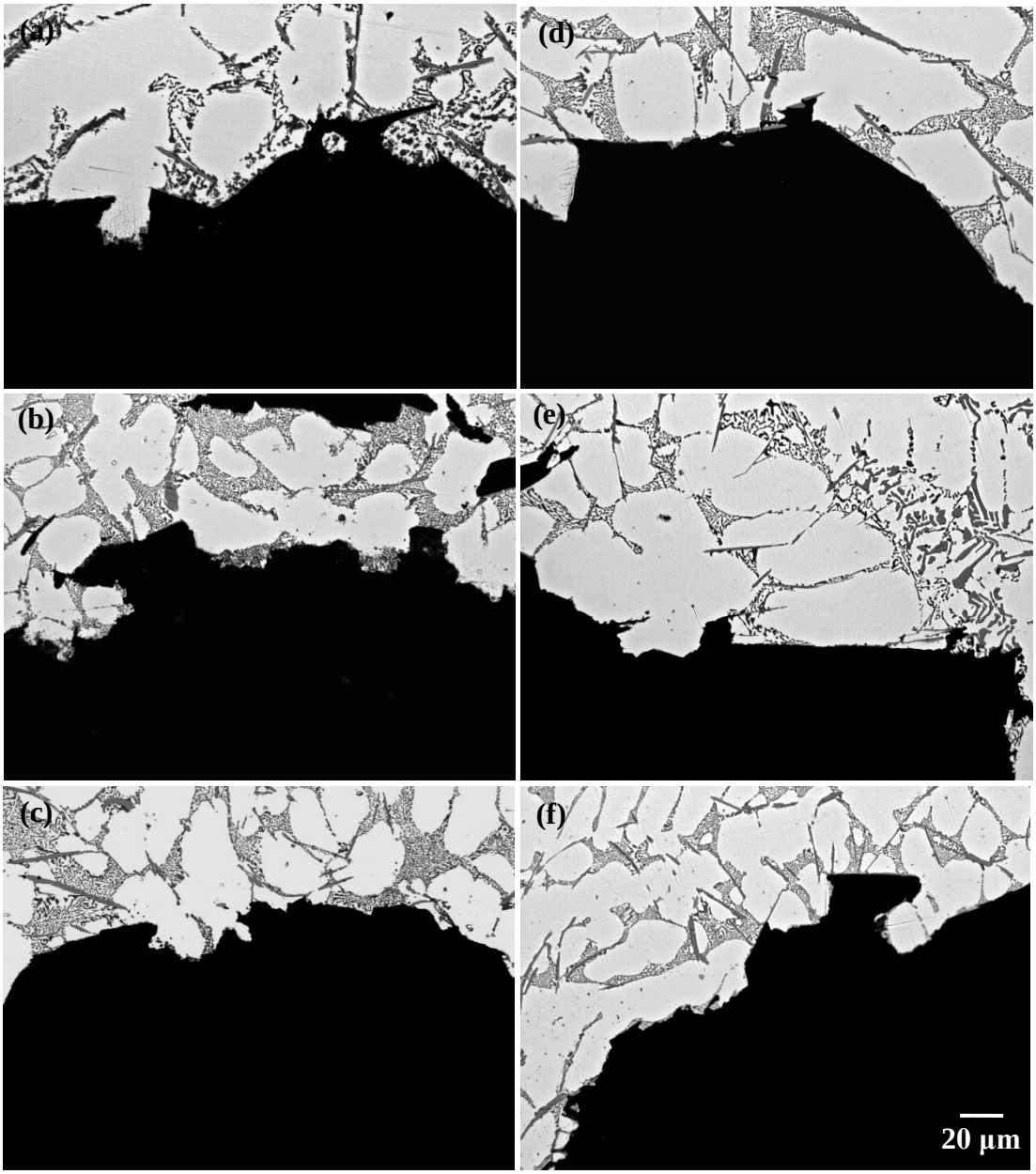

Fig.2.10 Microstructures of the cross-sections of the tensile specimens with 1.0 Fe and different Mn/Fe ratio under different cooling rates, 1.0 Fe: (a) 3.2˚C/s, (b) 8.1˚C/s, (c) 15.5˚C/s; 1.0 Fe + 0.35: (d) 3.2˚C/s, (e) 8.1˚C/s, (f) 15.5˚C/s; 1.0 Fe + 0.5: (g) 3.2˚C/s, (h) 8.1˚C/s, (i) 15.5˚C/s; 1.0 Fe + 0.65: (j) 3.2˚C/s, (k) 8.1˚C/s, (l) 15.5˚C/s.

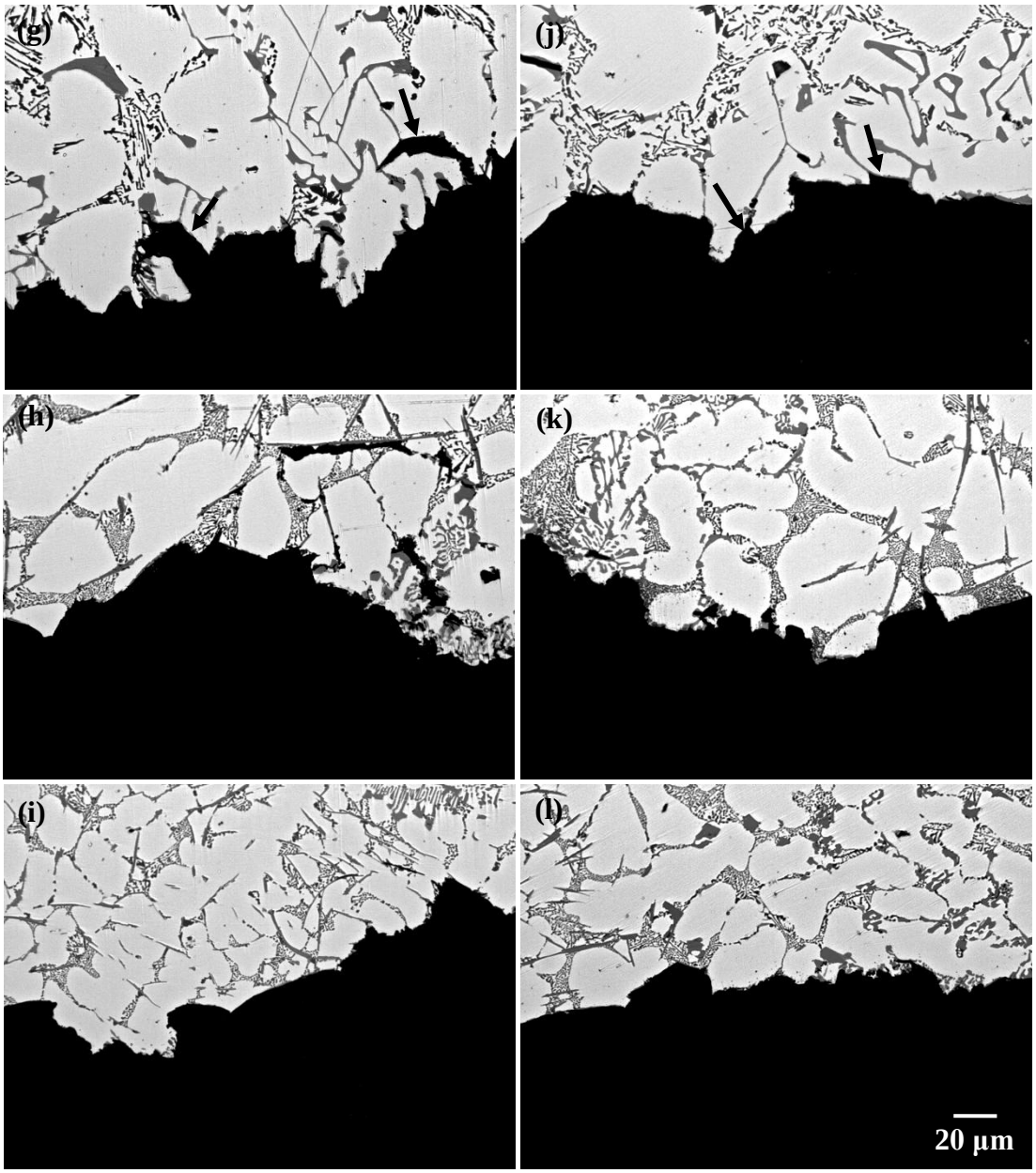

Fig.2.10 (Continued). The arrows in (g) and (j) indicated the large branches of the Chinese script Fe compound can easily act as the nucleation sites for cracks under loading. Arrows indicated the large branches of Chinese script Fe compound.

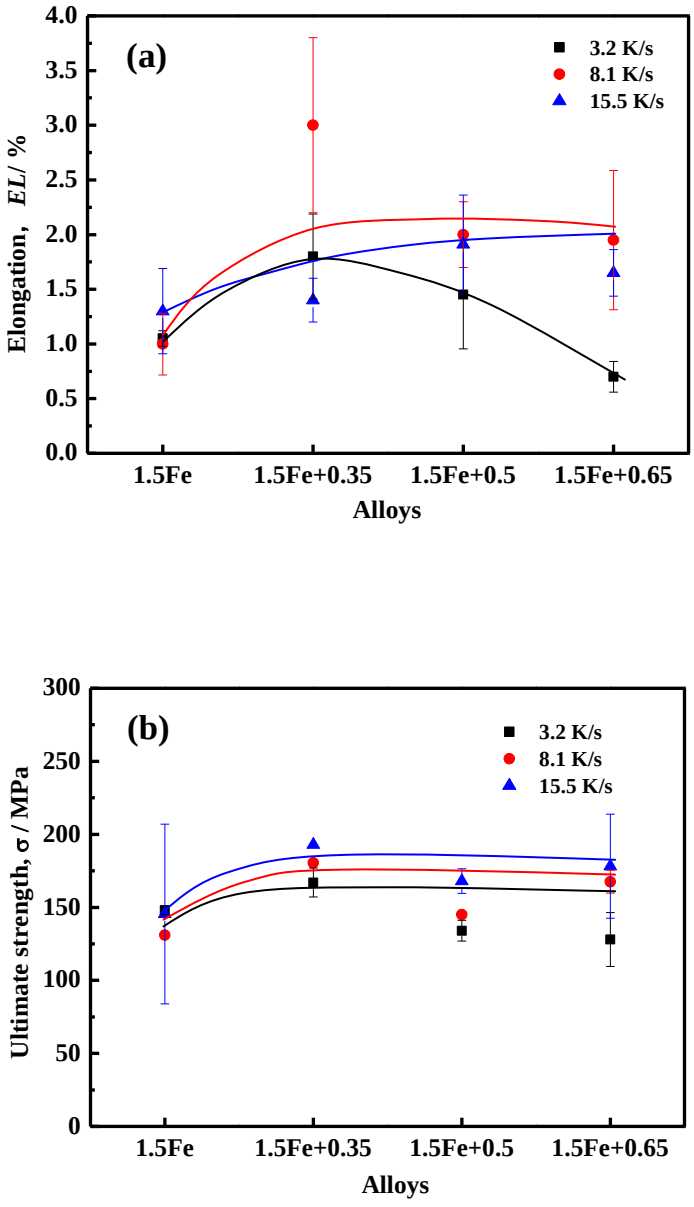

Fig.2.11 Mechanical properties of cast AA356 based alloys with 1.5 Fe and different Mn/Fe ratio under different cooling rates: (a) elongation, (b) UTS.

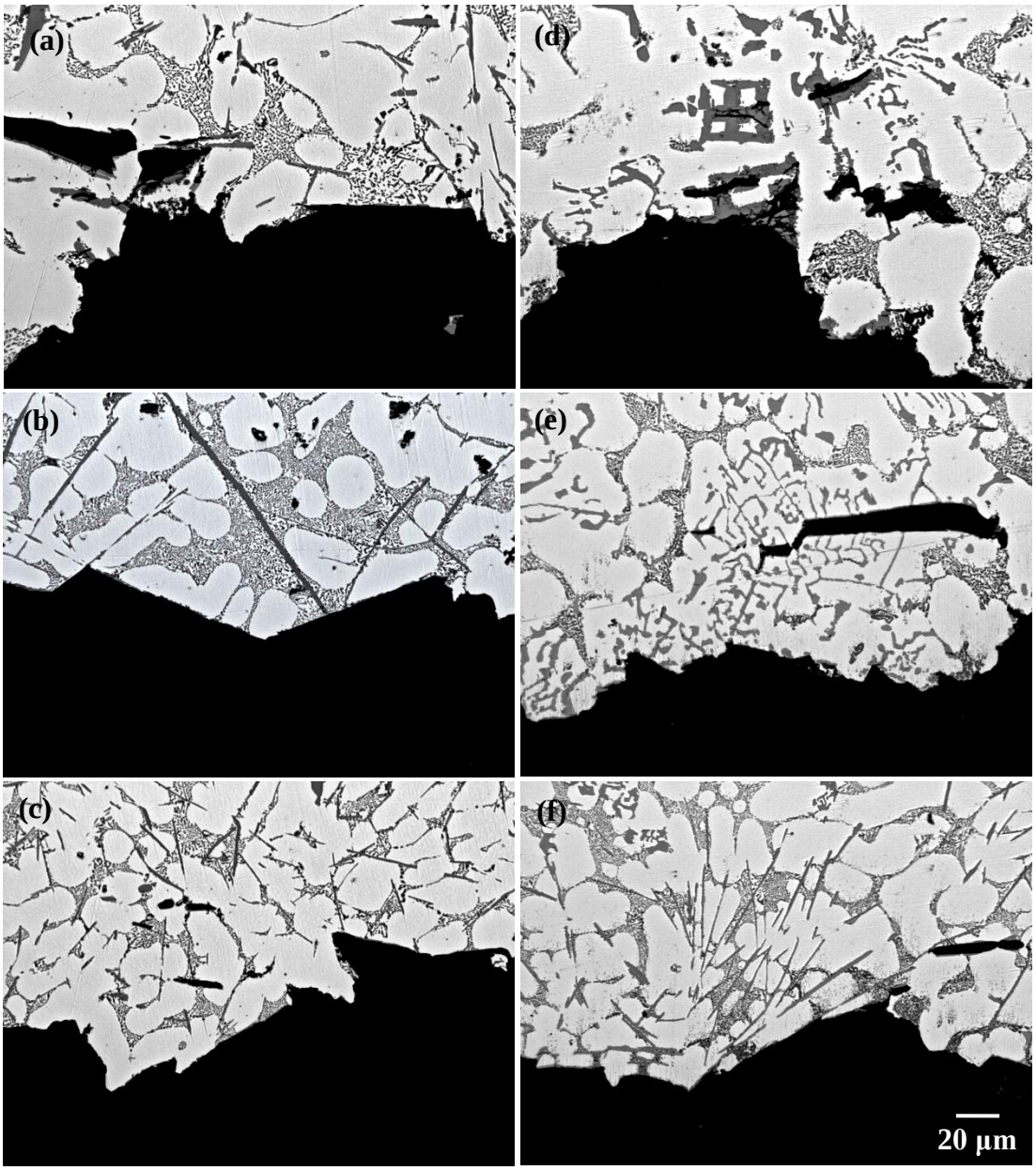

Fig. 2.12 Microstructures of the cross-sections of the tensile specimens with 1.5 Fe and different Mn/Fe ratio under different cooling rates, 1.5 Fe: (a) 3.2˚C/s, (b) 8.1˚C/s, (c) 15.5˚C/s; 1.5 Fe + 0.35: (d) 3.2˚C/s, (e) 8.1˚C/s, (f) 15.5˚C/s; 1.5 Fe + 0.5: (g) 3.2˚C/s, (h) 8.1˚C/s, (i) 15.5˚C/s; 1.5 Fe + 0.65: (j) 3.2˚C/s, (k) 8.1˚C/s, (l) 15.5˚C/s.

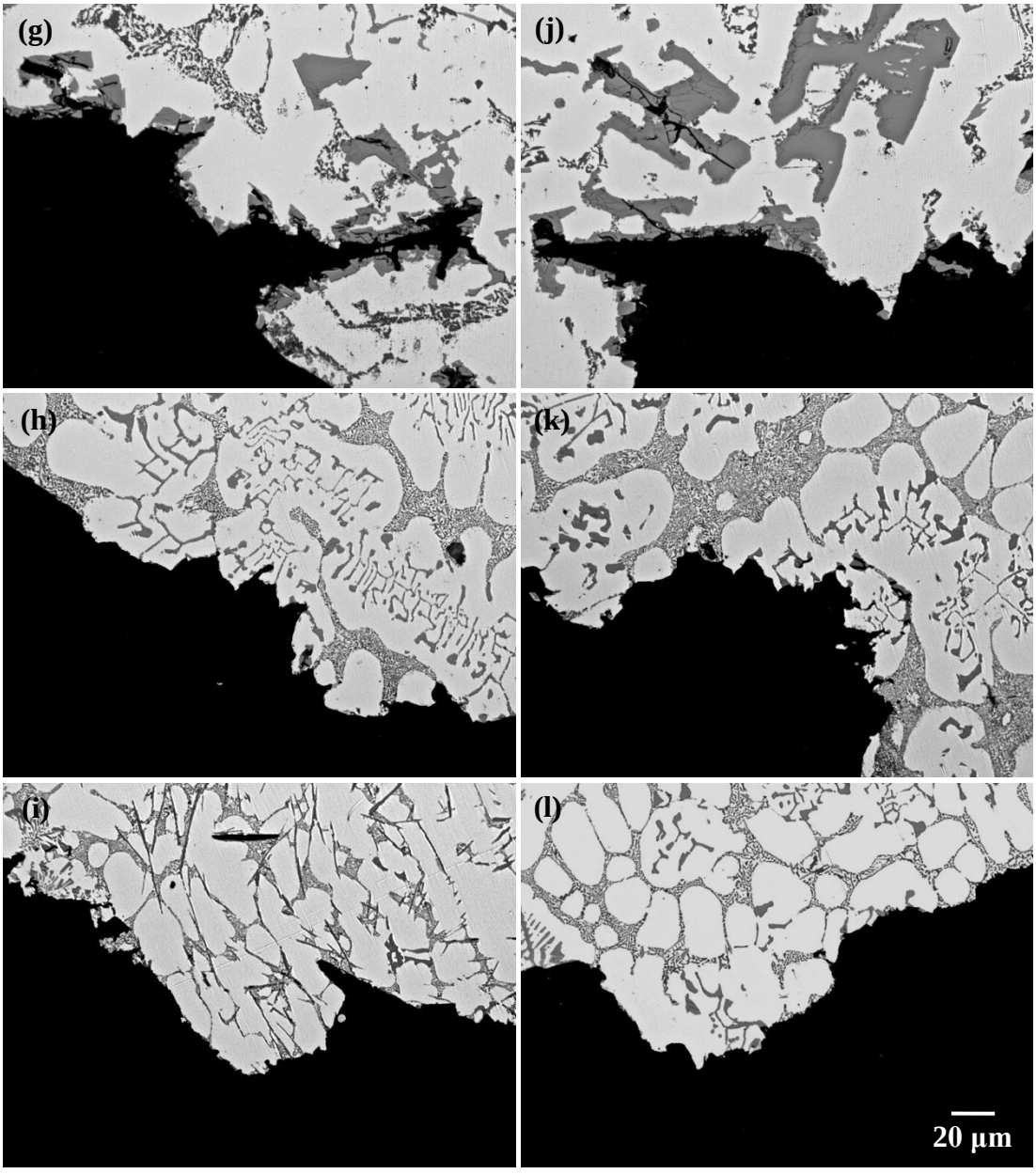

Fig. 2.12 (Continued).

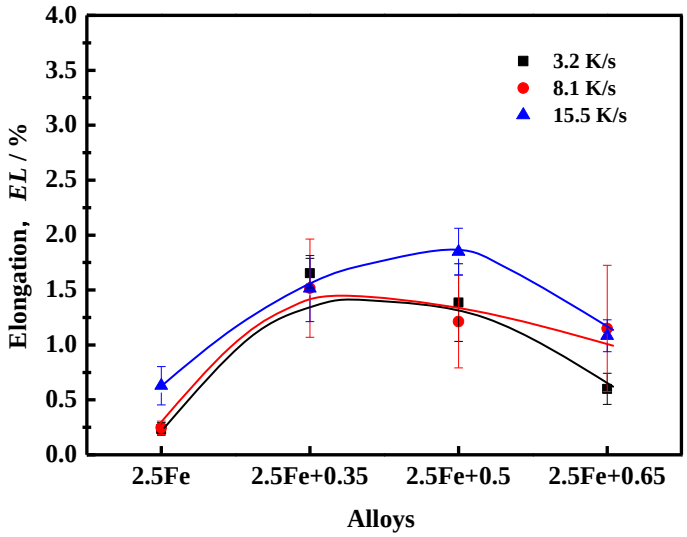

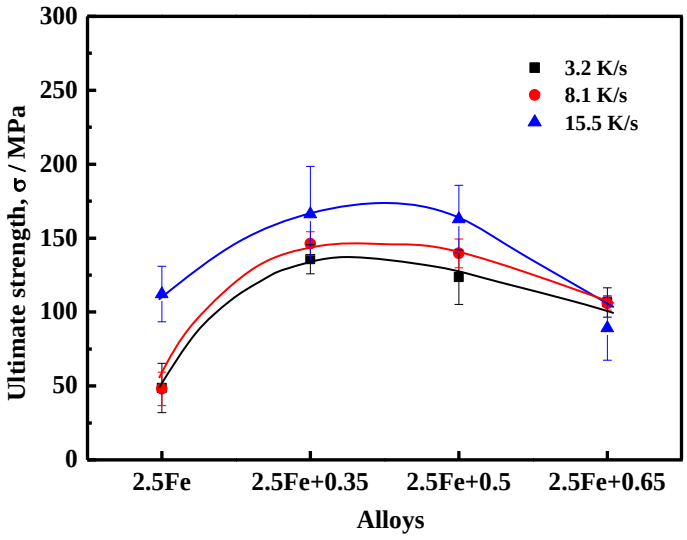

Fig.2.13 Mechanical properties of cast AA356 based alloys with 2.5 Fe and different Mn/Fe ratio under different cooling rates: (a) elongation, (b) UTS.

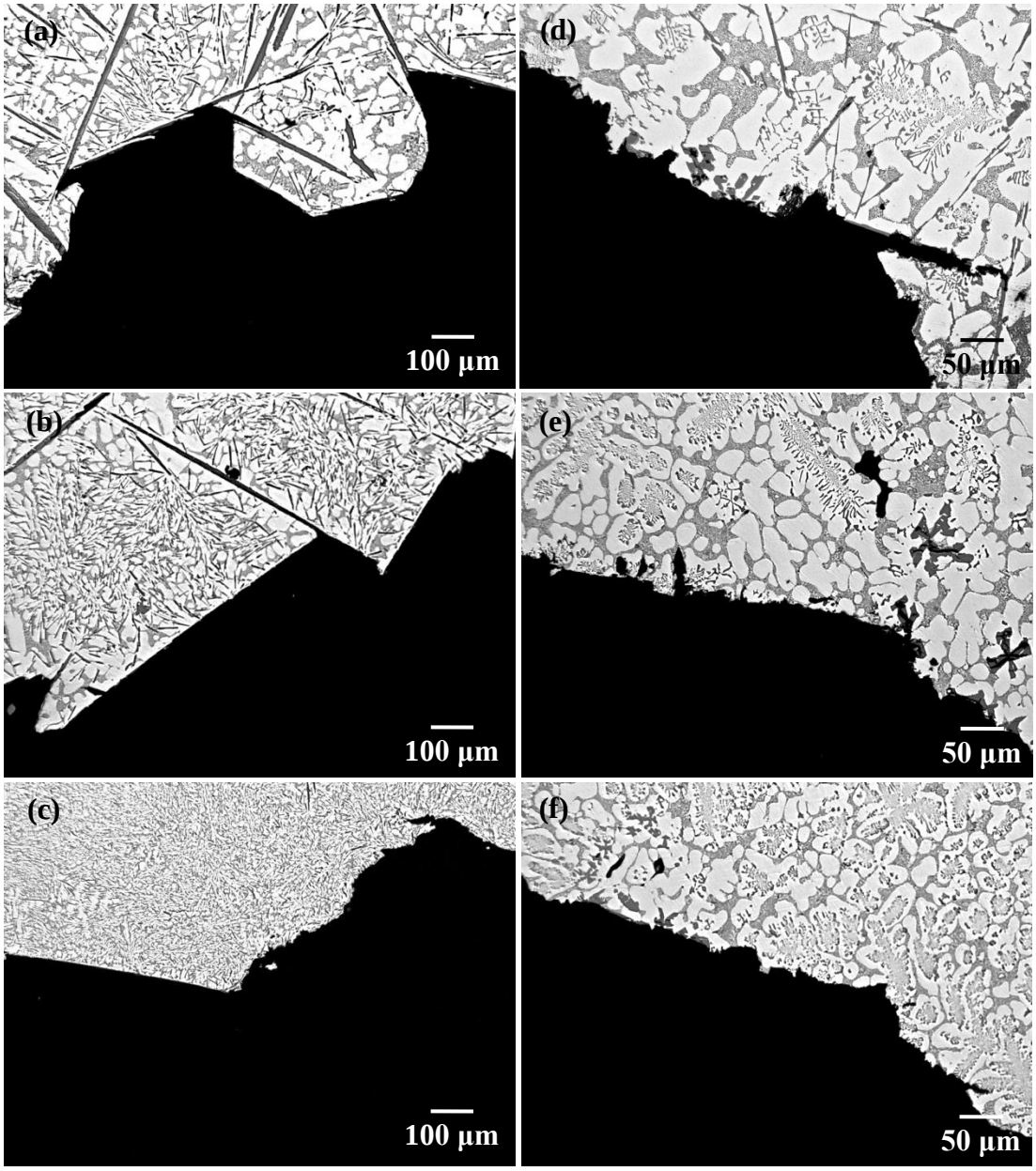

Fig. 2.14 Microstructures of the cross-sections of the tensile specimens with 2.5 Fe and different Mn/Fe ratio under different cooling rates, 2.5 Fe: (a) 3.2˚C/s, (b) 8.1˚C/s, (c) 15.5˚C/s; 2.5 Fe + 0.35: (d) 3.2˚C/s, (e) 8.1˚C/s, (f) 15.5˚C/s; 2.5 Fe + 0.5: (g) 3.2˚C/s, (h) 8.1˚C/s, (i) 15.5˚C/s; 2.5 Fe + 0.65: (j) 3.2˚C/s, (k) 8.1˚C/s, (l) 15.5˚C/s.

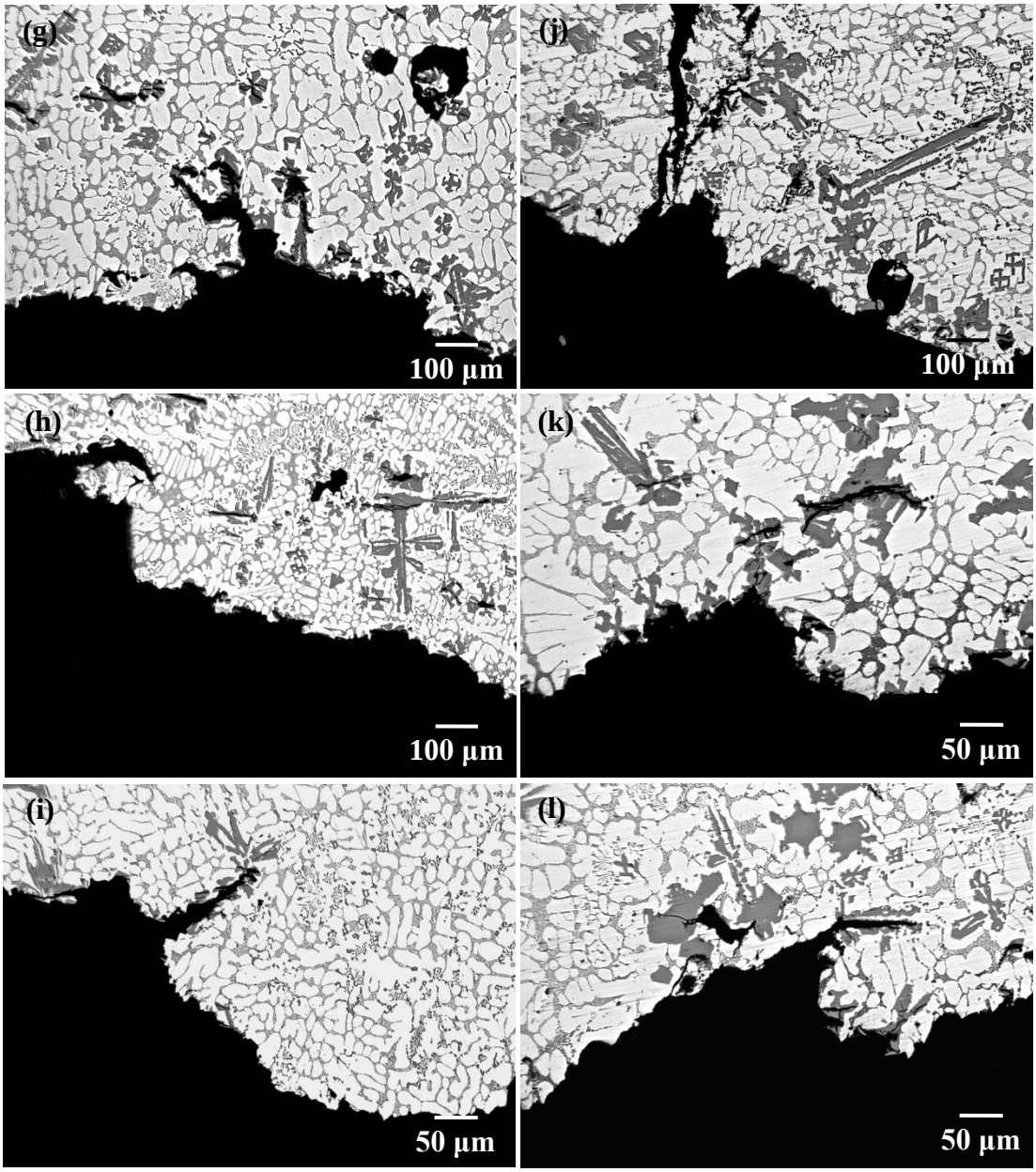

Fig. 2.14 (Continued).

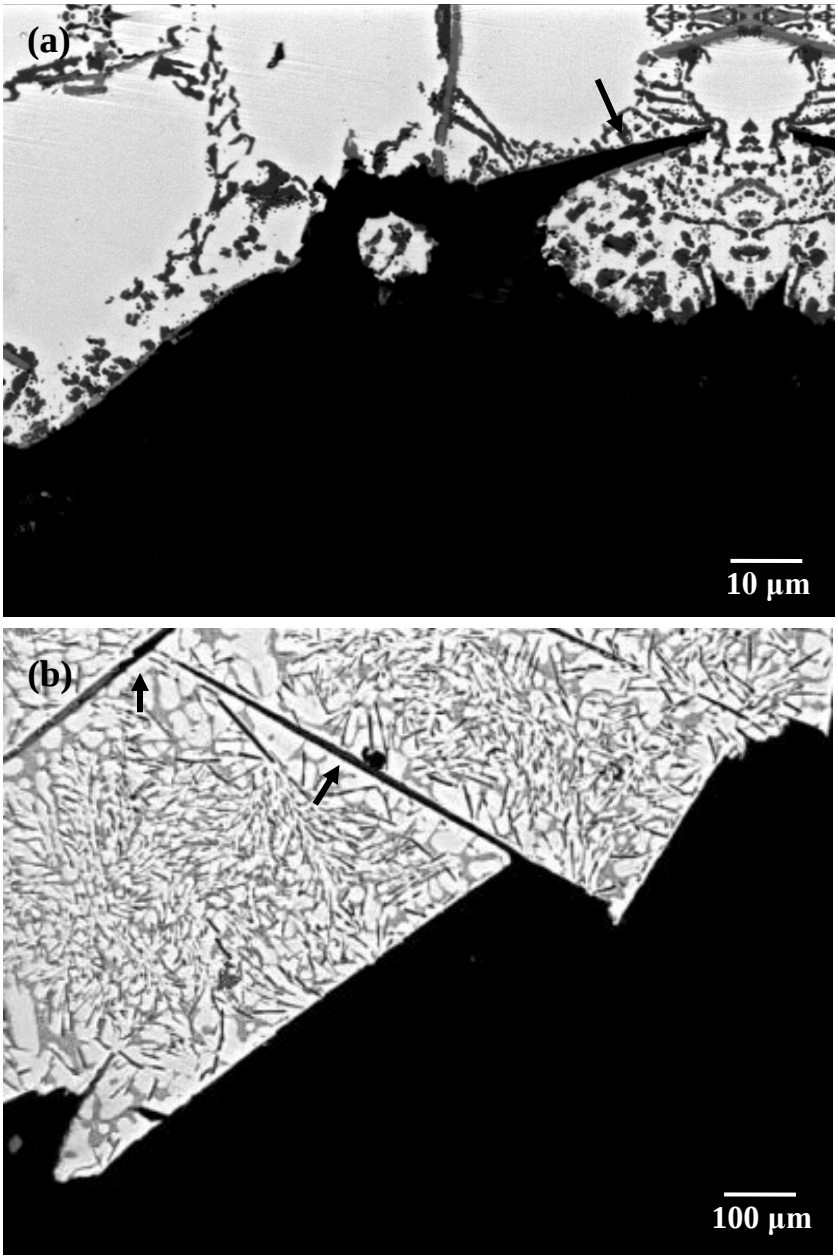

Fig. 2.15 Microstructures of the cross-sections of the tensile specimens with 1.0 Fe and 2.5 Fe. The arrows indicated the cracks located inside the platelet Fe compounds.

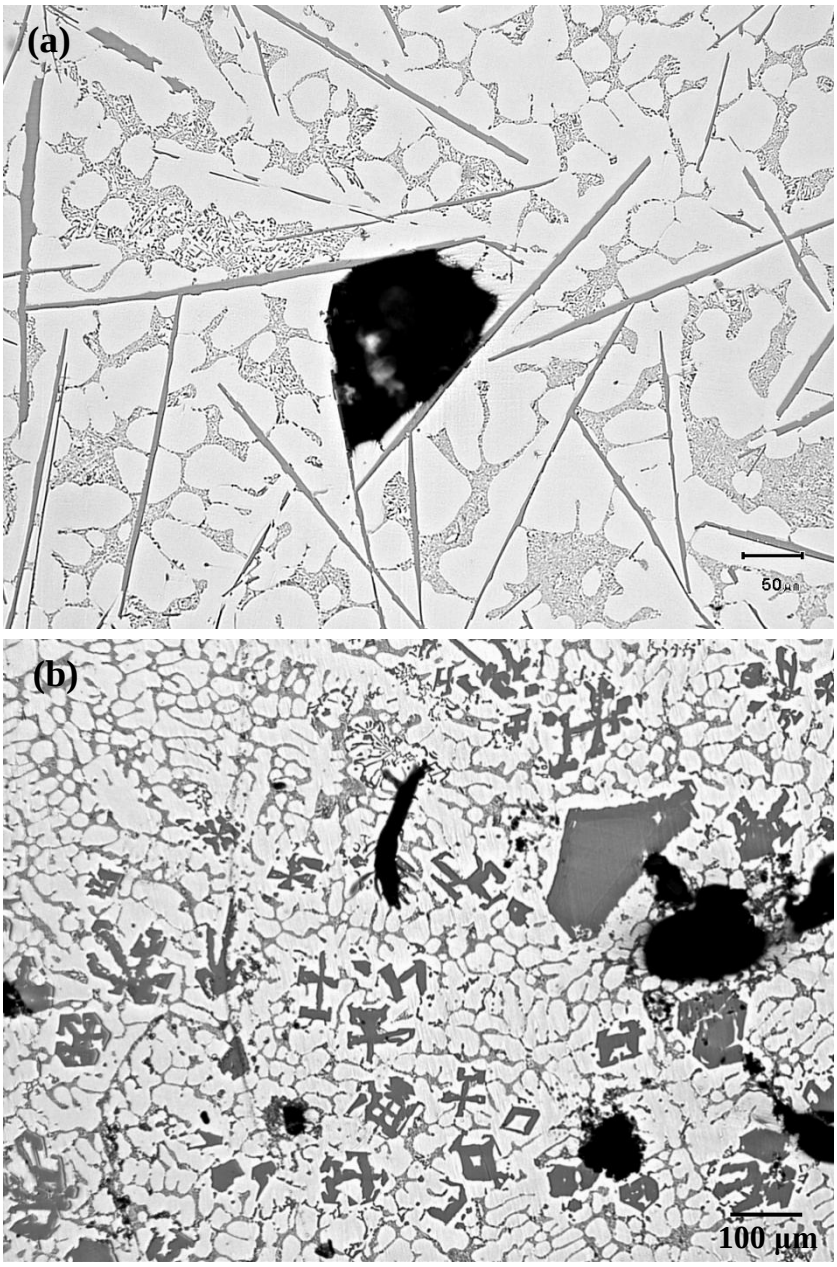

Fig. 2.16 Microstructures of the alloy 2.5 Fe and 2.5 Fe + 0.65 solidified at low cooling rate. The large size of platelet Fe compounds block the feeding channel of the liquid during solidification leads to the formation of pore (a) and the formation of the polyhedral shape Fe compound also along with the formation of pore (b).

Chapter 3

Influence of Fe content, Mn/Fe ratio and cooling rate on morphology of Fe intermetallic compounds in cast AA356 based alloys

In cast Al-Si alloys, the platelet β type Fe intermetallic compound has been considered as most detrimental Fe compounds to their mechanical properties, especially ductility. When the Fe is inevitable, to enhance the properties of the cast aluminum alloys, the modification of Fe compounds from the platelet β type Fe compound to a more compact and less harmful α type Fe compound having the Chinese script morphology becomes the efficient and important way.

This chapter mainly investigated how did three factors, Fe content, Mn/Fe ratio and cooling rate individually and combined influence this modification process in cast AA356（JIS, AC4C） based alloys. The special shape stainless steel mold was utilized during casting to generate the different cooling rates. The results were mainly revealed by the morphology analysis. The results revealed that with increasing the Fe content in the alloy without Mn addition, the size of the platelet β type Fe compound increases significantly under the same cooling rate. The Mn addition was effective to modify the platelet β type Fe compound to more compact Chinese script and/or polyhedral shape α type Fe compound. The amounts these two kinds of α type Fe compounds mainly depends on the Mn/Fe ratio

and the cooling rate at a given Fe content.

3.1 Introduction

Cast Al-Si alloys are widely used in automotive industry due to their excellent properties such as high strength/weight ratio, low cost of recycling and etc. Depending on the purity of the base material, the Al-Si alloys contain various amounts of impurity elements. Fe is always present in aluminum as a dominant impurity. It comes into aluminum from ores, anodic mass, master alloys, as well as from the steel equipment used in melting and casting [1]. In the recycled alloys, for example in the aluminum alloy scraps, the Fe concentration usually is very high. It has been widely accepted that Fe is the most detrimental impurity in cast Al-Si alloys due to the formation of Fe intermetallic compounds, as shown in ternary phase diagram of Al-Si-Fe system in Fig. 3.1 [2]. Fe intermetallic compounds are formed by reacting of Fe with Al and Si during solidification process due to its small solid solubility in the Al matrix [3]. Fe intermetallic compounds are assumed to act as stress raisers and are points of weak bond, causing reduction in mechanical properties, particularly the ductility of cast alloys. The reduction of mechanical properties depends on their amount, size and type. In the Al-Si alloys with high Si content, there are two main Fe compounds with their dominant morphology, the platelet β type Fe compound and the Chinese script α type Fe compound. Among them, β type Fe compound appearing as the platelet shape (needle-like in the 2-D cross-section image), has been identified as the dominant and most detrimental one in Al-Si alloy castings [4-6], as shown in Fig. 3.2 (a). The metallurgically preferable phase is α-$A1_8Fe_2Si$ with the morphology of Chinese script. It performs a less deleterious effect on strength properties than that of platelet β type Fe compound does. These effects are due to its more compact shape and its more diffuse interface with the Al matrix. Chinese script shape presents less of an internal stress concentration than do sharp platelet β type Fe

compound. However, in the Al-Si alloys without modifier, the Fe compounds usually solidify as platelet β type Fe compound instead of Chinese script α type Fe compound. Hence, it is important to control Fe intermetallic compounds by refining their size and by modifying them to the less harmful morphologies.

Mn is most widely used to modify the platelet β type Fe compound to less harmful $Al_{15}(Fe,Mn)_3Si_2$ compound with a Chinese script morphology, which is also confusingly called as α type Fe compound, as shown in Fig. 3.2 (b). Mn addition favors the α-$Al_{15}(Fe,Mn)_3Si_2$ compound to be the dominant one [7,8]. If Fe and Mn contents are sufficiently high, the third kind of Fe compound, which has the similar composition and crystal structure as that of the Chinese script α type Fe compound, also confusingly known as the α type Fe compound but with the polyhedral shape [9,10], as shown in Fig. 3.2 (c). This compound has been thought not to embrittle the alloy, but reduce the machinability and its formation should be avoided [7].

Efforts are made to keep the Fe contents in Al alloys as low as possible. Clearly, the strict requirement for low levels of Fe in the cast aluminum alloys significantly increases costs. So how to improve the mechanical properties of cast aluminum alloys with high Fe content becomes important and necessary. When the Fe compounds are inevitable, the Chinese script α type Fe compound or the small size Fe compounds are preferable [11].

Mn was usually added into the alloy as a modifier to modify the platelet β type Fe compound to the Chinese script α type Fe compound [12]. Although the addition of Mn to Al-Si alloys has been widely investigated and documented, the amount of Mn needed to neutralize Fe has not been well established, especially with the change of the cooling rate [14]. Several researchers have been working to find the critical Fe:Mn ratio, known as the sludge factor or Iron Equivalent Vale (IEV) to avoid the formation of polyhedral shape Fe

compounds [14-18]. The previous works mainly revealed the influences of the Mn and Fe content on the type and size of different Fe compounds [18-20] or the cooling rate on the evolution of different Fe compounds during the modification process separately [21-22]. Still very limited work has reported systematically about the influences of the Fe content, the Mn/Fe ratio and cooling rate on the modification of Fe compounds. This chapter mainly investigate the individually and combined influences of the Mn/Fe ratio and cooling rate on the modification of Fe compounds in cast AA356 based alloys with different Fe contents.

3.2 Experimental procedures

The master alloy Al-7.0mass% Si-0.35mass% Mg was molten in a graphite crucible under an Ar protective atmosphere by an electrical resistance furnace. The nominal compositions of the experimental AA356 based alloys are given in Table 3.1. The iron was added in the form of Fe wire, and Fe contents in each alloy are 1.0wt.%, 1.5wt.%, 2.0wt.% and 2.5wt.%, respectively. Mn was added in the form of the Al-9.93 wt.% Mn. Different Mn contents were added to make sure the Mn/Fe ratio are 0, 0.35, 0.5 and 0.65, respectively at each given Fe content. In the present work, neither grain refiner nor eutectic modifier was added to the melt. Samples are named as x Fe or x Fe + y in the text, where the x represents the Fe content (in mass %) and y represents the Mn/Fe ratio. Each alloy was cast into a stainless steel mold, as shown in Fig. 3.3. The thickness of the mold walls was designed getting thinner gradually from the bottom (60 mm) to the top (40 mm) to get the wedge shape cast. Hence, the different heights of the cast show the different cooling rates. During casting, the thermocouples were set in the center of the mold at different locations of the mold from its bottom (20 mm, 30 mm, 40 mm, 50 mm, 60 mm, 70 mm, 80 mm and 90 mm from the bottom of the mold), to monitor the cooling curves. The average cooling rate at each location was calculated from the beginning to the onset of the eutectic temperature

(around 570^{o}C) in each cooling curve. In addition, the stainless steel cup mold system as shown in Fig. 3.4 was used to generate the low cooling rate. The cup molds at the room temperature were filled by dipping into the melt which was holding at 720 ˚C, temporarily immersing it to attain thermal equilibrium with the melt. The molds with their liquid metal were then removed from the melt and solidified in air. The K-type thermocouples were located in the central areas of the cup molds to monitor the cooling curves during air cooling just after taking out the cup molds from the molten alloys. The calculated cooling rates based on the cooling curves obtained by two kinds of molds during casting were showed in Fig. 3.5.

Microstructures of the alloys were studied by an optical microscope (OM). Electron probe micro-analyzer (EPMA) was utilized to measure the elements distribution inside the Fe intermetallic compounds and WDS was conducted to measure the composition of Fe intermetallic compounds. Samples for the microstructural analysis were prepared by standard techniques with the final polishing stage using the 0.05 μm colloidal silica.

3.3 Results

3.3.1 Identification of Fe intermetallic compounds in the present work

Basically, the different Fe compounds in cast Al-Si alloys have their dominant morphologies, e.g. the β type Fe compound appeared as platelet and α type Fe compound appeared as Chinese script or polyhedral shape. This is the easy and typical way to identify the different Fe compounds in Al-Si alloys. Hence, it is necessary to make sure that this method is correct or incorrect in the whole work. The EPMA and WDS were used in this work to analysis the compositions of Fe compounds with different morphologies. The results were showed in Fig. 3.7, Fig. 3.8, Table 3.2 and 3.3. The locations conducted WDS analyses were marked by solid red circles in the BEI images in each Fe compound. Based

on the EPMA and WDS analysis results, it is clear that in this work, it is correct to identify the different Fe compounds by their characteristic morphologies.

3.3.2 Effect of Fe content

Microstructures of the alloys with different Fe contents at the low cooling rate (3.6K/s, 90 mm) were showed in Fig. 3.9. The size of the platelet β type Fe compound particles significantly increases with increasing the Fe content. The larger size platelet β type Fe compound particles marked by the arrows in Fig. 3.9 (d) and (e) demonstrated that with increasing the Fe content, the β type Fe compound crystallized at higher temperature, before the crystallization temperature of α-Al phase. Longer growth time made the size of the β type compound much larger.

3.3.3 Effect of Mn/Fe ratio

The addition of Mn can modify the platelet β type Fe compound to α type Fe compound which appeared as both Chinese script and polyhedral shape, as shown in Fig. 3.10. In the alloy with both low Fe content and low Mn/Fe ratio, the alloy 1.0 Fe + 0.35, almost all of the Fe compounds appeared as the platelet shape, as shown in Fig. 3.10 (a). With increasing the Mn/Fe ratio, some of the platelet shape β type Fe compounds were modified to the Chinese script α type Fe compounds, marked by arrows in Fig. 3.10 (b). When the Mn/Fe ratio reached up to 0.65, most of the platelet β type Fe compounds were modified to Chinese script Fe compounds, as shown in Fig.3.10 (c). However, still some platelet β type Fe compounds existed, as shown in Fig.3.10 (c) marked by arrows.

By increasing the Fe content from 1.0wt.% to 1.5wt.% with the Mn/Fe ratio of 0.35, most of the Fe compounds were modified to the Chinese script α type Fe compounds, as shown in Fig.3.10 (d). With increasing the Mn/Fe ratio to 0.5, all the Fe compounds appeared as α type with morphologies of both Chinese script and polyhedral shape, as

shown in Fig. 3.10 (e). With increasing the Mn/Fe ratio to 0.65, the amounts of polyhedral shape Fe compounds increased, as shown in Fig. 3.10 (f).

In the alloy 2.0 Fe + 0.35, Fe compounds appeared as platelet, Chinese script and polyhedral shape, as shown in Fig. 3.10 (g). With increasing the Mn/Fe ratio to 0.5 at this Fe content, almost all the platelet β type Fe compounds were replaced by α type Fe compounds. The amounts of the polyhedral shape α type Fe compounds greatly increased, as shown in Fig. 3.10 (h). When the Mn/Fe ratio was increased to 0.65, most of the Fe compounds became as the polyhedral shape, as shown in Fig. 3.10 (i).

When the Fe content was 2.5wt.%, the modification of the Fe compounds by Mn addition showed the similar tendency as that of the alloys with 2.0wt.% Fe and different Mn/Fe ratio, as shown in Fig. 3.10 (j)-(l). The difference is that at the same Mn/Fe ratio, the amounts of the polyhedral shape α type Fe compounds increased.

3.3.4 Effect of cooling rate

Microstructures of the alloys with different Fe contents at different cooling rates were showed in Fig. 3.11. In the alloy without Mn addition, all the Fe compounds appeared in the form of platelet shape, as shown in Fig. 3.11. Changing the cooling rate can not modify the Fe compound in the type. However, the size of the Fe compounds was refined by high cooling rate significantly. With increasing the cooling rate from 0.67˚C/s to 17.3˚C/s, the size of the β type Fe compounds was refined from the large one to the small one, regardless of the Fe content.

In the alloy 1.0 Fe + 0.35, with increasing the cooling rate, Fe compounds tended to solidified as platelet instead of Chinese script, as shown in Fig. 3.12 (a)-(d). In the alloy 1.0 Fe + 0.5 and 1.0 Fe + 0.65, with increasing the cooling rate, the amounts of platelet Fe compounds increased, as shown in Fig. 3.12 (e)-(l). Moreover, at the same cooling rate,

more Mn addition (large Mn/Fe ratio) can make more Fe compounds solidify as Chinese script instead of platelet Fe compounds.

In the alloy 2.5 Fe + 0.35, with increasing the cooling rate from 0.67˚C/s to 17.3˚C/s, Fe compounds solidified as platelet and Chinese script. High cooling rate restricted the formation of polyhedral shape Fe compound, as shown in Fig. 3.13 (a)-(d). In the alloy 2.5 Fe + 0.5 and 2.5 Fe + 0.65, with increasing the cooling rate, Fe compounds solidified as Chinese script and small polyhedral shape instead of large size polyhedral shape, as shown in Fig. 3.13 (e)-(k). With increasing the cooling rate, the size of Fe compounds decreased. Also, the Chinese script α type Fe compound is preferentially formed, comparing with the formation of polyhedral shape Fe compound.

It is indicted that the high cooling rate favored the formation of the platelet β type Fe compound instead of Chinese script Fe compound in the alloys with low Fe content and different Mn/Fe ratio. In addition, high cooling rate can restrict the formation of the polyhedral shape Fe compound in the alloy with the high Fe content and high Mn/Fe ratio.

3.4 Discussion

The platelet β type Fe compound is known as very detrimental to the mechanical properties of cast Al-Si alloys, especially ductility. The high Fe content tends to cause the larger size platelet β type Fe compound rather than increasing its number density, as shown in Fig. 3.9. This larger size platelet β type Fe compound, which is believed to be more detrimental, is considered to be formed earlier and hence more unconstrained growth occurs. The Fe content is the main factor that influences the morphology of the Fe compounds in cast Al-Si alloys. Increasing the cooling rate can restrict the growth of the larger size Fe compounds and other phases, which is beneficial to the mechanical properties of alloys.

The addition of Mn results in the modification of the morphology and type of intermetallic compounds from platelet β type Fe compound to Chinese script and/or polyhedral shape α type Fe compounds. Couture revealed that if the iron content exceeded 0.45 mass %, the Mn content should not be less than the half of the Fe content to modify all of the platelet β type Fe compounds [14]. However, in this work, this ratio was greatly affected by both the Fe content and cooling rate.

At the low Fe content, the high Mn/Fe ratio and low cooling rate favor the formation of the Chinese script α type Fe compound, as shown in Fig. 3.12 (i) and (j). Decreasing the Mn/Fe ratio and increasing the cooling rate result in the amounts increase of platelet β type Fe compounds, as shown in Fig. 3.12 (a), (b), (k) and (l). On the other hand, at the high Fe content, high Mn/Fe ratio and low cooling rate favor the formation of the polyhedral shape α type Fe compound, as shown in Fig. 3.13 (e) and (i). Decreasing Mn/Fe ratio and increasing cooling rate result in the amounts decrease of polyhedral shape α type Fe compounds accompanied by the amounts increase of Chinese script α type Fe compounds, as shown in Fig. 3.13 (a), (d), (h) and (k).

Therefore, in order to modify the platelet β type Fe compound to Chinese script α type Fe compound and to avoid the formation of the polyhedral shape α type Fe compound, the critical Mn/Fe ratio and cooling rate should be mainly considered at a given Fe content. In the alloy with 1.0wt.% Fe, the Mn/Fe ratio of 0.65 is a little bit large at the cooling rate of 0.67˚C/s. At the cooling rate of 3.6˚C/s, the Mn/Fe ratio should be larger than 0.65 to modify the remained platelet β type Fe compound at the cooling rate of 3.6˚C/s, as shown in Fig.3.12 (i) and (j). If increasing the cooling rate at this Fe content, to modify all the platelet Fe compounds to Chinese script Fe compounds, the Mn/Fe ratio should be much larger, as shown in Fig.3.12 (k) and (l). In the alloys with 2.5wt.% Fe, it is difficult to modify all the

Fe compounds appeared Chinese script without solidifying as both platelet and polyhedral shape by alerting the Mn/Fe ratio and cooling rate, as shown in Fig. 3.13. From the microstructures, the high cooling rate can refine the size of Fe compound. The Mn/Fe ratio of 0.5 at high cooling rate is beneficial to obtain the better morphology in which the Fe compounds appeared as Chinese script and small size polyhedral, without platelet Fe compound, as shown in Fig. 3.13 (h).

Additionally, most of Fe compounds appeared as platelet shape at the low Fe content with high Mn/Fe ratio and as Chinese script shape at the high Fe content with high Mn/Fe at high cooling rate, as shown in Fig.3.12 (l) and Fig. 3.13 (k). It is considered that the platelet β type Fe compound can solidify earlier than Chinese script α type Fe compound. The formation of the polyhedral shape Fe compound mainly came from the growth of the Chinese script Fe compound. This phenomenon will be explained in Chapter 3.

3.5 Conclusions

The influence of Fe content, Mn/Fe ratio and cooling rate on the modification process of Fe intermetallic compounds in cast AA356 based alloys was investigated. The results can be drawn as follows:

1. Fe content greatly influences the size of the platelet β type Fe compound in the alloys without Mn addition. The size of the β type Fe compound increases significantly with increasing the Fe content.

2. Mn addition was effective to modify platelet β type Fe compound to more compact compounds, Chinese script and/or polyhedral shape α type Fe compound. The ratio of these different Fe compounds was greatly affected by the Mn/Fe ratio and the cooling rate at a given Fe content.

3. At high cooling rate, in the alloy with low Fe content and high Mn/Fe ratio and high Fe content and high Mn/Fe ratio, Fe compounds mainly appeared as platelet shape and Chinese script separately. It is indicated that the platelet β type Fe compound can solidify earlier than Chinese script α type Fe compound. The formation of the polyhedral shape Fe compound mainly came from the growth of the Chinese script Fe compound.

References

[1] N. A. Below, A. A. Aksenov and D. G. Eskin：*Iron in aluminum alloys*, (Taylor & Francis Inc, New York, 2002) pp. 1-7.

[2] G. Effenberg and S. Ilyenko: *Landolt-Börnstein, Ternary Alloy Systems Phase Diagrams, Crystallographic and Thermodynamic Data, Subvol. D, Part 1, Springer-Verlag Berlin, Heidelberg*, (2008) pp.53-54.

[3] L. Wang, D. Apelian and M.M. Makhlouf: AFS Transactions, 146 (1999) 231-238.

[4] L. Backerud, G. Chai and J. Tamminen: *Solidification Characteristics of Aluminium Alloys*, Foundry Alloys Vol. 2 (AFS/Skanaluminum,1990) pp. 71-84.

[5] S. Shivkumar, L. Wang and D. Apelian: JOM 43 (1991) 26-32.

[6] P. Ashtari, H. Tezuka and T. Sato: Scr. Mater. 51 (2004) 43-46.

[7] L.F. Mondolfo: *Aluminum Alloys: Structure and Properties*, (Butterworths, London, 1976), 661-663.

[8] M.V. Kral: Mater. Lett, 59 (2005) 2271-2276.

[9] X.J. Cao and J. Campbell: Int. J. Cast Met. Res. 13 (2000) 175-184.

[10] X.J. Cao and J. Campbell: *Shape Casting: The John Campbell Symposium*, ed. by M. Tiryakiogly and P. N. Crepeau, (The Minerals, Metals & Materials Society, 2005) pp. 255–262.

[11] S. Seifeddine and I. L. Svensson: Metall. Sci. and Technol. 27-1 (2009) 11-20.

[12] P. Ashtari, H. Tezuka and T. Sato: Mater. Trans. 44-12 (2003) 2611-2616.

[13] P. N. Crepeau: AFS Trans. 103 (1995) 361-366.

[14] A. Couture: AFS Int. Casting Metals J. 6 (1981) 9-17.

[15] Y. Osame, K. Toyoda, Y. Tsumura, M. Suzuki, S. Furuya and K. Nagayama: J. Jpn. Inst. Light Met., **36** (1986) 813-818.

[16] A.N. Lakshmannan, S.G. Shabestari, J.E. Gruzleski and Z. Metallkd, **86** (1995) 457-464.

[17] X.J. Cao, N. Saunders and J. Campbell: J. Mat. Sci., **39** (2004) 2303-2014.

[18] S.G. Shabestari: Mater. Sci. Eng. A. 383 (2004) 289-298.

[19] J.Y. Hwang, H.W. Doty and M.J. Kaufman: Mater. Sci. Eng. A. 488 (2008) 496-504.

[20] C.M. Dinnis, J.A. Tayor and A.K. Dahle: Metall. Mater. Trans. A. 37A (2006) 3283-3291.

[21] B. Dutta and M. Rettenmayr: Mater. Sci. Eng. A. 283 (2000) 218-224.

[22] Y.H Zhang, Y.C. Liu, Y.J. Han, C.Wei and Z.M. Gao: J. Alloys Compd. 473 (2009) 442-445.

Table 3.1 Nominal compositions of cas AA356 based alloys with different Fe and Mn contents. The Mn/Fe ratios in each set are 0, 0.35, 0.5 and 0.65 respectively. The samples are named as x Fe or x Fe+ y in the text, where the x represents the Fe content (in mass %) and y represents the Mn/Fe ratio.

Alloys	Elements (mass %)					Mn/Fe ratio
	Al	Si	Mg	Fe	Mn	
Set 1	Bal.	7.00	0.35	-	-	-
Set 2	Bal.	7.00	0.35	1.0	0, 0.35, 0.5, 0.65	0, 0.35, 0.5 0.65
Set 3	Bal.	7.00	0.35	1.5	0, 0.525, 0.75, 0.975	0, 0.35, 0.5, 0.65
Set 4	Bal.	7.00	0.35	2.0	0, 0.7, 1.0, 1.3	0, 0.35, 0.5, 0.65
Set 5	Bal.	7.00	0.35	2.5	0, 0.875, 1.25, 1.625	0, 0.35, 0.5, 0.65

Table 3.2 WDS quantitative analysis of Fe intermetallic compounds in the alloy 2.5 Fe + 0.35 at the cooling rate of 3.6˚C/s.

Shape of Fe intermetallic compounds	Al	Si	Fe	Mn	(Fe+Mn)/Si	Total
	wt.%	wt.%	wt.%	wt.%	atomic ratio	wt.%
Platelet	58.25	16.09	23.92	1.74	1/1.25	100.00
Chinese script	64.70	10.18	18.53	6.59	1/0.80	100.00
Polyhedral shape	60.80	10.98	19.25	8.97	1/0.77	100.00

Table 3.3 WDS quantitative analysis of Fe intermetallic compounds in the alloy 2.5 Fe at the cooling rate of 17.3˚C/s.

Shape of Fe intermetallic compounds	Al	Si	Fe	Mn	(Fe+Mn)/Si	Total
	wt.%	wt.%	wt.%	wt.%	atomic ratio	wt.%
Platelet 1	73.71	10.80	15.37	0.10	1/1.39	100.00
Platelet 2	68.67	15.06	22.89	0.05	1/1.31	100.00

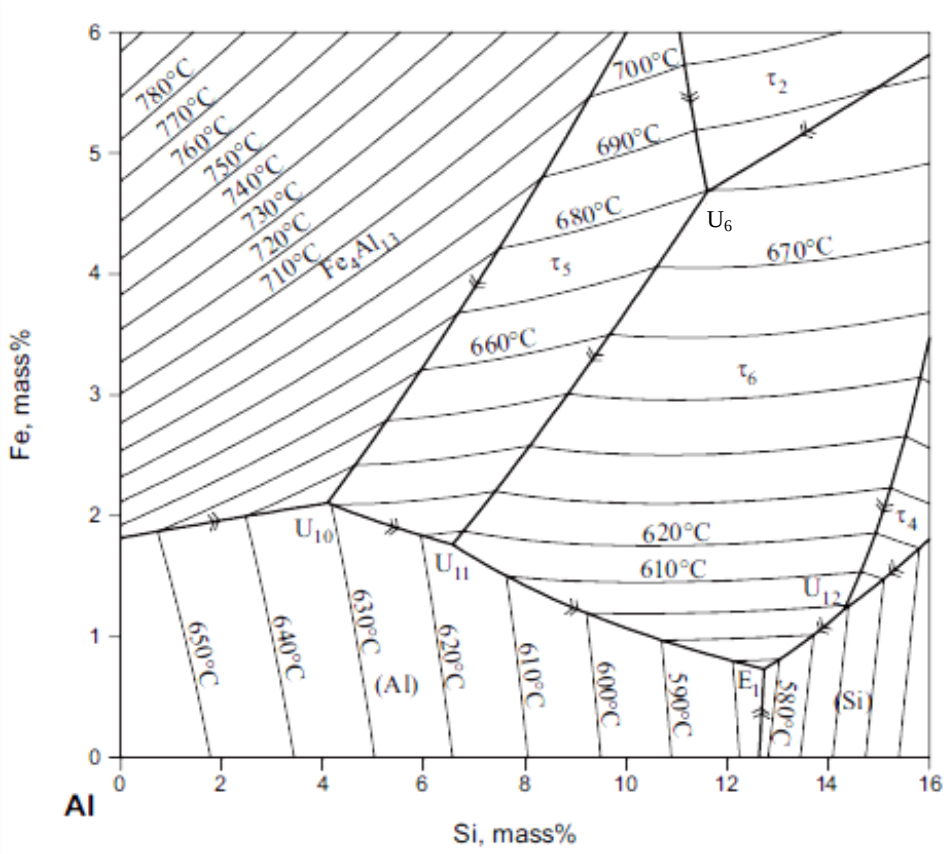

Fig. 3.1 Calculated liquidus surface of the Al-Fe-Si ternary phase diagram [2], where τ4 represents δ–Al_3FeSi_2, τ5 represents α-Al_8Fe_2Si and τ6 represents β–Al_5FeSi, respectively. Fe_4Al_3 also was confusedly named as θ–Al_3Fe.

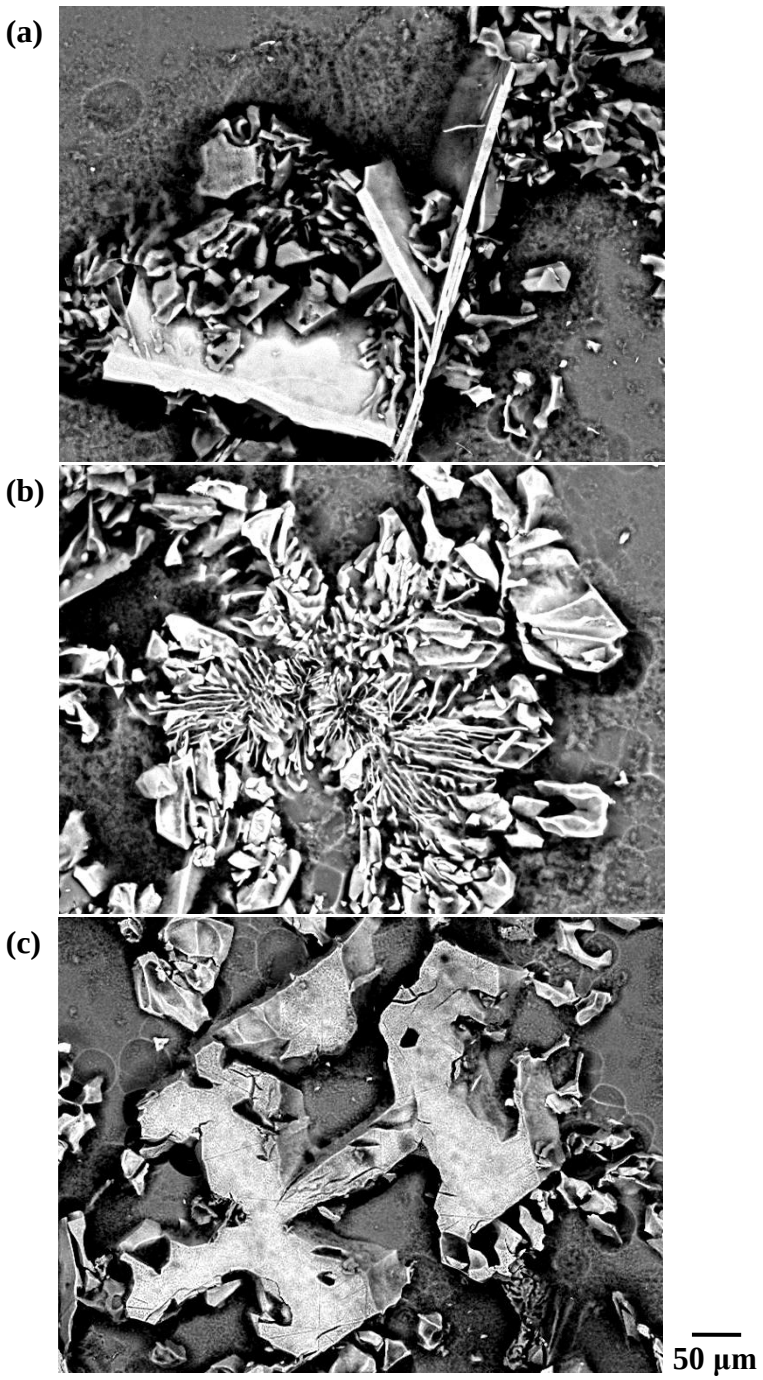

Fig. 3.2 Morphology of different Fe compounds after deep etching: (a) platelet β type Fe compound, (b) Chinese script α type Fe compound, (c) polyhedral shape α type Fe compound.

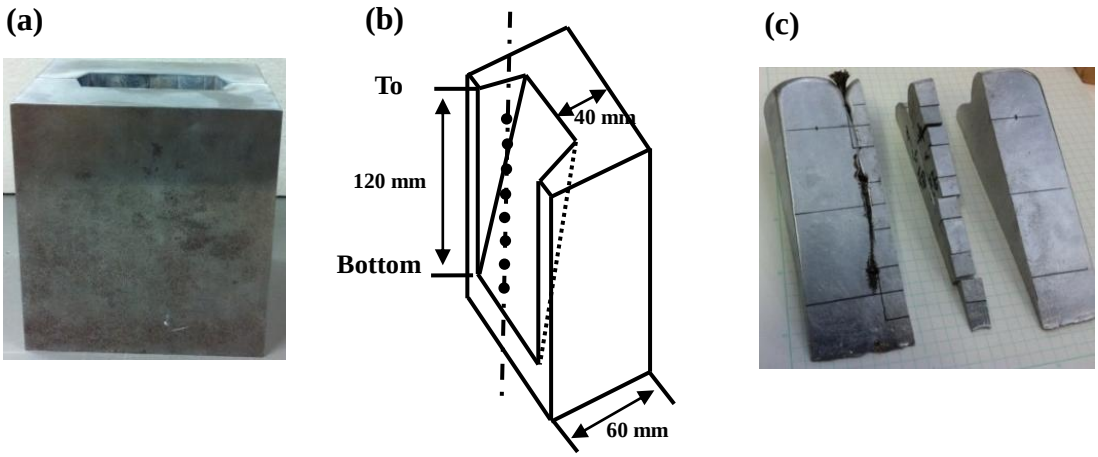

Fig. 3.3 The stainless steel mold for casting (a) and its half schematic drawing (b). The locations of the thermocouples during casting were marked by solid circles. They are 20mm, 30mm, 40mm, 50mm, 60mm, 70mm, 80mm and 90mm from the bottom of the mold. The wedge-shaped specimen obtained by this mold (c).

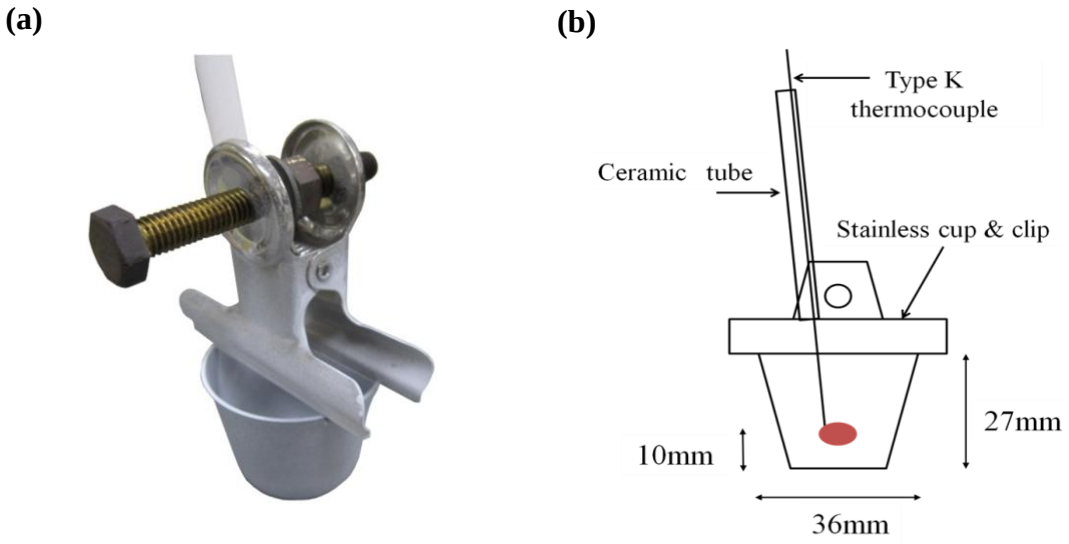

Fig. 3.4 The stainless cup mold system used to generate the low cooling rate.

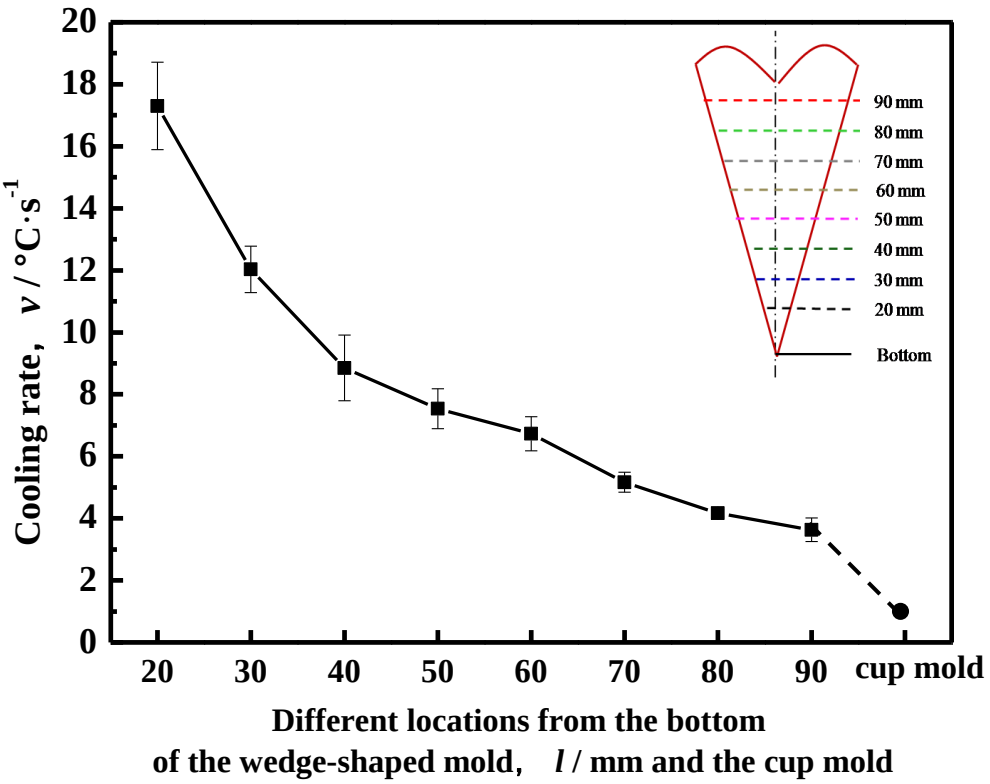

Fig. 3.5 Values of the cooling rates are averaged for the alloys with different Fe contents and no Mn addition.

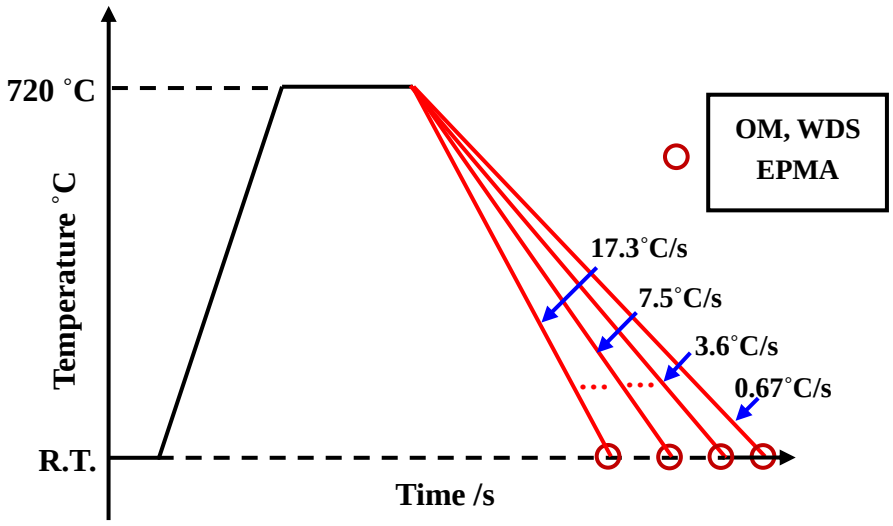

Fig. 3.6 Schematic illustration of the casting process utilized the wedge-shape mold and the stainless steel cup mold.

(a) Platelet

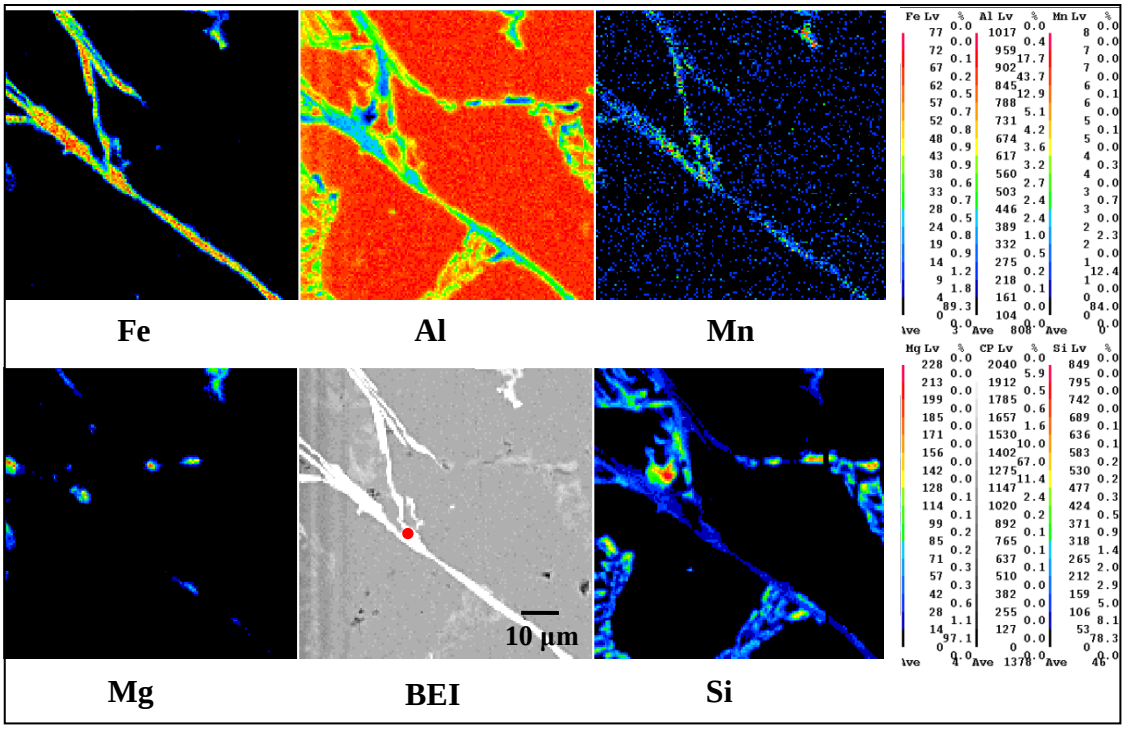

(b) Chinese script

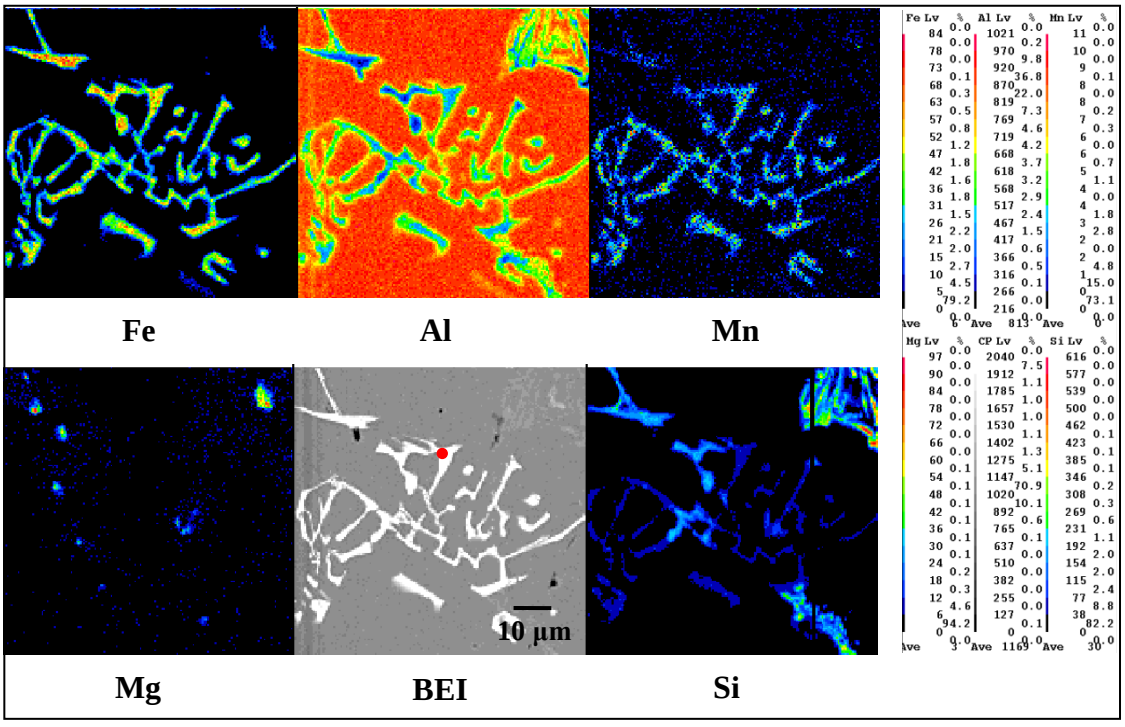

(c) Polyhedral shape

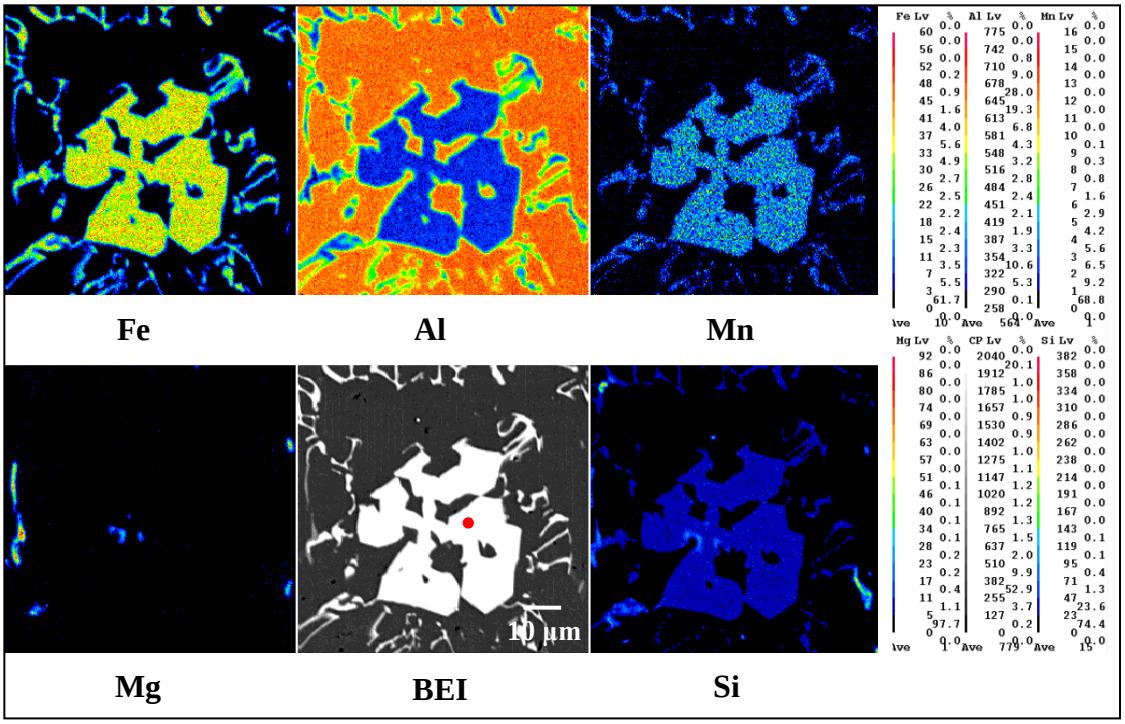

Fig. 3.7 Chemical composition analysis by EPMA color mapping of the (a) platelet Fe compound, (b) Chinese script Fe compound and (c) polyhedral shape Fe compound in the alloy 2.5 Fe + 0.35 at the cooling rate of 3.6˚C/s. The locations to make the WDS analysis were marked by red solid circles in the BEI images.

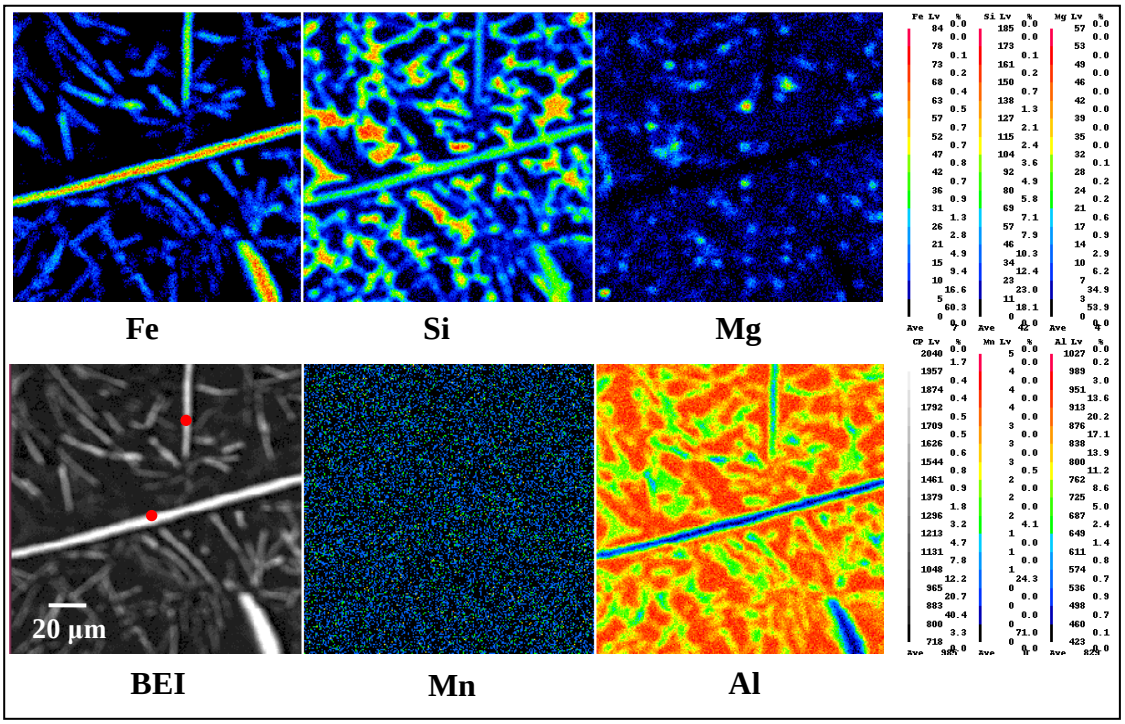

Fig. 3.8 Chemical composition analysis by EPMA color mapping of platelet Fe compounds in the alloy 2.5 Fe at the cooling rate of 17.3˚C/s. The locations to make the WDS analysis was marked by red solid circle in the BEI image.

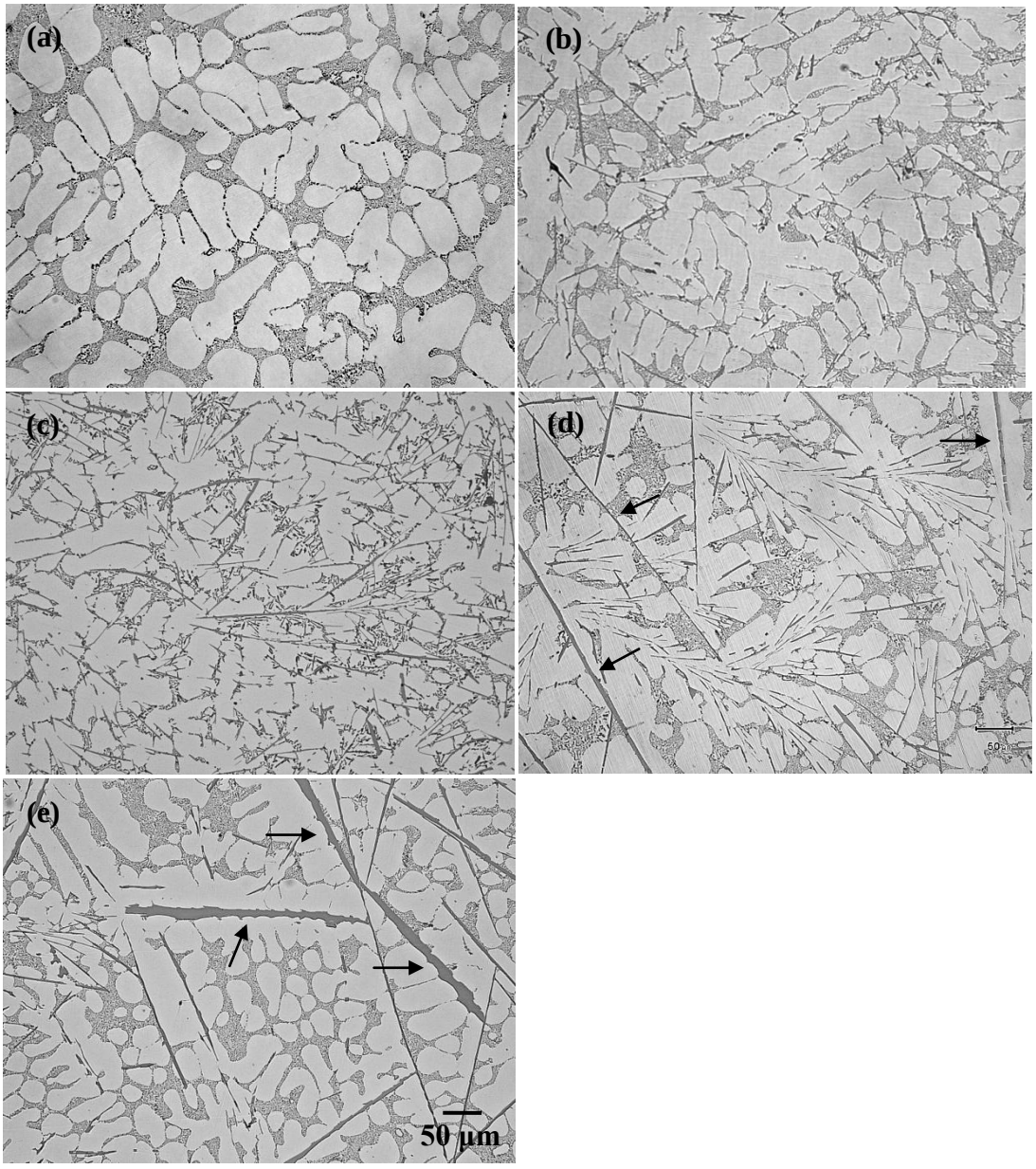

Fig. 3.9 Microstructures of the alloys with different Fe contents at the cooling rate of 3.6˚C/s from the bottom of the mold: (a) Fe-free, (b) 1.0 Fe, (c) 1.5 Fe, (d) 2.0 Fe. (e) 2.5Fe. The large size platelet β type Fe compound particles are indicated by the arrows.

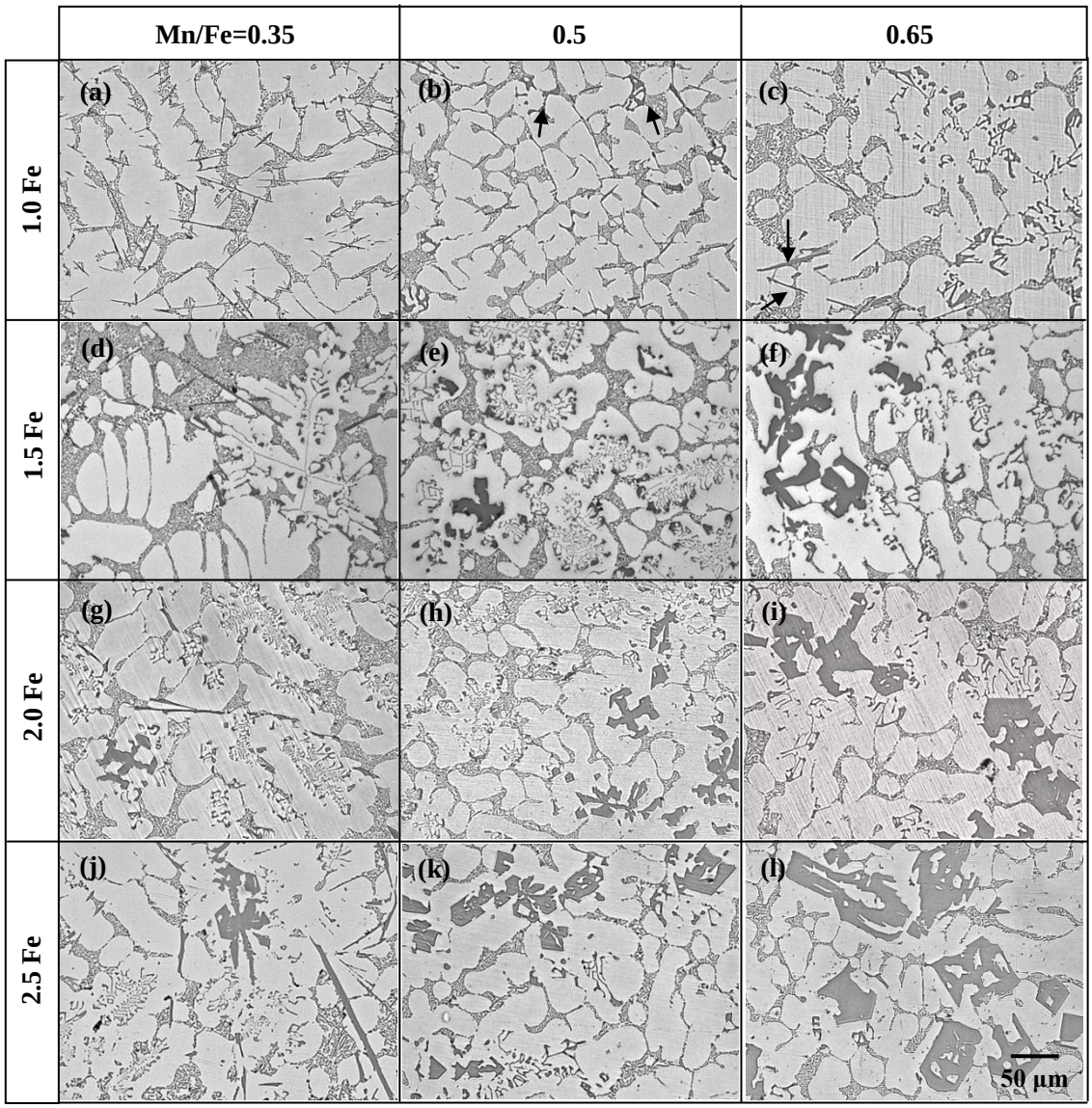

Fig. 3.10 Microstructures of the alloys with different Fe contents and Mn/Fe ratios at the cooling rate of 3.6˚C/s: (a) 1.0 Fe + 0.35 (b) 1.0 Fe + 0.5 (c) 1.0 Fe + 0.65 (d) 1.5 Fe + 0.35 (e) 1.5 Fe + 0.5 (f) 1.5 Fe + 0.65 (g) 2.0 Fe + 0.35 (h) 2.0 Fe + 0.5 (i) 2.0 Fe + 0.65 (j) 2.5 Fe + 0.35 (k) 2.5 Fe + 0.55 (l) 2.5 Fe + 0.65. Arrows in the images indicated the appearance of platelet Fe compound.

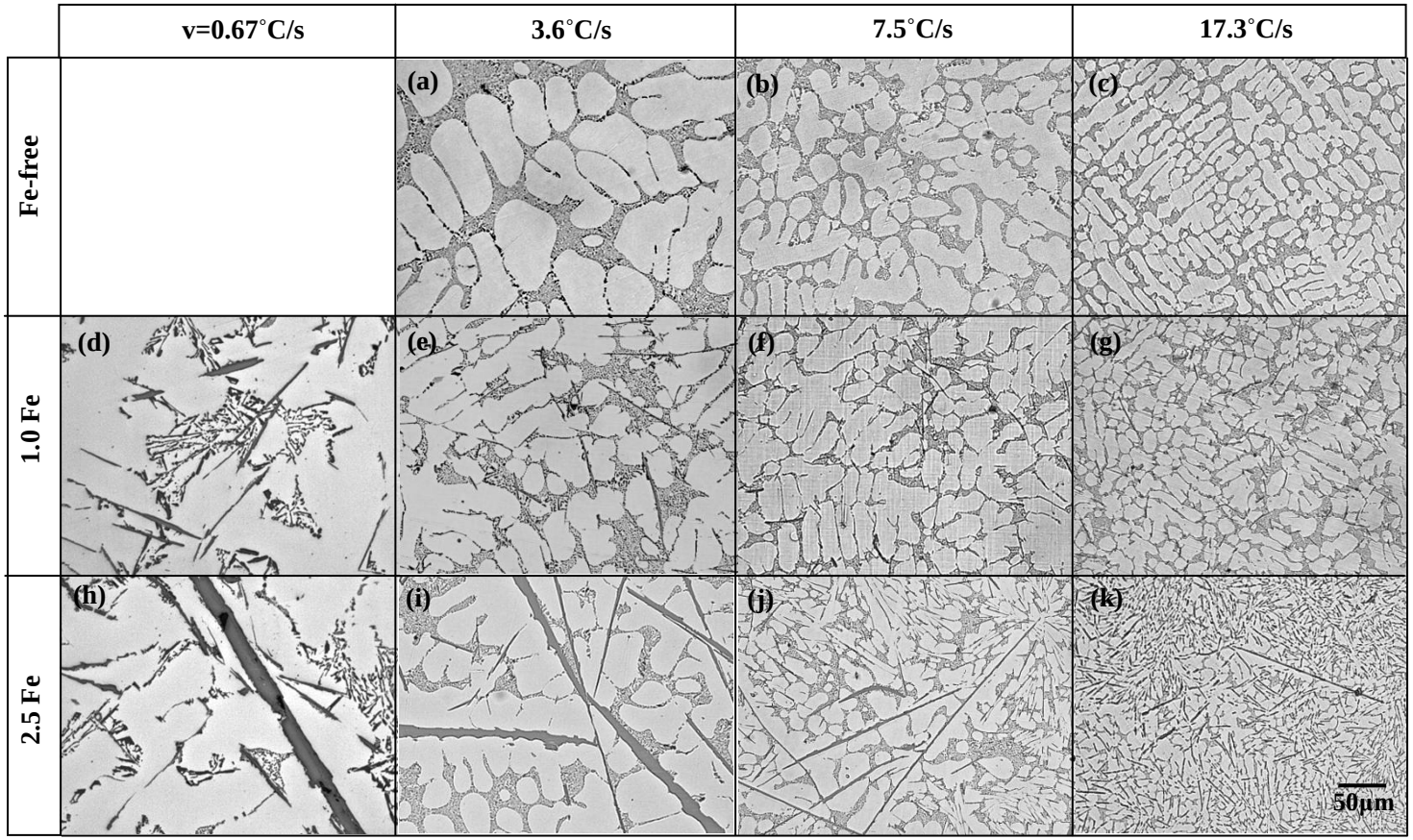

Fig. 3.11 Microstructures of the alloys with different Fe contents at different cooling rates, Fe-free: (a) 3.6˚C/s, (b) 7.5˚C/s, (c) 17.3˚C/s; 1.0 Fe: (d) 0.67˚C/s, (e) 3.6˚C/s, (f) 7.5˚C/s, (g) 17.3˚C/s; 2.5 Fe: (h) 0.67˚C/s, (i) 3.6˚C/s, (j) 7.5˚C/s, (k) 17.3˚C/s.

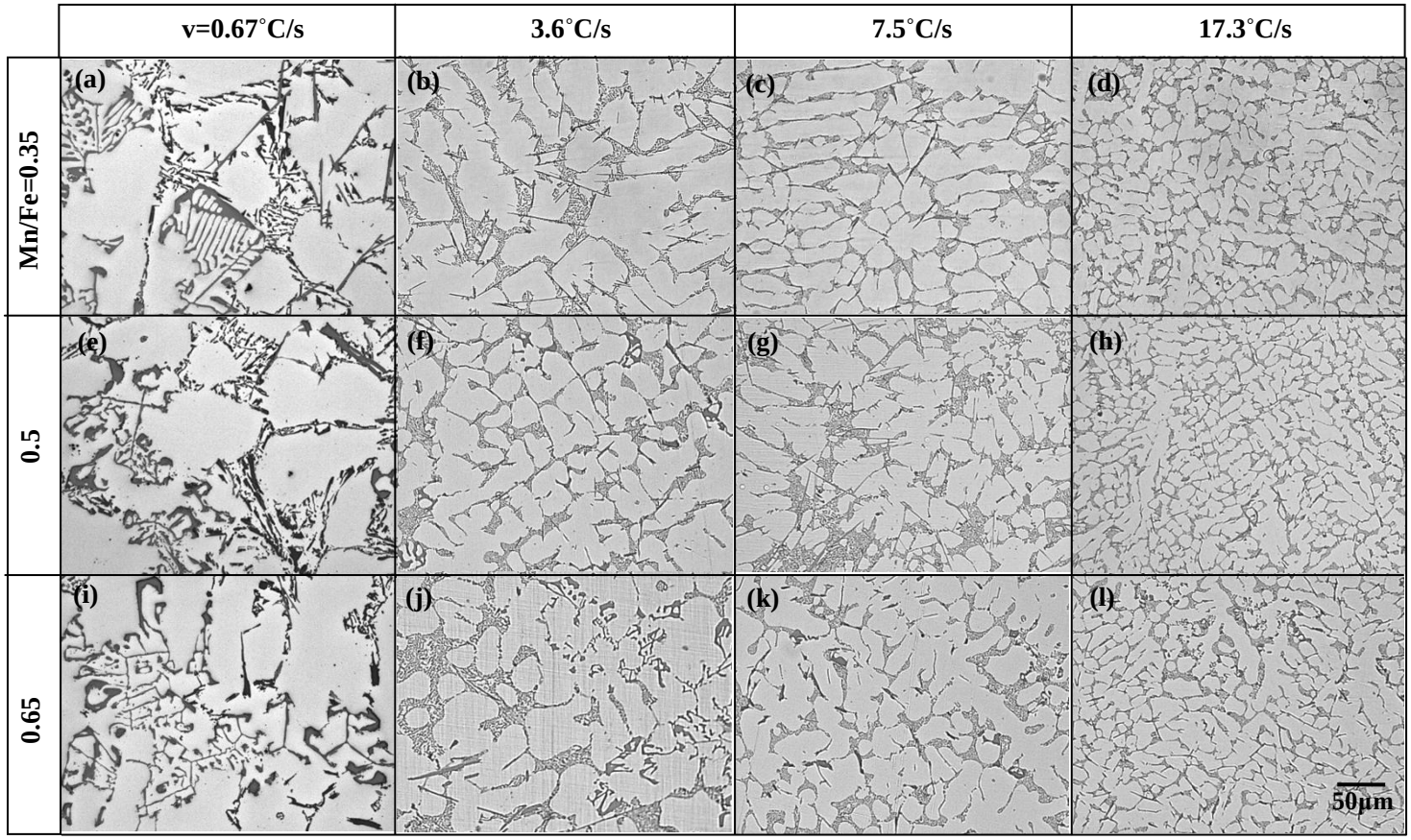

Fig. 3.12 Microstructures of the alloys with 1.0wt.% Fe and different Mn/Fe ratios at different cooling rates, 1.0Fe + 0.35: (a) 0.67˚C/s, (b)3.6˚C/s, (c) 7.5˚C/s, (d) 17.3˚C/s; 1.0 Fe + 0.5: (e) 0.67˚C/s, (f) 3.6˚C/s, (g) 7.5˚C/s, (h) 17.3˚C/s; 1.0 Fe + 0.65: (i) 0.67˚C/s, (j) 3.6˚C/s, (k) 7.5˚C/s, (l) 17.3˚C/s.

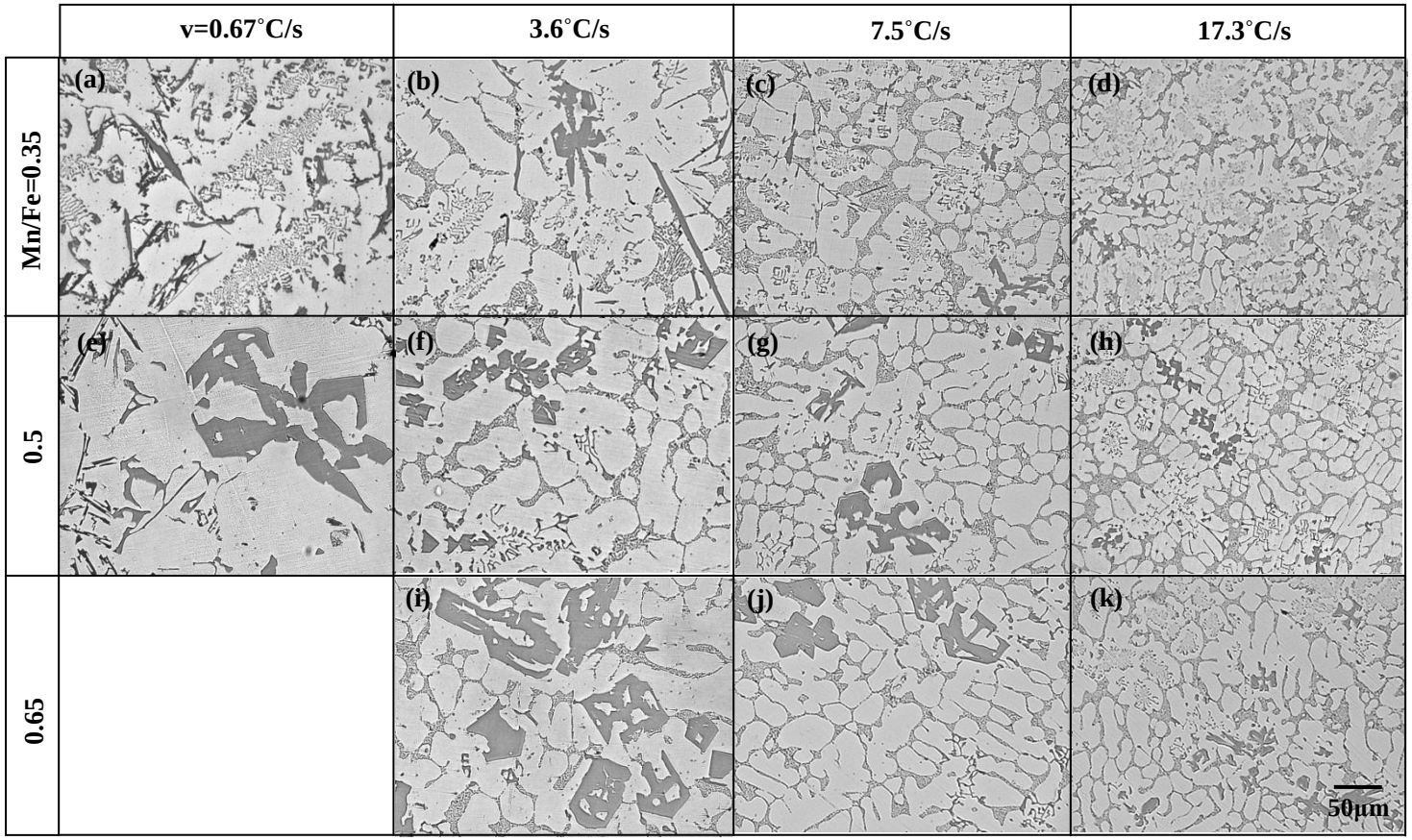

Fig. 3.13 Microstructures of the alloys with 2.5wt.% Fe and different Mn/Fe ratios at different cooling rates, 2.5Fe + 0.35: (a) 0.67˚C/s, (b)3.6˚C/s, (c) 7.5˚C/s, (d) 17.3˚C/s; 2.5 Fe + 0.5: (e) 0.67˚C/s, (f) 3.6˚C/s, (g) 7.5˚C/s, (h) 17.3˚C/s; 2.5 Fe + 0.65: (i) 3.6˚C/s, (j) 7.5˚C/s, (k) 17.3˚C/s.

Chapter 4

Evolution of Fe intermetallic compounds during solidification in cast AA356 based alloys with different Fe content and Mn/Fe ratio

Mn addition showed very effective influence on the modification of the platelet β type Fe compound to the less harmful Chinese script α type Fe compound, although sometimes it was over-modified to the polyhedral shape α type Fe compound, especially when the Fe and Mn concentrations were relative high. In order to control this modification process well to make the Fe compounds solidify as the Chinese script α type Fe compound, it is very important and essential to get the deep understanding about the evolution of Fe compounds in the modification process during solidification.

In this chapter, the evolution of Fe compounds during solidification was revealed by the quenching experiment. The comparing quenching experiments under different situation were conducted to reach this target. The results indicated that in the alloys without Mn addition, the Fe compounds only appeared as a platelet shape. In the alloys with low Fe content and low Mn addition, the Fe compound crystallized as the platelet β type compound at the beginning of the solidification. With the solidification proceeding, the Chinese script α type Fe compound became the dominant one. More Mn addition in the alloys with both the low and high Fe content, part of the Fe compound crystallized as the Chinese script at the

beginning of the solidification as well as the platelet shape. With the solidification proceeding, the growth of the Chinese script Fe compound accompanied by the decrease of the platelet β type Fe compound. In the alloy with high content Fe and high Mn addition, Fe compounds also can appear as the polyhedral shape. The formation of polyhedral shape α type Fe compound mainly came from two aspects, crystallized as the primary phase and the growth of Chinese script α type Fe compound. The ratio of these two parts of compounds mainly depends on the composition and cooling rate.

4.1 Introduction

The recycled aluminum alloys has many advantages such as low energy consumption of only 3-5% compared with the primary aluminum production [1]. However, the challenge for using the recycled aluminum alloys is that in the recycled alloys, the impurities concentrations are usually very high. Among them, the iron impurity content is one of the main factors to evaluate the property and determine the level of the prices of final product in cast Al-Si alloys. The Fe intermetallic compounds formed during solidification in cast Al-Si alloys degrade the mechanical properties and formability of the alloys, especially the platelet β type Fe compound. Its sharp shape and weak interface to the Al matrix can result in crack initiation and propagation [2].

Hence, efforts are made to keep the Fe concentrations in cast Al-Si alloys as low as possible. However, there is no known way to economically remove Fe from aluminum or its alloys so far. When the Fe is inevitable, how to decrease the damage influence of Fe impurity on the mechanical properties of cast Al-Si is very essential, especially when the Fe content is high.

As introduced in the former chapters, it is clear that in order to improve the mechanical properties of cast Al-Si alloys with Fe impurity, making the Fe compounds solidify as the

Chinese script α type Fe compound is a very effective way instead of the platelet β type Fe compound [4-6]. In Chapter 3, the formation of the platelet β type Fe compound can be restricted well by alerting the Mn/Fe ratio and cooling rate in a given Fe concentration. However, about the evolution of the Fe compounds during this modification process is still unclear. Very limited work reported this field, and still not unified conclusion has been conducted.

In this chapter, the quenching experiment was conducted to investigate the evolution of Fe compounds during solidification in the modification process from the platelet β type compound to the less harmful Chinese script α type Fe compound. In the industrial production process, to control Mn addition is a much easier way than introducing the higher cooling rate. Therefore, in this chapter the quenching experiments were prepared at low cooling rates to reveal the evolution of Fe compounds during solidification. On this basis, the solidification sequence of the AA356 based alloys with different Fe content and Mn/Fe ratio were discussed.

4.2 Experimental procedures

Some results obtained in Chapter 3 will be utilized in this chapter. Hence, the experimental procedures and chemical compositions of alloys used are the same as that introduced in Chapter 3. The chemical compositions of the experimental AA356 based alloys used in this study are given in Table 4.1. The manufacture process for the master alloy Al-7.0wt.% Si-0.35wt.% Mg was the same as that described in Chapter 3. The samples with different compositions are named as x Fe or x Fe+ y in the text, where the x represents the Fe content (in mass %) and y represents the Mn/Fe ratio. The alloys were remelted using an electrical resistance furnace and conducted water-quenching experiments. The stainless steel cup molds coated with a thin layer of boron nitride were used for quenching

experiments, as shown in Fig.4.1 (a) and (b). In order to get more detailed information about the evolution of the Fe compounds, two sets of the comparative quenching experiments were performed. The quenching experimental procedures were showed in Fig. 4.2 (a) and (b).

In the set 1, the cup molds at the room temperature were filled by dipping into the melt which was holding at 720 ˚C, temporarily immersing it to attain thermal equilibrium with the melt. The molds with their liquid metal were then removed from the melt and solidified in air. The K-type thermocouples were located in the central areas of the cup molds to monitor the cooling curves during air cooling just after taking out the cup molds from the molten alloys. The cooling rate of this kind of cup mold under this situation during air cooling is 0.59 ˚C /s, as shown in Fig. 4.3 (a). The onset of the air cooling was counted from the time taking out the cup molds from the melt. For each alloy composition, four interrupted water-quenched experiments were carried out at 5 s, 20 s, 50 s and 180 s timing from the start of the air cooling, where each time represented the special solidification stage. The air cooling time used in the following text represents the period between onset of the air cooling and the water-quenched time.

In the set 2, before dipping into the melt, the cup molds were kept in another furnace which temperature was 720 ˚C for 2 minutes to get the thermal equilibrium. The cup molds were then dipped into the melt keeping around 5s to attain thermal equilibrium. The molds with their liquid metal were removed from the melt and solidified in air. The K-type thermocouples were located in the central areas of the cup molds to monitor the cooling curves during air cooling just after taking out the cup molds from the molten alloys, as shown in Fig. 4.1 The cooling rate of this kind of cup mold under this situation during air cooling is 0.67 ˚C /s, as shown in Fig. 4.3 (b). The onset of the air cooling was counted from

the time taking out the cup molds from the melt. For each alloy composition, four or five interrupted water-quenched experiments were carried out at different stage of the solidification, where the temperature were 660 ˚C, 620 ˚C, crystallized temperature of α-Al phase, 580 ˚C and eutectic temperature, respectively, as shown in Fig. 4.7 (a), Fig. 4.8 (a), Fig. 4.9 (a), Fig. 4.10 (a), Fig. 4.11 (a), Fig. 4.12 (a), Fig. 4.13 (a) and Fig. 4.14 (a). The corresponding air cooling times to the temperatures in different alloys were a little bit different depending on the different compositions. Onset of the air cooling was counted from the time taking out the cup molds from the melt. After such the air cooling time, the cup mold with its melt was immediately moved into another furnace where the temperature was set as the corresponding temperature to the air cooling time in each alloy for holding 60 minutes. The cup mold with its melt was quenched into the water at the room temperature.

Microstructures of the alloys were studied by an optical microscope (OM). Chemical analysis of different Fe compounds was performed by an energy dispersive spectroscopy (EDS) system attached to an FE-SEM. Samples for the microstructural analysis were prepared by standard techniques with the final polishing stage using the 0.05 μm colloidal silica.

4.3 Results

In Chapter 3, with increasing the cooling rate, in the alloy with low Fe content and high Mn/Fe ratio (1.0 Fe + 0.65), most of the Fe compounds appeared as the platelet shape instead of Chinese script α type Fe compound. However, in the alloy with high Fe content and high Mn/Fe ratio (2.5 Fe + 0.65), with increasing the cooling rate, most of the Fe compounds appeared as the Chinese script instead of the polyhedral shape as it showed in the low cooling rate, as shown in Fig. 4.4. It indicated that the platelet β type Fe compound can solidify earlier than Chinese script α type Fe compound during solidification.

Meanwhile, the formation of the polyhedral shape α type Fe compound seemed mainly coming from the growth of the Chinese script α type Fe compound.

To prove this hypothesis and get further understanding of the evolution of Fe compounds during solidification, the comparing water-quenched experiments during air cooling were conducted. The results are showed in the figures from Fig. 4.7 to Fig. 4.14.

In the set 1 of the quenching experiment, the Fe compounds appeared as the very small size platelet shape at the beginning of the solidification in the alloy 1.0 Fe + 0.5, as shown in Fig. 4.5 (a). With increasing the air cooling time, the size of these small platelet Fe compounds increased along with the decrease of their number density, as shown in Fig. 4.5 (b) and (c). Almost no compound appeared as Chinese script shape even the air cooling time was 50s. However, when the air cooling time reached to 180s, most of Fe compounds showed the Chinese script. Meanwhile, the amount and volume fraction of platelet Fe compound decreased, as shown in Fig. 4.5 (c) and (d). This is the direct evidence to prove that the Fe compound crystallized as the platelet β type compound at the beginning of the solidification. With the solidification proceeding, the Chinese script α type Fe compound became the dominant one.

In the alloy 2.5 Fe + 0.5, even at the beginning of the solidification, most of Fe compounds appeared as the Chinese script shape and some of them appeared as the small size polyhedral shape, as shown in Fig. 4.6 (a). With increasing the air cooling time, the size and ratio of the polyhedral shape Fe compound particles greatly increased along with the decrease of the ratio of the Chinese script Fe compound particles, as shown in Fig. 4.6 (b). Most of Fe compounds appeared as the polyhedral shape at the air cooling time of 50s, 180s and full solidification, as shown in Fig. 4.6 (c)-(e). It is clearly demonstrated that most of

the polyhedral shape Fe compound particles came from the growth of the Chinese script Fe compound particles.

From the Fig. 4.5 (a) and (b), there should be a doubt that this kind of small size platelet β type Fe compound crystallized during quenching instead of reflecting the real solidification at this temperature. In addition, in the microstructures showed in Fig. 4.5 and Fig. 4.6, the crystallization phases and residual liquid phase was not clear. Hence, the comparing quenching experiments were carried out which containing preheating the cup molds before dipping and holding process at different temperature before quenching. The results of the set 2 quenching experiments were showed in Fig. 4.7-Fig. 4.14.

In the set 2 of the quenching experiment, in the alloy 1.0 Fe, at the beginning of the solidification Fe compounds solidified as small size platelet shape, as shown in Fig. 4.7 (b) and (c) indicated by arrows. However, when the quenching temperature was near α-Al crystallized temperature with holding 60 minutes, the abnormal growth large size platelet β type Fe compound located inside of α-Al grains appeared, marked by arrows in Fig. 4.7 (d). It indicated that only some of the primary platelet β type Fe compounds mentioned above in Fig. 4.7 (b) and (c) can grow to the large size at this temperature. Also, from the location relationship between this abnormal growth β type Fe compound and α-Al grains, during the solidification, this primary β type Fe compound can solidify before α-Al. Holding at 580 ˚C for 60 minutes, no such a big Fe compound appeared as shown in Fig. 4.7 (d). Instead, most of the Fe compounds grew to the medium size. It indicated that with holding the liquid at high temperature, the Fe element in the residual liquid tend to diffuse to the Fe compounds already solidified, instead of the nucleation.

In the alloy 1.5 Fe, the solidification showed the similar tendency as that of the alloy 1.0 Fe. The difference was that at the same quenching temperature and holding time, the size of

platelet shape Fe compounds was a little bit larger, as shown in Fig. 4.8. When the Fe content increased to 2.5wt.%, as shown in Fig. 4.9, at the quenching temperature 620˚C, the big size platelet Fe compound appeared. The high concentration of Fe can make the primary Fe compound grew at much higher temperature (more than 620˚C).

Additionally, comparing the full solidification cooling curves of these three alloys, as shown in Fig. 4.7, Fig. 4.8 and Fig. 4.9, with increasing the Fe content from 1.0wt.% to 2.5wt.%, the crystallization temperature of α-Al increased from 603.3˚C to 609.5˚C. It indicated that with increasing the Fe content, the crystallization temperature of the primary platelet β type Fe compound increased. The α-Al phase can nucleate on the primary platelet phase and make its crystallization temperature increase.

In the alloy with low Fe content and low Mn/Fe ratio (1.0 Fe + 0.35), at the beginning of the solidification, the Fe compound solidified as small platelet shape, as shown in Fig.4.10 (b) and (c). At the quenching temperature of 609.3˚C with holding 60 minutes before quenching, large size Chinese script α type Fe compound appeared inside of the α-Al. It indicated that nucleation and growth of this kind of Fe compound in this composition happened before or at this temperature. The nucleation temperature of this phase should be higher than that of α-Al. Meanwhile, comparing Fig. 4.10 (d) and (e), at this temperature, the driving force of the growth of Chinese script α type Fe compound bigger than that of the growth of platelet β type Fe compound and made it grow to the abnormal size. However, at lower temperature (580˚C), the platelet β type Fe compound became more stable, and can grow to the large size as well. It indicate that the transformation of Fe compounds from platelet β type Fe compound to Chinese script α type Fe compound mainly happened at high temperature, higher than 580˚C in this composition.

Increasing the Mn/Fe ratio at 1.0 Fe content, more Mn addition made the Chinese script α type Fe compound can solidified at the beginning of the solidification as well as the platelet shape β type Fe compound. Meanwhile, more Mn addition made the Chinese script α type Fe compound stable and platelet β type Fe compound unstable at higher temperature. The transformation from β type Fe compound to α type Fe compound happened more completely. Hence, at 580˚C holding 60 minutes，in alloy 1.0 Fe + 0.65, almost all the Fe compound showed the Chinese script shape, as shown in Fig.4.12 (e). Mn addition can make α type Fe compound more stable during solidification. In addition, with increasing the Mn addition, the amount of small size platelet Fe compounds decreased, as shown in Fig. 4.10 (d), Fig. 4.11 (d) and Fig. 4.12 (d). It indicated that more Fe solidified as Chinese script shape with increasing the Mn addition.

In the alloy 1.5 Fe +0.5, it showed the similar tendency as that of the alloy 1.0 Fe + 0.65, as shown in Fig. 4.13. At the beginning of the solidification, Fe compound solidified as both small platelet shape and Chinese script shape. With the solidification proceeding, the Chinese script α type Fe compound became the dominant one. Almost all the Fe compounds appeared as the Chinese script after the full solidification.

In the alloy 2.5 Fe + 0.35, it has the similar tendency as that of the alloy 1.0 Fe +0.5, as shown in Fig. 4.14. At the quenching temperature of 609.3˚C with holding 60 minutes before quenching, large size Chinese script α type Fe compound appeared inside of the α-Al. The driving force for the growth of Chinese script α type Fe compound at this temperature is bigger than that of the growth of platelet β type Fe compound and makes it grow to the abnormal size. However, at lower temperature (580˚C), the platelet β type Fe compound became more stable too (due to not enough Mn addition), and can grow to the large size as well. After full solidification, part of the Fe compounds showed the platelet shape.

In addition, in the alloy 1.0 Fe + 0.65 and the alloy 2.5 Fe + 0.35 at the quenching temperature of 660˚C with holding 60 minutes, some of the Fe compound solidified as α type Fe compound and grew to the large size polyhedral shape, as shown in Fig. 4.15 (a) and (b). Chinese script Fe compounds appeared near this kind of Fe compound without growth. Both the compositions of these polyhedral shape and Chinese script shape compounds were analyzed by EDS and the results were shown in Table 2. The compositions of these two compounds were corresponding to that of α type Fe compound [3]. The formation of this kind of polyhedral shape Fe compound at 660 ˚C after holding 60 minutes indicated that when the Fe and Mn contents were high, some of the Fe could crystallize as the polyhedral shape at the beginning of the solidification. The polyhedral shape Fe compound can act as the nucleation site for the Chinese script Fe compound, as shown in Fig. 4.15 (a) and (b).

4.4 Discussion

In order to increase the mechanical properties of cast Al-Si alloys with Fe impurity, some alloying elements are added to modify the platelet β type Fe compound to the less harmful Chinese script α type Fe compound. Mn is widely used and shows a very effective influence on this modification process, especially when the Fe content is low. So far, the effect of Mn on the modification process from the platelet β type Fe compound to the Chinese script α type Fe compound is clear. However, what happened during the solidification in this modification process, i.e. the evolution of the Fe compounds during solidification is unclear. Still very limited research work focuses on this field. In this work, the water-quenched experiments were conducted to reveal the evolution of the Fe compounds during the solidification.

In the alloys without Mn addition, only platelet Fe compound solidified during solidification. With increasing the Fe content, the growth of the platelet Fe compound happened at higher temperature, as shown in Fig. 4.7 (c), Fig. 4.8 (c) and Fig.4.9 (c).

Mn addition alerted the solidification sequence of the Fe compounds. Accompanied by the Mn addition, α type Fe compound appeared. Both of the two sets of the quenching experiments indicated that in the alloys with Mn addition, the platelet β type Fe compound solidified at the beginning of the solidification. With solidification proceeding, Chinese script α type Fe compound appeared along with disappearance of the β type Fe compound. In the set 1 of the quenching experiment, the growth of the Chinese script α type Fe compound to the polyhedral shape is very clear, as shown in Fig. 4.6. In the set 2 of the quenching experiment, in the alloy 2.5 Fe + 0.35 water-quenched at α-Al crystallization temperature after holding 60 minutes, part of the Fe compounds appeared as the polyhedral shape, as shown in Fig. 4.16. However, in the microstructure of the water-quenched sample at lower temperature, almost no polyhedral shape Fe compound appeared, as shown in Fig. 4.14 (e) and (f). It indicated that the growth of the polyhedral shape Fe compound from the Chinese script Fe compound happened at high temperature, higher or around α-Al crystallization temperature.

Fe content, Mn/Fe ratio (or Mn addition at a given Fe content) and growth time for the Fe compounds (cooling rate) can determine the detail of the solidification sequence of the Fe compounds. The cooling rates used in this work were very close, 0.59˚C/s and 0.67˚C/s (the same cup molds with and without preheating process). Hence, the influence of the cooling rate on the solidification sequence of the Fe compounds was not discussed in this chapter. However, the holding time (60 minutes) before quenching can be treated as very small cooling rate. It is very clear that the holding process is very beneficial to the

transformation from the platelet β type Fe compound to the Chinese script α type Fe compound, as well as the formation of the polyhedral shape Fe compound. This is consistent with the conclusion of Chapter 3. The high cooling rate will restrict the formation of the α type Chinese script Fe compound from the transformation of the platelet β type Fe compound and the formation of the polyhedral shape α type Fe compound from the growth of the Chinese script α type Fe compound.

In the alloy with 1.0 Fe, only the platelet Fe compound solidified during solidification. From the quenching experiment and the microstructure analysis, the formation of the platelet Fe compound mainly happened at three different stage of the solidification. In Fig. 4.17 (a), the large size Fe compound marked by arrows indicated that this kind of the Fe compound solidified before the crystallization of the α-Al phase. More compounds located between the α-Al grains indicated that these compounds formed along with the growth of the α-Al phase. The small size Fe compounds appeared together with the eutectic Si indicated that during the eutectic reaction, small amount of the Fe compounds formed, as shown in Fig. 4.17 (b). Hence, the solidification sequence of the alloy 1.0 Fe under the low cooling rate 0.67˚C/s can be concluded as follow (the formation of Mg_2Si phase was not included):

$$L \rightarrow \beta\text{-}Al_5FeSi + L \quad (3.1)$$

$$L \rightarrow Al + L \quad (3.2)$$

$$L \rightarrow Al + \beta\text{-}Al_5FeSi + L \quad (3.3)$$

$$L \rightarrow Al + Si + L \quad (3.4)$$

$$L \rightarrow Al + Si + \beta\text{-}Al_5FeSi \quad (3.5)$$

In the alloy 1.5 Fe and 2.5 Fe, the solidification sequences are the same as mentioned above, as shown in Fig. 3.18 and Fig. 3.19. The difference is that the amount ratio of the Fe

compounds solidified at different stages. With increasing the Fe content, more Fe compounds will solidify before the crystallization of α-Al.

In the alloy with low Fe content and low Mn/Fe ratio (1.0 Fe + 0.35), at the beginning of the solidification, the platelet β type Fe compound solidified, as shown in Fig. 4.10 (b) and (c). With the solidification proceeding, the Chinese script Fe compound formed. Comparing the Fig. 4.10 (d) with Fig. 4.10 (g), with holding at high temperature for 60 minutes, more Fe compounds will solidify as the Chinese script. This is another evidence to prove the transformation from the platelet β type Fe compound to the Chinese script α type Fe compound. In addition, in the microstructure of the sample after full solidification, almost all the Chinese script Fe compound located inside the α-Al grains, as shown in Fig. 4.10 (g). Hence, the solidification sequence of the alloy 1.0 Fe + 0.35 under the low cooling rate 0.67˚C/s is summarized as follow.

$$L \rightarrow \beta\text{-}Al_5FeSi + L \quad (3.6)$$

$$L + \beta\text{-}Al_5FeSi \rightarrow \alpha\text{-}Al_{15}(Fe,Mn)_3Si_2 + L \quad (3.7)$$

$$L \rightarrow Al + L \quad (3.8)$$

$$L \rightarrow Al + \beta\text{-}Al_5FeSi + L \quad (3.9)$$

$$L \rightarrow Al + Si + L \quad (3.10)$$

$$L \rightarrow Al + Si + \beta\text{-}Al_5FeSi \quad (3.11)$$

The alloy 1.0 Fe + 0.5 had the same sequence as that of the alloy 1.0 Fe + 0.35. More Mn addition made more Fe compounds solidified as the Chinese script, as shown in Fig. 4.11.

In the alloy 1.0 Fe + 0.65, at 660 ˚C after holding 60 minutes, Fe compounds solidified as polyhedral shape, Chinese script as well as platelet shape, as shown in Fig. 4.12 (b) and 4.15 (a). It seems like that these Chinese script and polyhedral shape Fe compounds do not

come from the transformation of platelet β type Fe compound. In addition, in the Fig. 4.12 (d), in the dot cycle area some Fe compounds solidified as platelet shape. However, in Fig. 4.12 (e), no Fe compound appeared as the platelet shape. Instead, small size Chinese script appeared between α-Al grains. It indicated that the transformation from the platelet β type Fe compound to the Chinese script α type Fe compound can occur around lower temperature (580˚C) as well. Hence, the solidification sequence of the alloy 1.0 Fe + 0.65 under the low cooling rate 0.67˚C/s can be s as follow.

$$L \rightarrow \beta\text{-}Al_5FeSi + L \quad (3.12)$$

$$L \rightarrow \alpha\text{-}Al_{15}(Fe,Mn)_3Si_2 + L \quad (3.13)$$

$$L + \beta\text{-}Al_5FeSi \rightarrow \alpha\text{-}Al_{15}(Fe,Mn)_3Si_2 + L \quad (3.14)$$

$$L \rightarrow Al + L \quad (3.15)$$

$$L \rightarrow Al + \beta\text{-}Al_5FeSi + L \quad (3.16)$$

$$L + \beta\text{-}Al_5FeSi \rightarrow \alpha\text{-}Al_{15}(Fe,Mn)_3Si_2 + L \quad (3.17)$$

$$L \rightarrow Al + Si + L \quad (3.18)$$

$$L \rightarrow Al + Si + \beta\text{-}Al_5FeSi \quad (3.19)$$

The alloy 1.5 Fe + 0.5 and the alloy 2.5 Fe + 0.35 had the same sequence as that of the alloy 1.0 Fe + 0.65. In the alloy 1.5 Fe + 0.5, more Fe and Mn concentrations made the edge of the Chinese script Fe compound much thicker but still showed the Chinese script, as shown in Fig. 4.13 (f). In the alloy 2.5 Fe + 0.35, due to the low Mn addition, a lot of Fe compounds still showed the platelet shape. Hence, in order to modify all the platelet shape β type Fe compounds to Chinese script α type Fe compound, more Mn addition is required.

4.5 Conclusions

The evolution of the Fe intermetallic compounds during solidification in based AA356 cast alloys was investigated by water-quenched experiment. Two factors, Fe content and

Mn/Fe ratio were alerted individually and combined in the modification process during solidification to reveal their influence on the evolution of Fe compounds. Additionally, the solidification sequence of the alloys was discussed based on the quenching experiments and microstructural analysis. The results are concluded as follows:

1. Fe content is the main factor which can influence the solidification sequence and the evolution of the Fe compounds. In the alloy without Mn addition, only platelet Fe compound appeared. With increasing the Fe content, the growth of the platelet Fe compound happened earlier (at higher temperature). More growth time made the final size of platelet Fe compound much bigger.

2. Mn addition was very effective to modify the platelet β type Fe compound to the less harmful Chinese script α type Fe compound. In the alloys with low Fe content and low Mn addition, the Fe compound crystallized as the platelet β type Fe compound at the beginning of the solidification. With the solidification proceeding, the Chinese script α type Fe compound became the dominant one. The growth of the Chinese script Fe compound during solidification accompanied by the decrease of the platelet β Fe compound. More Mn addition in the alloys with both the low and high Fe content, at the beginning of the solidification, part of the Fe compound crystallized as the Chinese script and/or polyhedral shape. With the solidification proceeding, the growth of the Chinese script Fe compound accompanied by the decrease of the platelet β Fe compound as well.

3. In the alloy with high content Fe and high Mn addition, Fe compounds will appear as the polyhedral shape. The formation of polyhedral shape α type Fe compound mainly came from two aspects, crystallized as the primary phase and the growth of Chinese script α type Fe compound. The ratio of these two parts of compounds mainly depends on the composition and cooling rate.

References

[1] M. E. Schlesinger: *Aluminum Recycling, CRC Press,* (2007), pp. 47.

[2] J. A. Taylor: Procedia Materials Science, **1**(2012), 19-33.

[3] M. V. Kral: Materials Letters, 59 (2005), 2271-2276.

[4] L. Backerud, G. Chai and J. Tamminen: *Solidification Characteristics of Aluminium Alloys*, AFS/Skanaluminum, Foundry Alloys Vol. 2 (1990), 71-84.

[5] S. Shivkumar, L. Wang and D. Apelian: JOM, **43** (1991), 26-32.

[6] P. Ashtari, H. Tezuka and T. Sato: Scr. Mater. **51** (2004), 43-46.

Table 4.1 Nominal compositions of AA356 based alloys with different Fe and Mn contents for quenching experiments. The samples are named as x Fe or x Fe+ y in the text, where the x represents the Fe content (in mass %) and y represents the Mn/Fe ratio.

Alloys	Elements (mass %)					Mn/Fe ratio
	Al	Si	Mg	Fe	Mn	
Set 1	Bal.	7.00	0.35	1.0	0, 0.35, 0.5, 0.65	0, 0.35, 0.5 0.65
Set 2	Bal.	7.00	0.35	1.5	0, 0.75	0, 0.5
Set 3	Bal.	7.00	0.35	2.5	0, 0.875, 1.25	0, 0.35, 0.5

Table 4.2 Nominal compositions of the primary polyhedral shape and nearby Chinese script Fe compounds, as shown in Fig. 15 (b), in the alloy 2.5 Fe + 0.35water-quenched at 660 ˚C after holding 60 minutes

Compounds	Number	Al	Si	Fe	Mn	Mg	(Fe+Mn)/Si
		wt. %	wt. %	wt. %	wt. %	wt. %	atomic ratio
Polyhedral shape	1	61.8	6.9	21.6	9.7	0	1/0.44
	2	61.7	6.9	22.0	9.4	0	1/0.43
	3	61.2	7.0	22.1	9.7	0	1/0.44
Chinese script	1	61.5	7.2	23.3	8.0	0	1/0.46
	2	64.4	7.2	22.2	6.1	0	1/0.50
	3	62.1	7.4	23.7	6.8	0	1/0.47
	4	72.4	7.6	16.3	3.6	0	1/0.75
	5	63.0	8.8	23.7	4.6	0	1/0.62

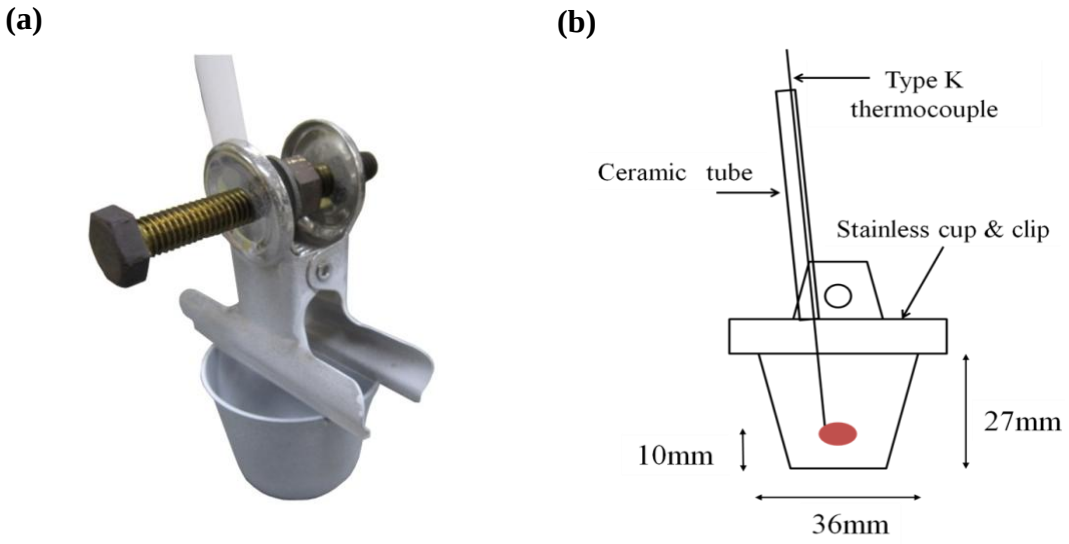

Fig. 4.1 A stainless steel cup mold system for quenching experiments (a) and its schematic drawing (mm) (b).

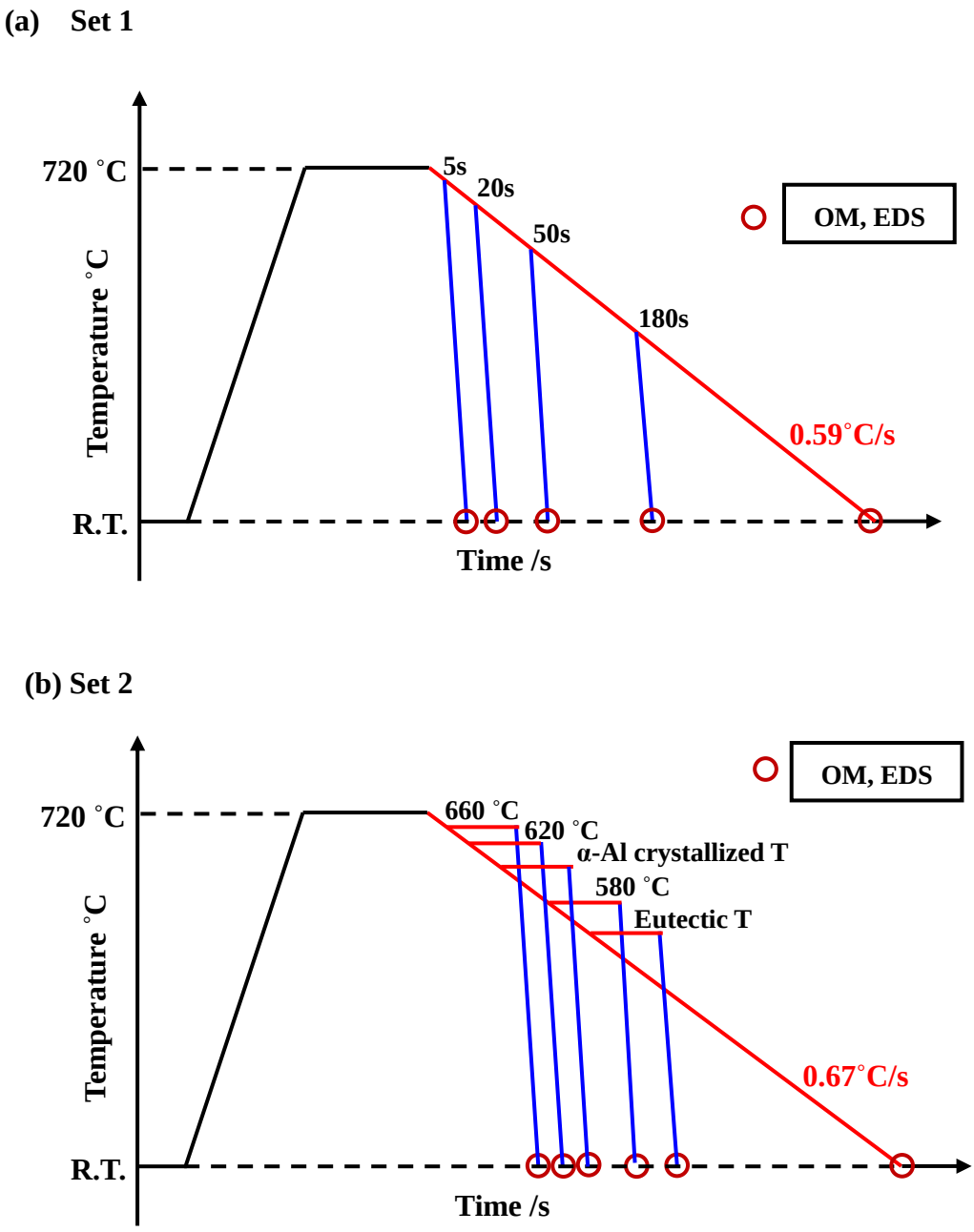

Fig. 4.2 Schematic illustration of two sets of the quenching experiments: (a) Set 1, (b) Set 2.

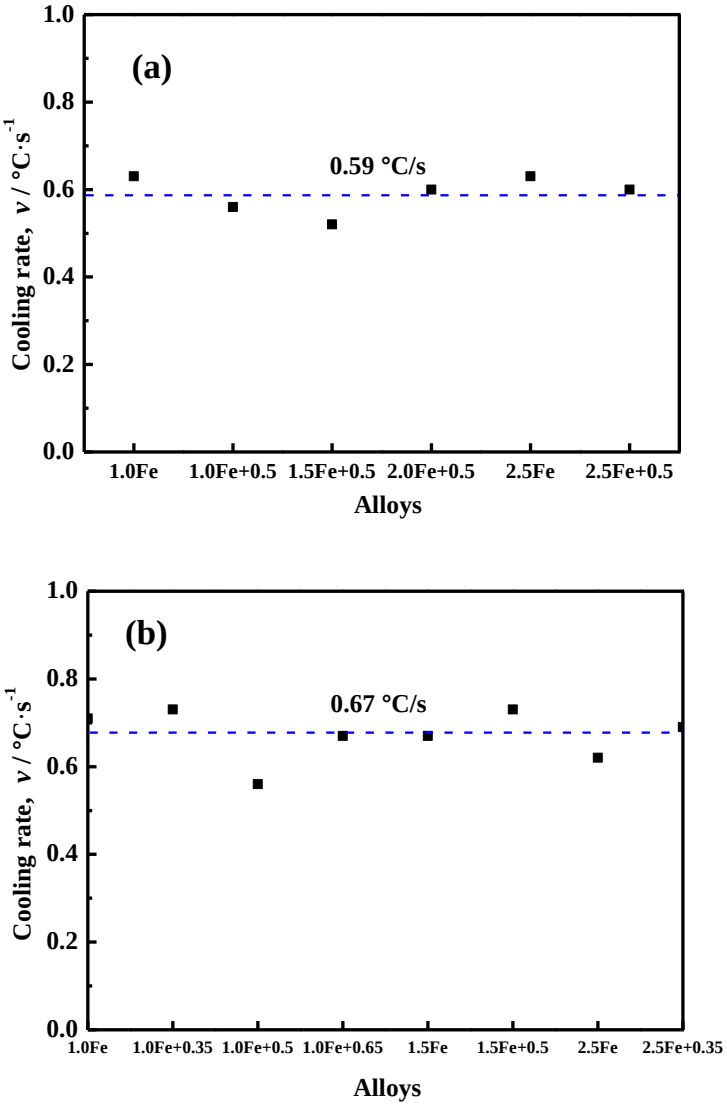

Fig. 4.3 Cooling rates of the alloys with different chemical compositions and their average cooling rate: (a) with the cup mold at the room temperature before dipping into the molten alloys, (b) with the cup mold kept at 720 ˚C before dipping into the molten alloys.

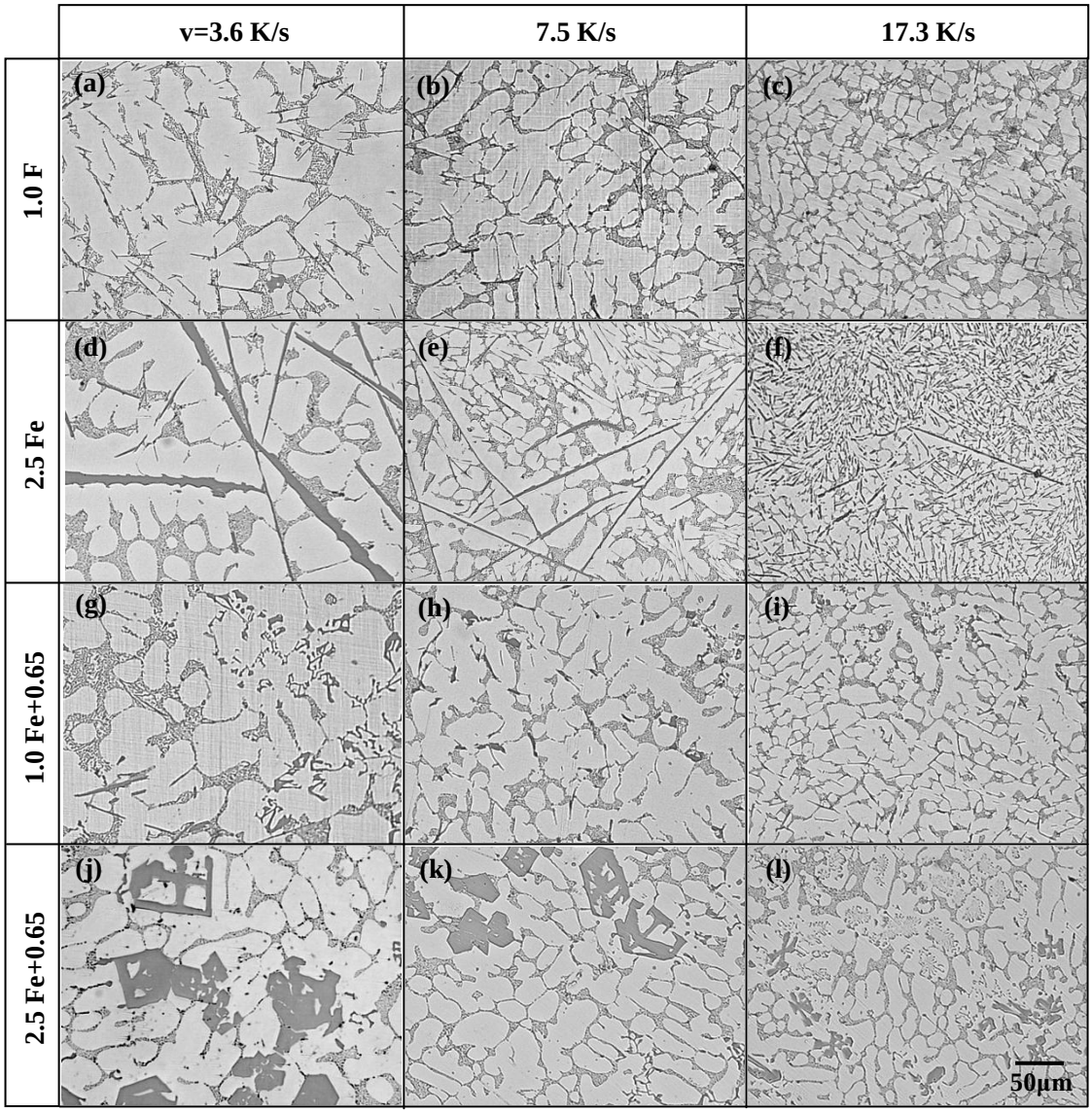

Fig. 4.4 Microstructures of the alloys at different cooling rates, 1.0 Fe: (a) 3.6˚C/s, (b) 7.5˚C/s, (c) 17.3˚C/s; 2.5 Fe: (d) 3.6˚C/s, (e) 7.5˚C/s, (f) 17.3˚C/s; 1.0 Fe + 0.65: (g) 3.6˚C/s, (h) 7.5˚C/s, (i) 17.3˚C/s; 2.5 Fe + 0.65: (j) 3.6˚C/s, (k) 7.5˚C/s, (l) 17.3˚C/s.

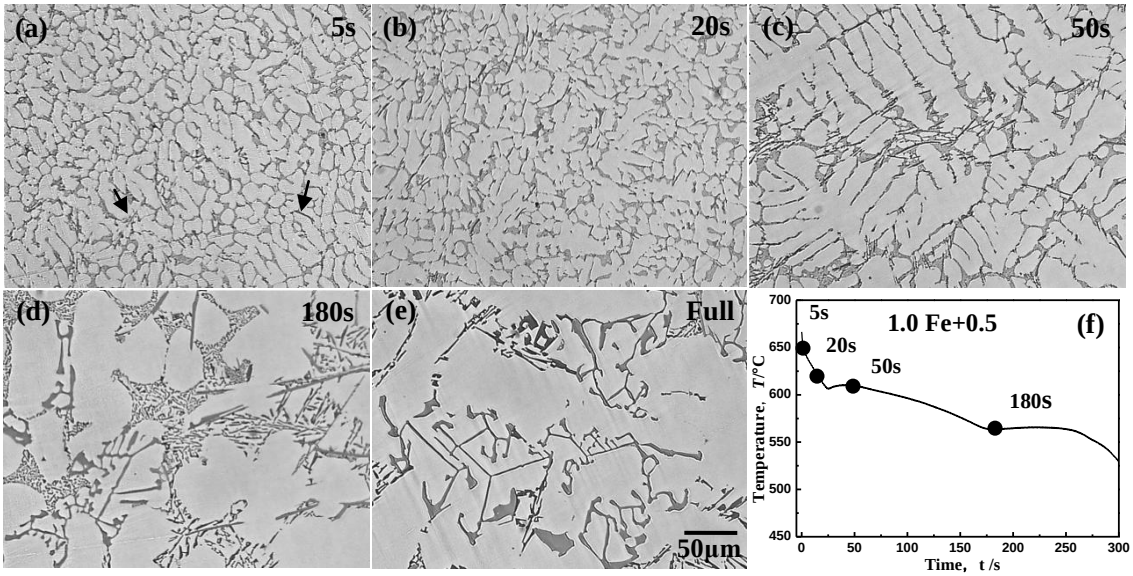

Fig. 4.5 Microstructures of the alloy 1.0 Fe + 0.5 water-quenched after different air cooling time: (a) 5 s, (b) 20 s, (c) 50 s, (d) 180 s and (e) after full solidification and (f) its full cooling curve indication quenching time as solid circles.

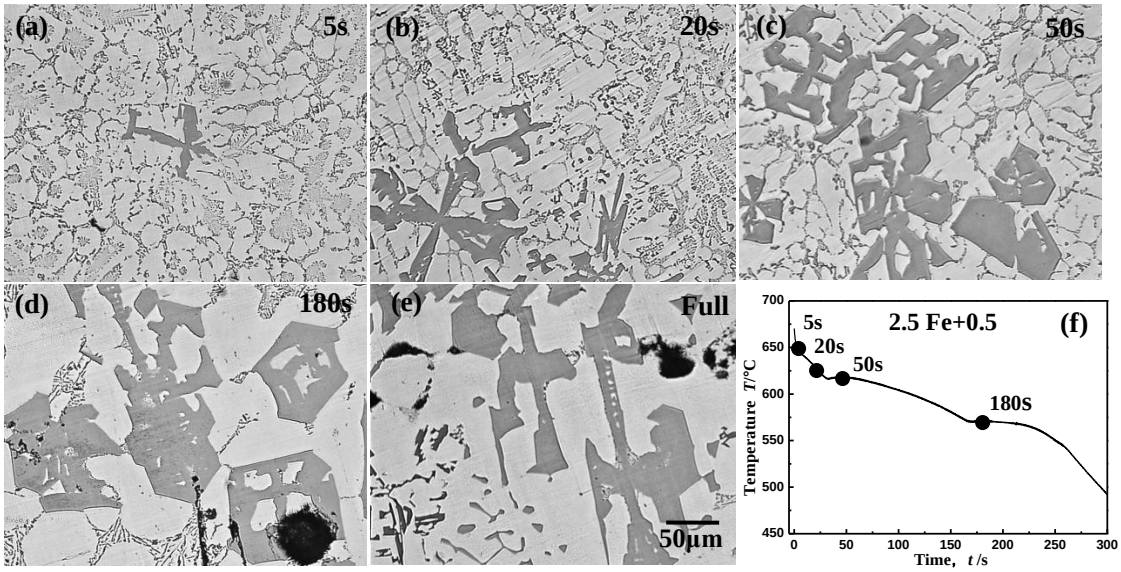

Fig. 4.6 Microstructures of the alloy 2.5 Fe + 0.5 water-quenched after different air cooling time: (a) 5 s, (b) 20 s, (c) 50 s, (d) 180 s and (e) after full solidification and (f) its full cooling curve indication quenching time as solid circles.

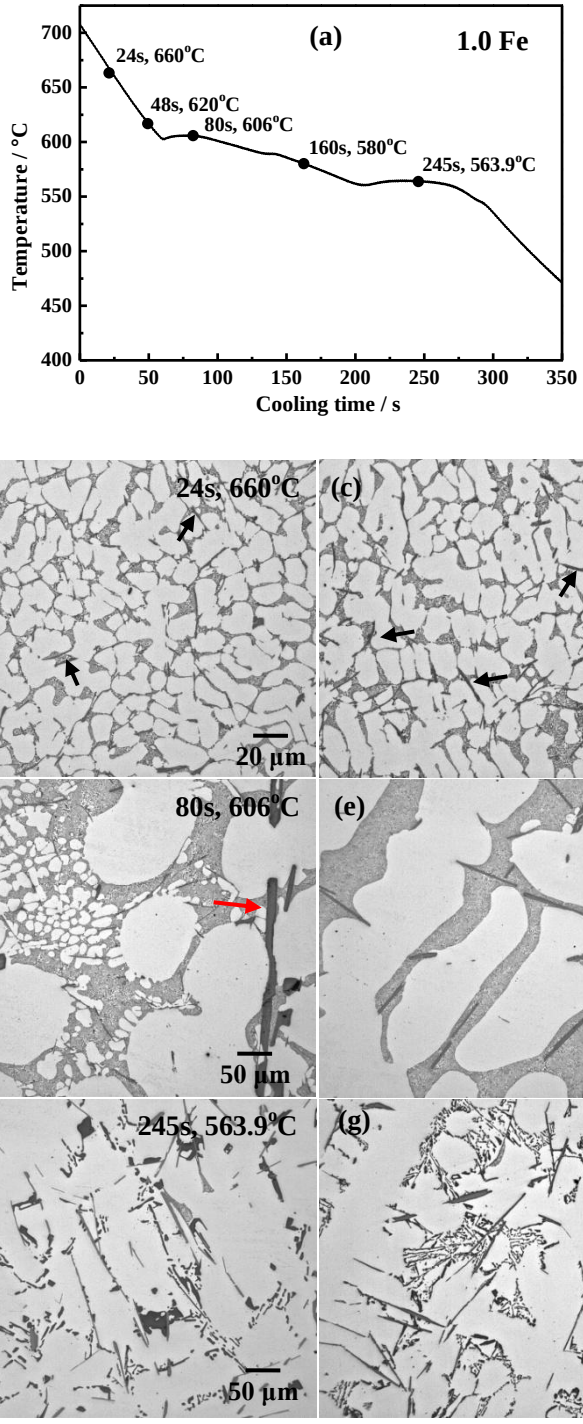

Fig. 4.7 Cooling curve of the alloy 1.0 Fe in the cup mold indication quenching time and corresponding quenching temperature with solid circles (a) and microstructures water-quenched after different air cooling time (with holding 60 minutes): (b) 24s, 660°C (c) 48s, 620°C (d) 80s, 606°C (e) 160s, 582°C (f) 245s, 563.9°C and (g) after full solidification. Platelet Fe compounds formed at high temperature were marked by arrows.

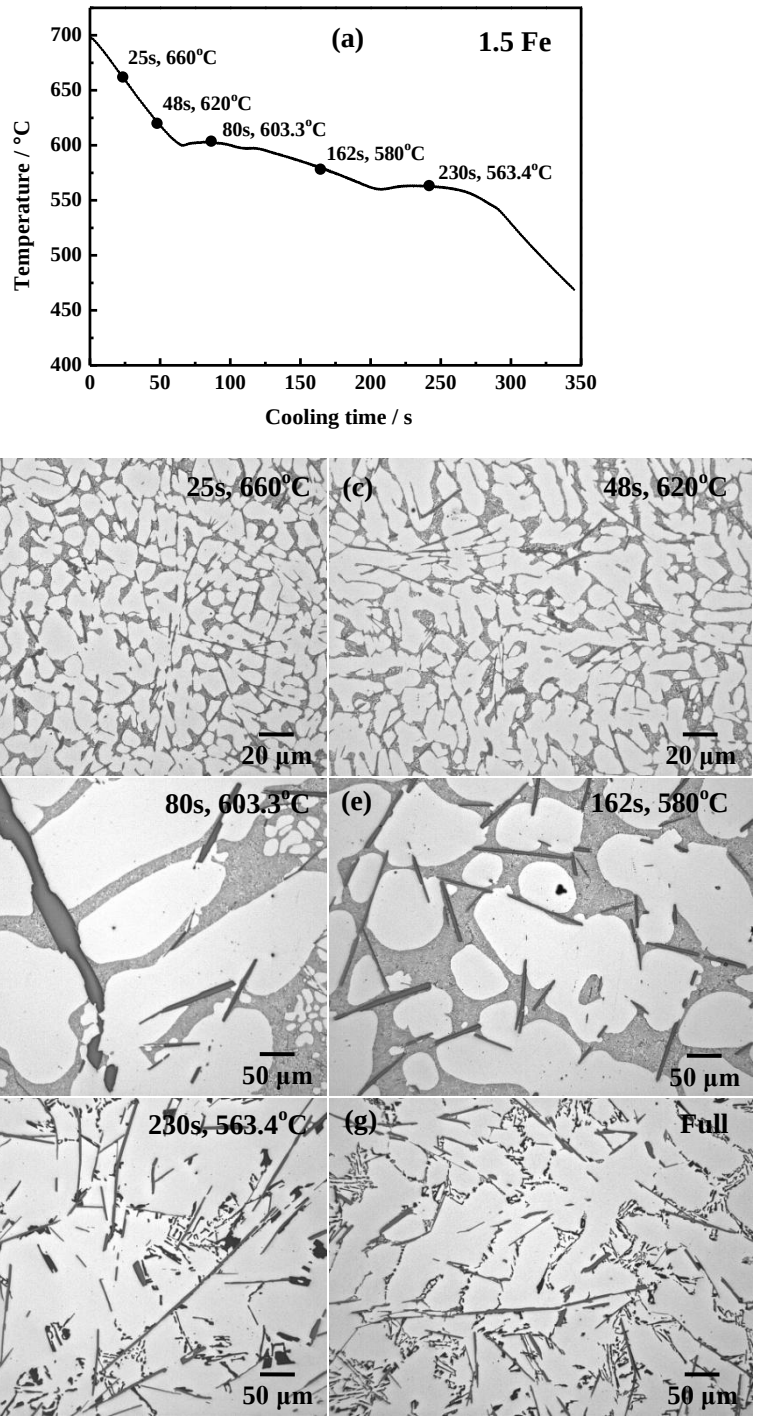

Fig. 4.8 Cooling curve of the alloy 1.5 Fe in the cup mold indication quenching time and corresponding quenching temperature with solid circles (a) and microstructures water-quenched after different air cooling time (with holding 60 minutes): (b) 25s, 660°C (c) 48s, 620°C (d) 80s, 603.3°C (e) 162s, 580°C (f) 230s, 563.4°C and (g) after full solidification.

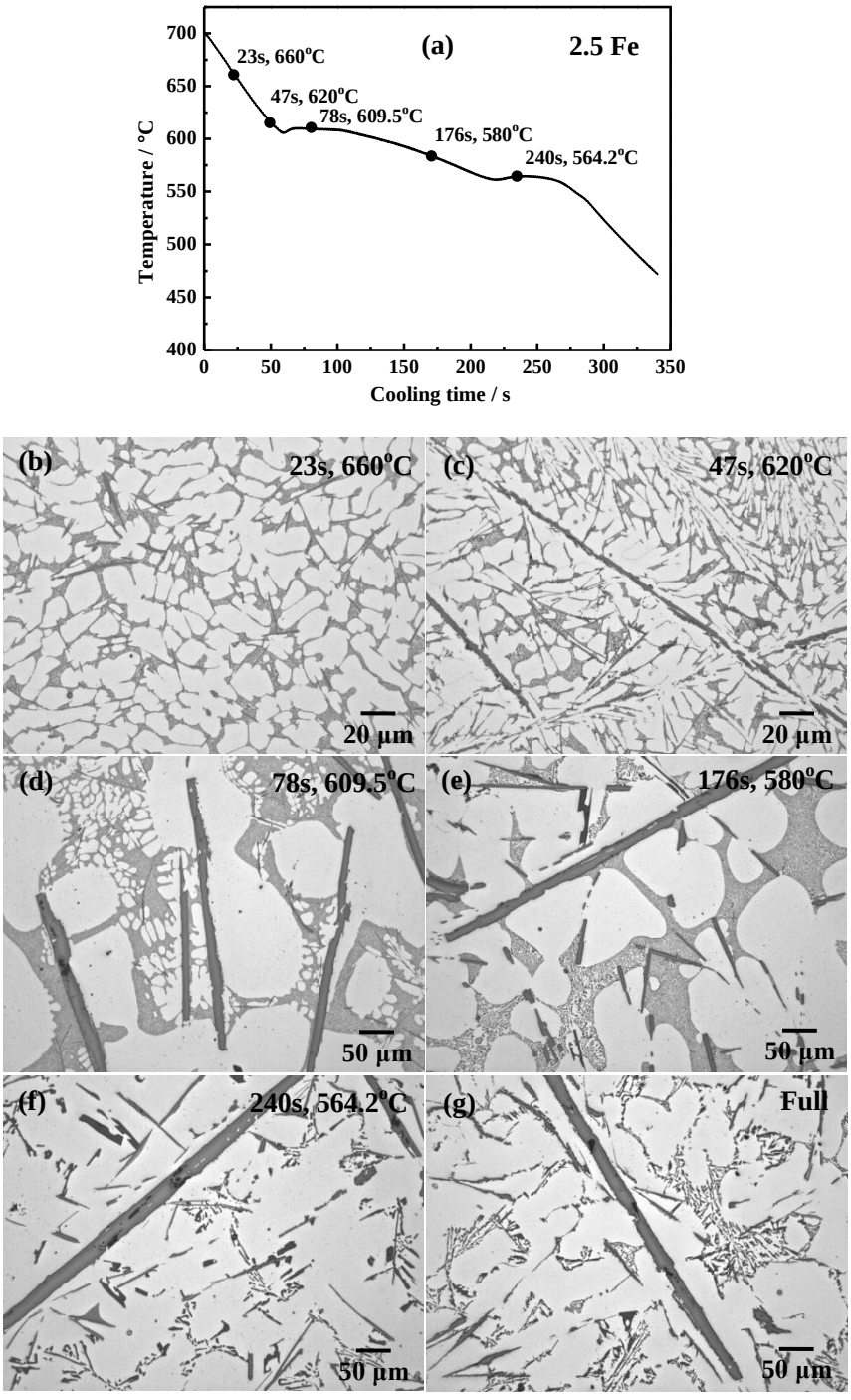

Fig. 4.9 Cooling curve of the alloy 2.5 Fe in the cup mold indication quenching time and corresponding quenching temperature with solid circles (a) and microstructures water-quenched after different air cooling time (with holding 60 minutes): (b) 23s, 660°C (c) 47s, 620°C (d) 78s, 609.5°C (e) 176s, 580°C (f) 240s, 564.2°C and (g) after full solidification.

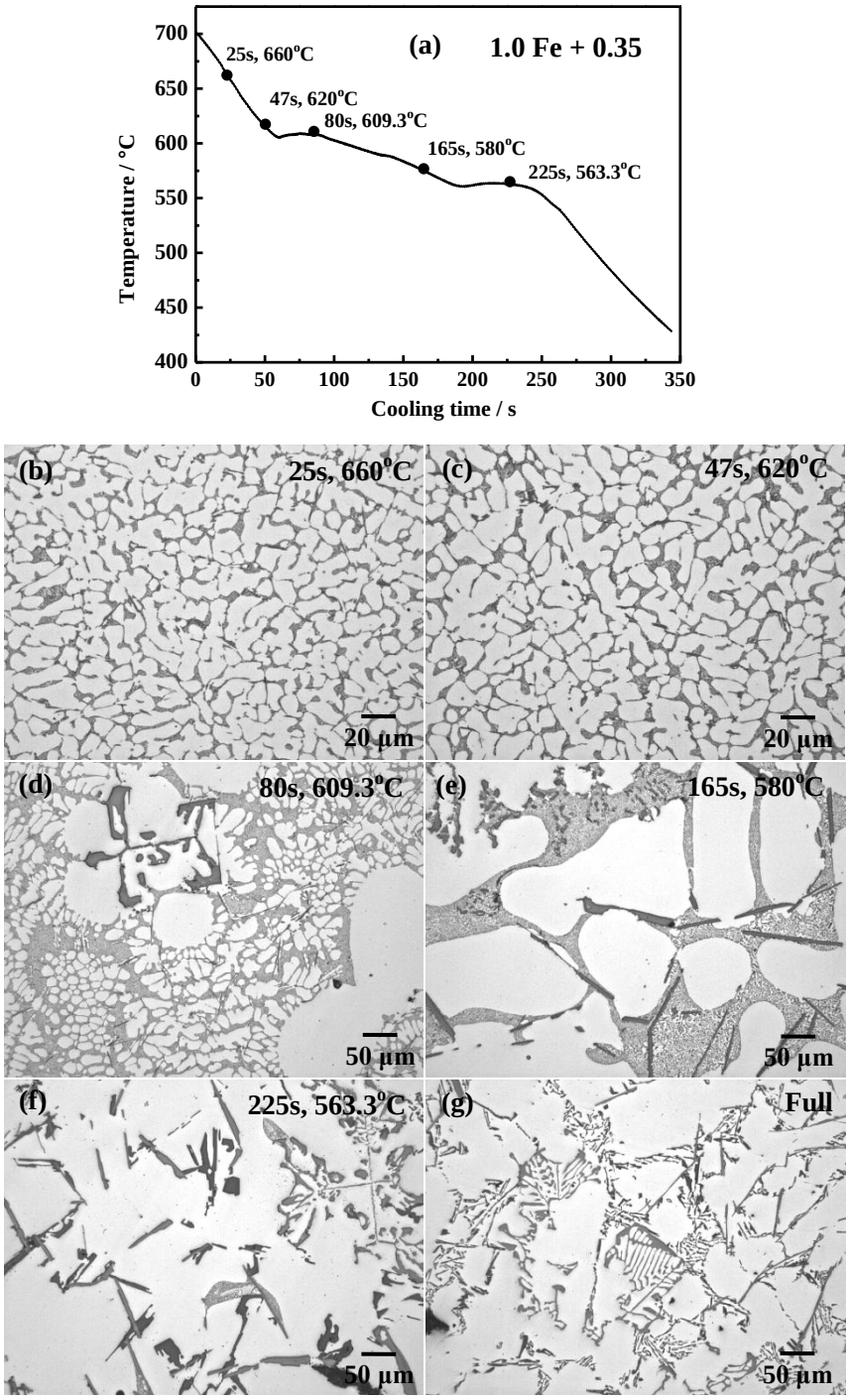

Fig. 4.10 Cooling curve of the alloy 1.0 Fe + 0.35 in the cup mold indication quenching time and corresponding quenching temperature with solid circles (a) and microstructures water-quenched after different air cooling time (with holding 60 minutes): (b) 25s, 660°C (c) 47s, 620°C (d) 80s, 609.3°C (e) 165s, 575°C (f) 225s, 563.3°C and (g) after full solidification.

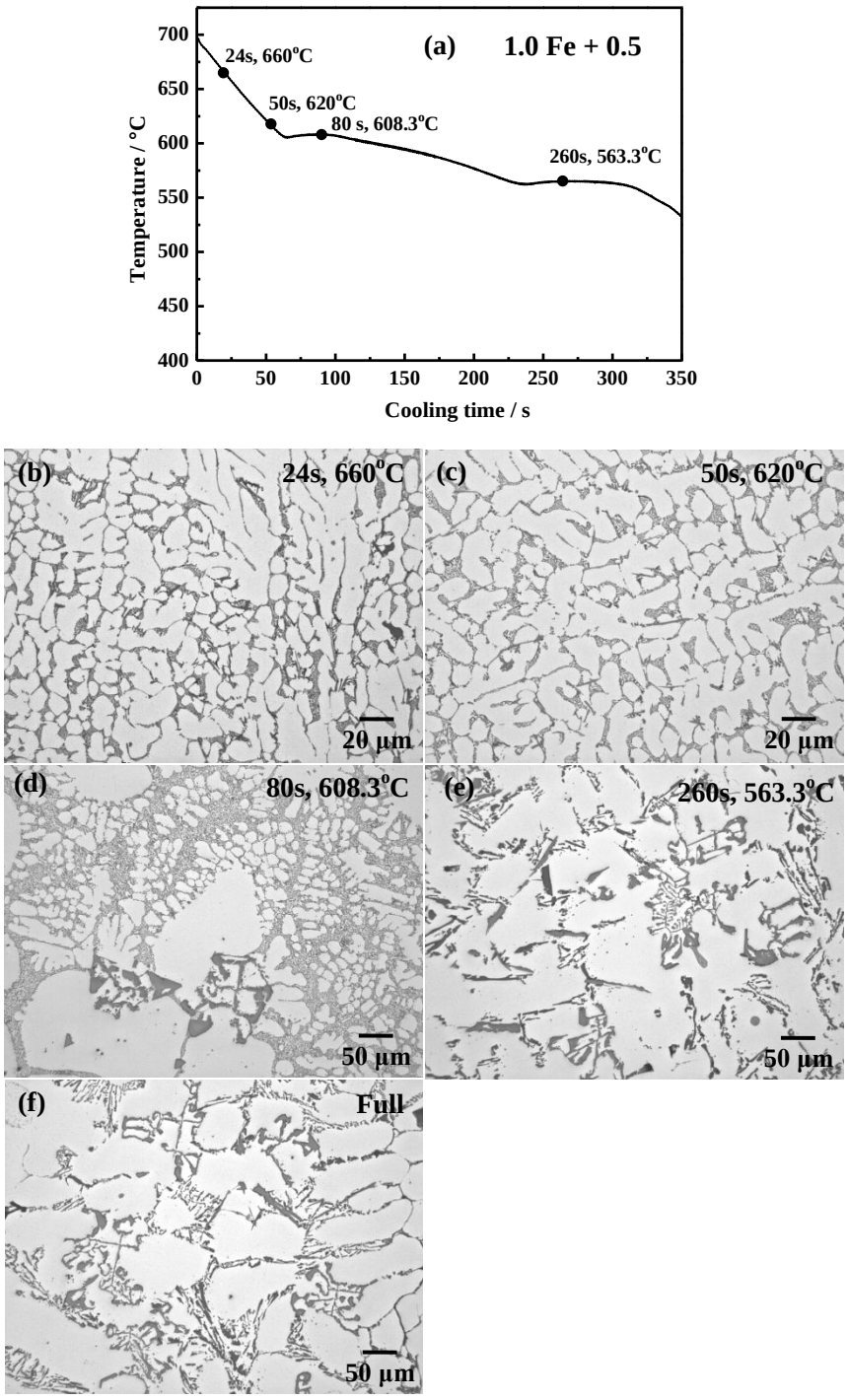

Fig. 4.11 Cooling curve of the alloy 1.0 Fe + 0.5 in the cup mold indication quenching time and corresponding quenching temperature with solid circles (a) and microstructures water-quenched after different air cooling time (with holding 60 minutes): (b) 24s, 660°C (c) 50s, 620°C (d) 80s, 608.3°C (e) 260s, 563.3°C and (f) after full solidification.

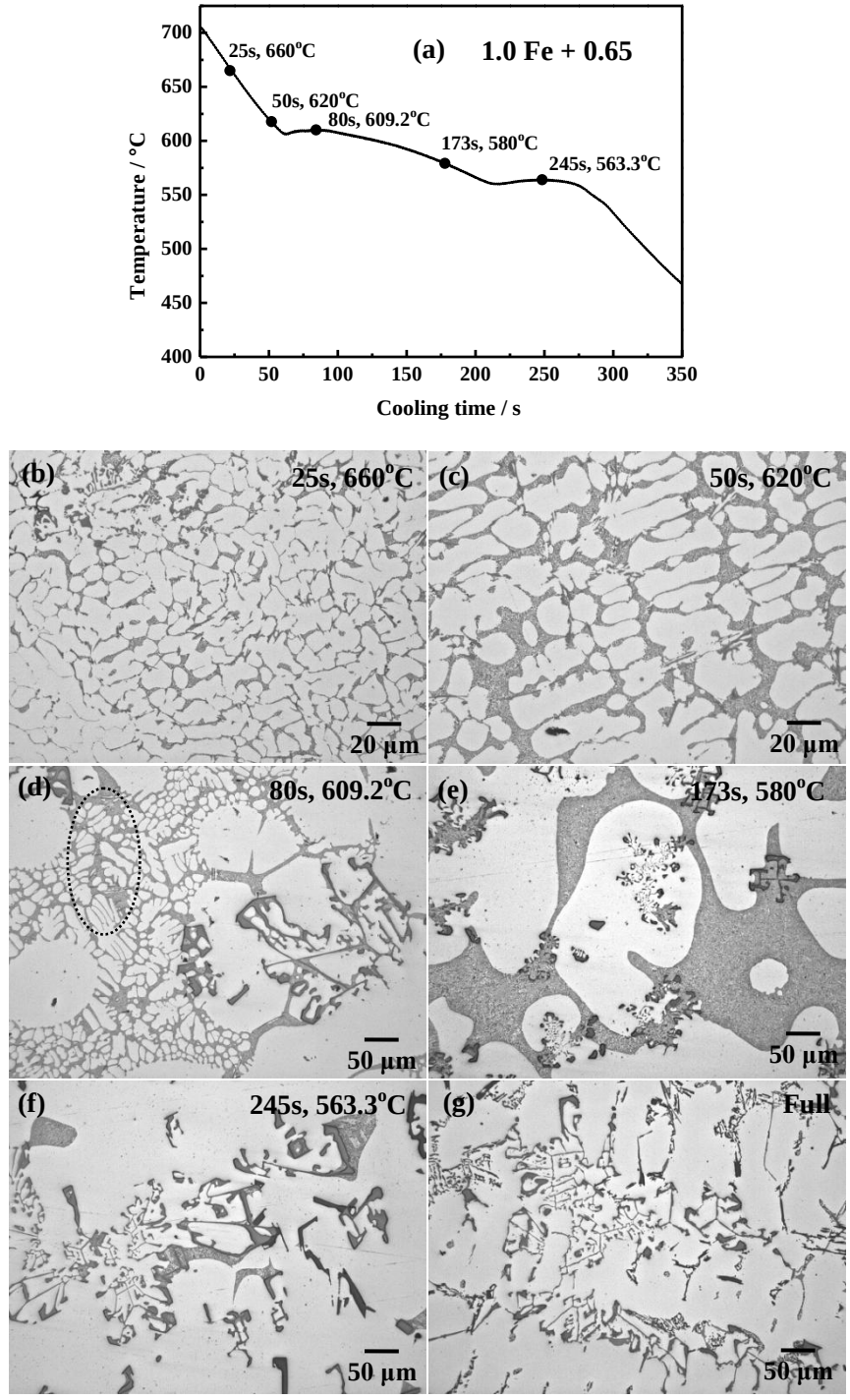

Fig. 4.12 Cooling curve of the alloy 1.0 Fe + 0.65 in the cup mold indication quenching time and corresponding quenching temperature with solid circles (a) and microstructures water-quenched after different air cooling time (with holding 60 minutes): (b) 25s, 660°C (c) 50s, 620°C (d) 80s, 609.2°C (e) 173s, 582°C (f) 245s, 563.3°C and (g) after full solidification.

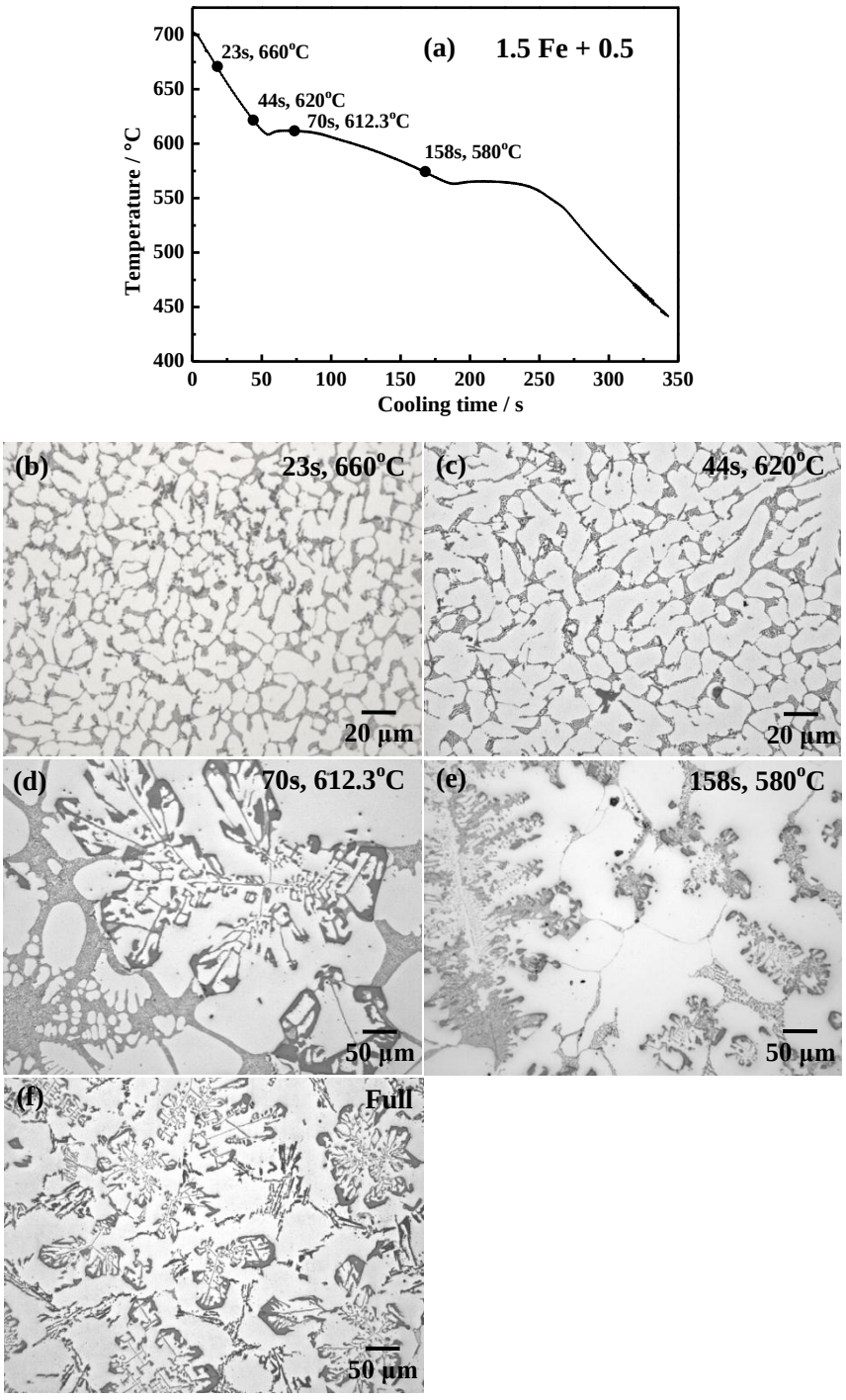

Fig. 4.13 Cooling curve of the alloy 1.5 Fe + 0.5 in the cup mold indication quenching time and corresponding quenching temperature with solid circles (a) and microstructures water-quenched after different air cooling time (with holding 60 minutes): (b) 23s, 660°C (c) 44s, 620°C (d) 70s, 612.3°C (e) 158s, 580°C and (f) after full solidification.

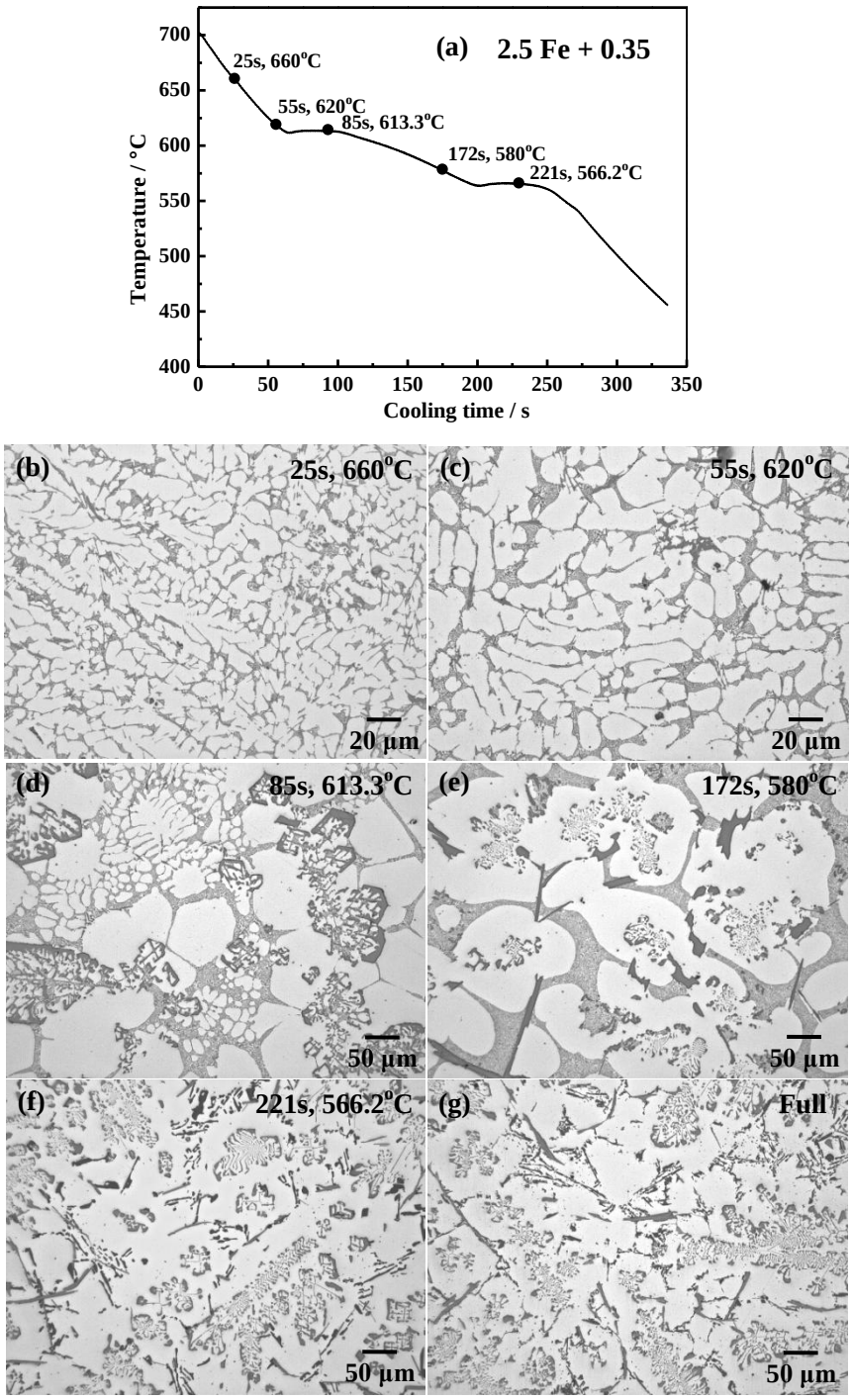

Fig. 4.14 Cooling curve of the alloy 2.5 Fe + 0.35 in the cup mold indication quenching time and corresponding quenching temperature with solid circles (a) and microstructures water-quenched after different air cooling time (with holding 60 minutes): (b) 25s, 660°C (c) 55s, 620°C (d) 85s, 613.3°C (e) 172s, 580°C (f) 221s, 566.2°C and (g) after full solidification.

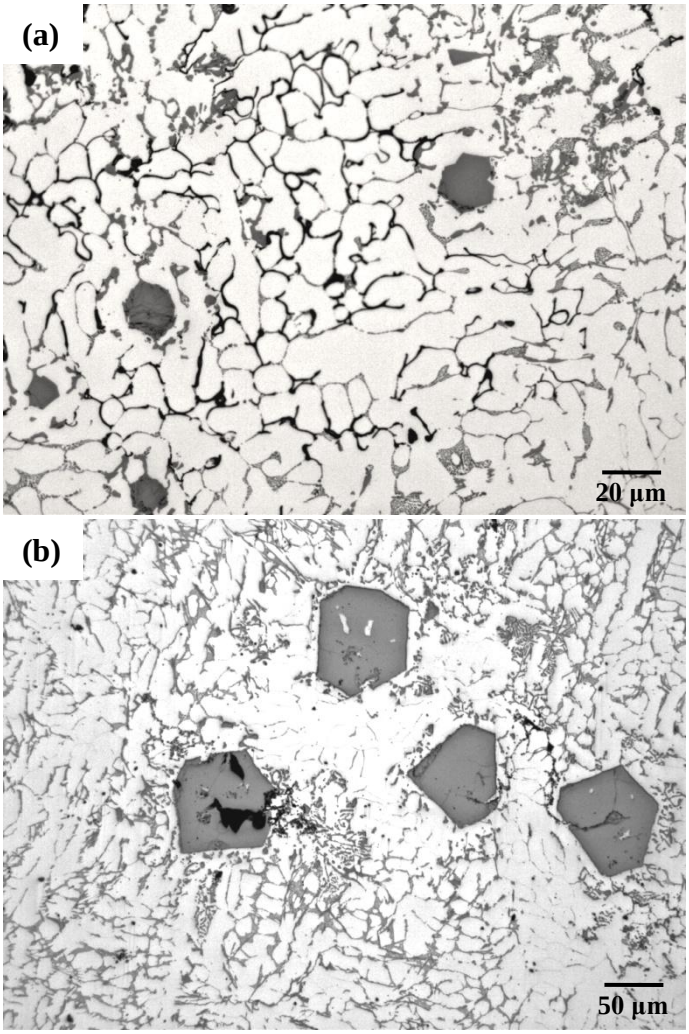

Fig. 4.15 Microstructures of the alloys 1Fe + 065 and 2.5 Fe + 0.35 water-quenched at 660^{o}C (after holding 60 minutes): (a) 1Fe + 0.65, (b) 2.5 Fe + 0.35. Polyhedral shape Fe compound solidified at the beginning of solidification.

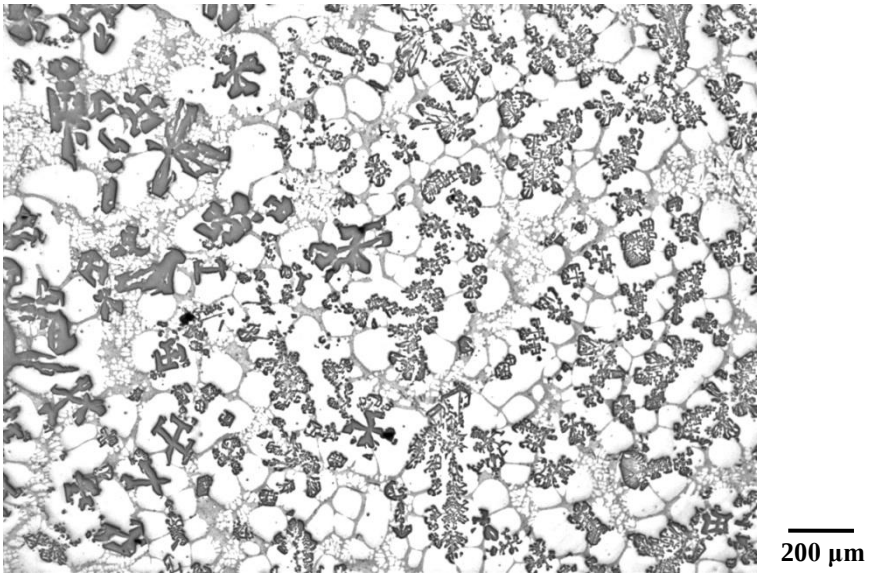

Fig. 4.16 Microstructure of the alloy 2.5 Fe + 0.35 water-quenched at α-Al crystallization temperature (after holding 60 minutes)

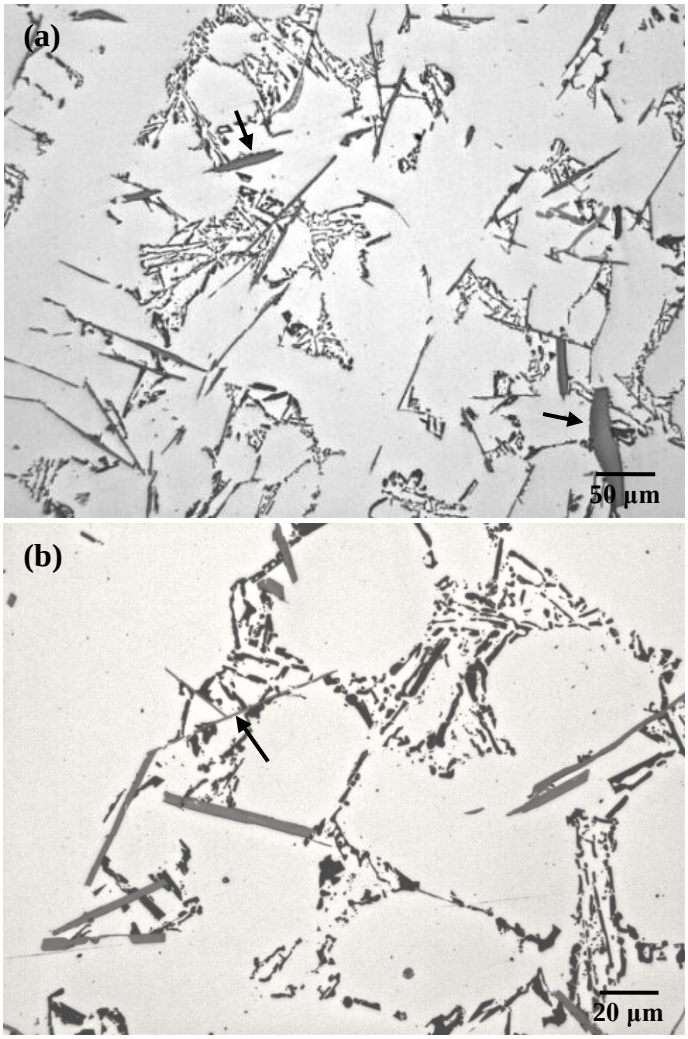

Fig. 4.17 Microstructures of the alloy 1.0 Fe after full solidification. Platelet Fe compounds located inside the α-Al grains and appeared together with eutectic Si phase were marked by arrows.

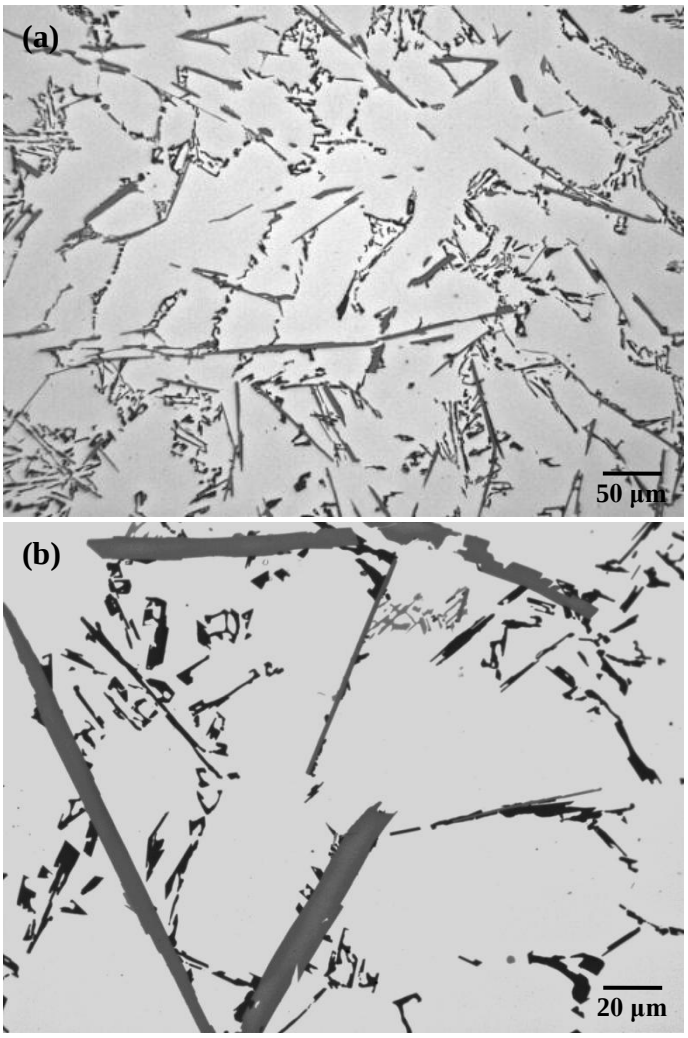

Fig. 4.18 Microstructures of the alloy 1.5 Fe after full solidification.

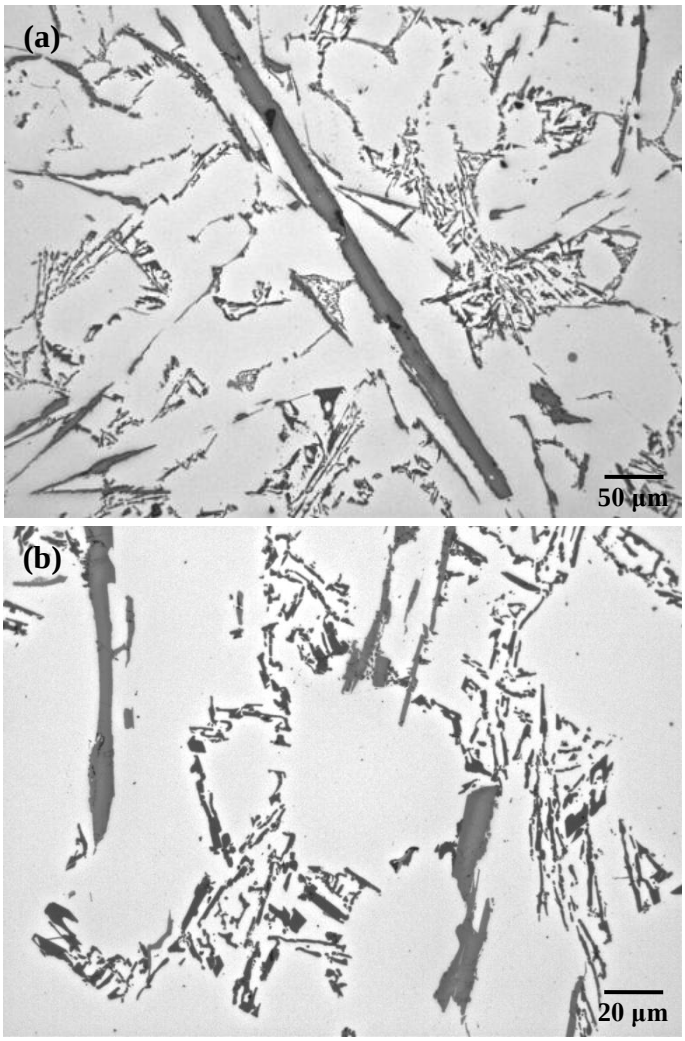

Fig. 4.19 Microstructures of the alloy 2.5 Fe after full solidification.

Chapter 5

Mechanisms of modification of Fe intermetallic compounds by different factors: Mn addition, Fe content and cooling rate in cast AA356 based alloys

In Chapters 2, 3 and 4, it was found that Fe content was the key factor to determine the size of Fe compounds in cast Al-Si alloys. With increasing the Fe content, the size of platelet β type Fe compound increased greatly. Mn addition can modify the Fe compound crystallized as Chinese script instead of platelet. More compact shape can reduce the detrimental influence of Fe compounds on the mechanical properties. The high cooling rate can refine the size of Fe compounds during solidification and improve the mechanical properties. However, the high cooling rate also can restrict the formation of Chinese script Fe compound from transformation of platelet shape Fe compound. Hence, in this chapter the mechanisms behind the evolution of Fe compounds by these factors will be discussed.

5.1 Introduction

The platelet β type Fe compound has been considered as the most detrimental Fe compounds in cast Al-Si alloys. To refine the big size of platelet compound to the small one or to convert the platelet β type Fe compound to Chinese script α type Fe compound are beneficial to improve the mechanical properties of alloys when the Fe is inevitable. Mn is widely used as a corrector to modify the type of Fe compound and the high cooling rate can

refine the size of Fe compounds.

In former Chapters, it was found that Fe content influenced the size of platelet β type Fe compound significantly in the alloys without Mn addition. With increasing the Fe content, the size of platelet β Fe compound increased greatly. Mn/Fe ratio and cooling rate can determine the type and size of Fe compounds in the cast at a given Fe content. Hence, it is important to investigate the mechanisms about how do these factors Mn addition, Fe content and cooling rate influence the evolution of Fe compounds in alloys during casting. In this chapter, the mechanisms of these factors will be discussed individually and combined.

5.2 Experimental procedures

Some results obtained in Chapter 3 and Chapter 4 will be utilized in this chapter. Hence, the experimental procedures and compositions of alloys used are the same as that introduced in these chapters. Nominal compositions of the alloys used independent in this chapter are shown in Table 5.1.The master alloy Al-7.0wt.% Si-0.35wt.% Mg were molten in a graphite crucible under an Ar protective atmosphere by an electrical resistance furnace. Mn was added in the form of the Al-9.93wt.% Mn. Different Mn contents in each alloy are 0.5 wt.%, 1.0 wt.% and 1.5 wt.%, respectively. The samples are named as x Mn in the text, where the x represents the Mn content (in mass %). The schematic illustration of the casting process was showed in Fig. 5.1. The mold used in Chapter 3 was utilized in this chapter showed in Fig. 5.2. Hence, the cooling rates at different locations of the mold from its bottom are the same here. (The influence of Mn addition on the cooling rate here is ignored due to its low content comparing with Al and Si contents.) Only three locations e.g. three different cooling rates were used in the following text: 90 mm-3.6^{o}C/s, 50mm-7.5^{o}C/s and 20mm-17.3^{o}C/s. The casting temperature of 720˚C was used throughout this study.

Microstructures of the alloys were studied by an optical microscope (OM). Electron probe micro-analyzer (EPMA) was utilized to analyze the elements distribution inside the Mn intermetallic compounds and wavelength dispersive spectroscopy (WDS) was utilized to obtain the composition of Mn compounds. Differential thermal analysis (DTA) was carried out to reveal the influence of Fe content and cooling rate on the solidification of Fe compounds. The phenol was used to dissolute the aluminum in the alloys at around 175^{o}C. After dissolution, the powder specimen was used to conducted the x-ray diffraction analysis. Samples for the microstructural analysis were prepared by standard techniques with the final polishing stage using the 0.05 μm colloidal silica.

5.3 Results and discussion

5.3.1 Mechanism of the growth of Fe intermetallic compound by Fe content

In Chapter 3 and 4, it was shown that with increasing the Fe content, the size of platelet β type Fe compound increased significantly under the same cooling rate. However, the increase of the number density of Fe compound was not obvious, as shown in Fig. 5.3. From the quenching experiment, in the alloy 1.0 Fe, water-quenched at 620^{o}C, only some small size platelet shape Fe compound appeared, even holding 60 minutes before quenching at this temperature, as shown in Fig. 5.4 (a). It indicated that the nucleation of this kind of Fe compound occurred at this temperature without growth. With increasing the Fe content, in the alloy 1.5 Fe, water-quenched at the same temperature 620^{o}C, it showed the similar small size platelet Fe compound, as shown in Fig. 5.4 (b). The size of Fe compound appeared a slight increase. In the alloy 2.5 Fe water-quenched at 620^{o}C, the size of platelet Fe compound increased greatly, as shown in Fig. 5.4 (c). Even water-quenched at 660^{o}C, the size of Fe compound is a lit big than that in the alloy 1.5 Fe water-quenched at 620^{o}C. It is clear that the increase of Fe content can make the platelet Fe compound growth occur at

high temperature.

Additionally, in the cooling curves of alloys 1.0 Fe and 1.5 Fe by the cup mold, it is clear that between stages indicated the growth of α-Al and eutectic Si phases, the stages indicated the growth of β compound, marked by arrows in Fig. 5.5 (a) and (b). With increasing the Fe content from 1.0wt.% to 1.5wt.%, the temperature of platelet β type Fe compound growth started increased from 588.8^{o}C to 597.8^{o}C. When the Fe content is 2.5wt.%, in the cooling curve, there is no clear staged indicated the growth of β type compound. In this alloy, the growth of β type Fe compound can happen at higher temperature, make the stages indicated the growth of α-Al and the growth of β type Fe compound coincident. This is another evidence to prove that increasing the Fe content can make the growth of platelet β type Fe compound occur at higher temperature. However, in the cooling curves, there is no peak which can indicate the growth of β compound before the formation of dendrite α-Al phase. In the alloy 1.0 Fe and 1.5 Fe under the cooling rate of 0.67^{o}C/s (cup mold with holding process), the amount of β type Fe compound formed before dendrite α-Al phase is very small. It can not produce a clear peak (or stage) in the cooling curve. In addition, the growth of the primary β Fe compound before the formation of α-Al should occur at the temperature higher but near the crystallization temperature of α-Al, hence the stage is not clear. For the alloy 2.5 Fe, in the cooling curve, the stage indicated the growth of platelet Fe compound is also not clear. However, from the Fig. 5.4 (d), the growth of this kind of Fe compound can occur at 620^{o}C. This is because that in the quenching experiment, before water-quenched, the melt was hold at 620^{o}C for 60 minutes. The large size platelet Fe compound appeared in Fig. 5.4 (d) should form during the holding period. In the real cast process (without holding process), the growth of this kind of big platelet Fe compound should occur at lower temperature but higher than the crystallization

temperature of α-Al. The stage indicated the growth of this big Fe compound is quite near the stage indicated the growth of α-Al phase. Hence, in the cooling curve of the alloy 2.5 Fe, the stage indicated the growth of platelet Fe compound is also not clear, as shown in Fig. 5.5 (c).

The similar results were observed by DTA analysis cooled at 0.5^{o}C/s, as shown in Fig. 5.6. In the alloy 1.0 Fe, the peak indicated the crystallization of β type Fe compound appeared. In the alloy 2.5 Fe, there is no clear peak indicated the crystallization of β type Fe compound.

Based on the explanation above, it is clear that increasing the Fe content can make the growth of platelet β type Fe compound occr at higher temperature. The longer growth time as well as the higher temperature itself lead to the formation of larger size platelet β type Fe compound, which will damage the tensile properties of cast Al-Si alloys significantly. Hence, the Fe content in cast Al alloys should be carefully controlled as low as possible.

5.3.2 Mechanism of modification of Fe intermetallic compound by Mn

The Mn addition can modify the platelet β type Fe compound to more compact Chinese script α type Fe compound (over-modified to polyhedral shape Fe compound when the Fe and Mn contents are high), as demonstrated in Chapter 3 and 4. The amount of different Fe compounds in the alloys after modification mainly depends on the Fe content and Mn/Fe ratio at the same cooling rate, as summarized in Table 5.2. The high cooling rate restricted the formation of Chinese script and polyhedral shape Fe compound comparing with the formation of platelet Fe compound.

In the alloy 1.0 Fe, water-quenched at α-Al crystallization temperature after holding 60 minutes, the platelet Fe compound grew to the very large size, as show in Fig. 5.7 (a).

However, in the alloy 1.0 Fe + 0.35, the Chinese script Fe compound grew to the large size instead of the growth of platelet Fe compound, as shown in Fig. 5.7 (a) and (b). It indicated that at high temperature, the Mn addition made the nucleation and growth of Chinese script Fe compound occur. And with the growth proceeding, the small size platelet Fe compounds primary crystallized will transform to Chinese script Fe compound. More Mn addition at low and high Fe contents made the nucleation of Chinese script Fe compound at higher temperature, even at 660^{o}C in the alloy 1.0 + 0.65 and the alloy 2.5 Fe + 0.35, as shown in Fig. 5.7 (c) and (d).

It is widely accepted that the addition of Mn basically expands α type Fe compound region in the phase diagram as shown in Fig. 5.8 (a) [1], comparing with the phase diagram of Al-Fe-Si system showed in Fig. 5.8 (b) [2]. However, there are two points which can not be explained well by this mechanism. First, in the Al-Fe-Si ternary system, the stoichiometry of α type Fe compound is α-Al_8Fe_2Si with crystal structure of hexagonal [3]. In the Al-Fe-Si-Mn quaternary system, the stoichiometry of α type Fe compound is widely accepted as α-$Al_{15}(Fe,Mn)_3Si_2$ with crystal structure of cubic. These two phases are quite different even both of them are confusingly called as α type Fe compounds. Second, at high cooling rate, in the alloy with low Fe content and low Mn/Fe ratio (1.0 Fe + 0.35 in Chapter 3), almost all the Fe compounds appeared as platelet β type. Even with high Mn/Fe ratio (1.0 Fe + 0.65), most of Fe compounds appeared as platelet β type as well. It is difficult to explain this phenomenon by this mechanism.

Hence, in this chapter, another model was proposed to reveal the mechanism of modification of Fe compounds by Mn addition. The alloy Al-7.0wt.% Si-0.35wt.% Mg without Fe content was used as based alloy. Mn was added in the based alloy to reveal the influence of Mn addition on the microstructure of hypoeutectic Al-Si alloy. Microstructures

of alloys with Mn only were showed in Fig. 5.9. With increasing the Mn addition, the Mn compounds appeared as Chinese script instead of thin platelet shape. In addition, the high cooling rate restricted the formation of Chinese script Mn compound, instead platelet Mn compound appeared. The EPMA and WDS analysis of this kind of compound were showed in Fig. 5.10 and Table 5.3. Based on the phase diagram of Al-Mn-Si system, as shown in Fig.5.11, this compound is more close to $Al_{15}Mn_3Si_2$ with crystal structure of cubic. It is very interesting that the stoichiometry of this Mn compound is very similar to that of the Fe compound α-$Al_{15}(Fe,Mn)_3Si_2$ in the alloys with both Fe and Mn.

Further analysis by XRD was conducted to supply more strong evidence, as shown in Fig.5.12. The alloys 1.5 Mn and 2.5 Fe + 0.65 at the cooling rate of 3.6^{o}C/s were analyzed. The peaks indicated the Mn compounds in the alloy of 1.5 Mn matched well with the $Al_{50}Mn_{12}Si_7$ with the crystal structure of cubic from the database [4]. From the stoichiometry and crystal structure of these two Mn compounds, it is reasonable to obtain that they are the same compound. The peaks indicated the Fe compounds in the alloy of 2.5 Fe + 0.65 also matched well with this Mn compounds. The difference is that the peaks shifted slightly to the higher degree. This is because that the Fe atom replaced the Mn atom in the cell of Mn compound. The replacement of Mn atom by Fe atom leads to the shift of peaks to the higher degree [3].

Hence, it can be assumed that the Chinese script Fe compound can nucleate by itself based on the crystal structure of $Al_{15}Mn_3Si_2$. In the alloy without Mn, at high temperature, the platelet Fe compound can nucleate without growth. With solidification proceeding, the size of platelet Fe compound can grow to the large one. Mn addition make the nucleation of Chinese script compound happen follow the crystal structure of Mn compound $Al_{15}Mn_3Si_2$. And this kind of Chinese script Fe compound is more stable and easily to grow at higher

temperature than platelet Fe compound. Hence, the growth of Chinese script Fe compound happened accompanied by the transformation from platelet compound to Chinese script compound with the solidification proceeding. More Mn addition can make the nucleation of this kind of Chinese script Fe compound occur at higher temperature, and lead to the transformation from platelet β type Fe compound to Chinese script α type Fe compound happen at higher temperature.

5.3.3 Mechanism of modification of Fe intermetallic compound by cooling rate

Another critical issue for iron intermetallic compounds and their effects is the timing at which the different phases form during solidification, and this is influenced by both the concentrations of the elements involved and cooling rates. The influence of the composition has been discussed above. Hereafter, the influence of cooling rate will be explained. In Chapter 3 and 4, with increasing the cooling rate, the size of Fe compounds can be refined. Instead, the number density of Fe compounds increased greatly with increasing the cooling rate.

Increasing the concentration of Fe (and/or Mn) in the alloy can results in the earlier formation of the dominant intermetallic compounds and hence more unconstrained growth of compounds is able to occur. In the alloy without Mn addition, high Fe content made the growth of platelet compound happen at higher temperature and extended the growth time. In the alloy with both Fe and Mn, high Mn addition made the formation of Chinese script and/or polyhedral shape Fe compound occur at higher temperature. Compounds that formed prior to the solidification of the α-Al grain network (i.e. that grow freely within the liquid phase) or that form independently at the same time as the dendritic network tend to grow relatively large. Increasing cooling rate can shorten the period for the growth of Fe compounds and hence refine the size of Fe compounds. The result from DTA analysis can

explain this phenomenon well, as shown in Fig. 5.13. The peaks indicated the growth of β compound shifted to the lower temperature. The growth time for platelet compound decreased with increasing the cooling rate.

On the other hand, as discussed in the 5.3.2 in this chapter, the growth of Chinese script Fe compounds accompanied by the decrease of platelet Fe compound. It indicated that during the modification process, the transformation form platelet β type Fe compound to Chinese script α type Fe compound happened. Increasing the cooling rate apparently can restrict this transformation process.

5.4 Prospect of remove Fe impurity in recycled Al alloys containing high Fe content

In the alloy 1.0 Fe + 0.65 and the alloy 2.5 Fe + 0.35, at the beginning of solidification, the polyhedral shape Fe compounds can form, even at 660^{o}C/s, as shown in Fig. 5.13 (a) and (b). In addition, in the alloy 2.5 Fe + 0.35 quenched at α-Al crystallization temperature after holding 60 minutes, more polyhedral shape Fe compounds formed, as shown in Fig. 5.13 (c). Hence, holding the molten alloys at the higher temperature (a little bit higher than α-Al crystallization temperature) can lead to the formation of large size polyhedral shape Fe compound. It is possible to remove these large size compounds by filter or sediment process. Additionally, in Chapter 4, in the microstructures of alloys 1.0 Fe, 1.5 Fe and 2.5 Fe water-quenched at α-Al crystallization temperature, as shown in Fig. 5.15, after holding 60 minutes at this temperature, the platelet Fe compound grew to the very large size. Hence, it is possible to remove the large size platelet Fe compound directly without modification process using the same method.

5.5 Conclusions

In this chapter, the mechanisms behind the evolution of Fe compounds by these factors will be discussed. The results can be drawn as follows:

1. Increasing Fe content can increased the size of platelet Fe compounds significantly. This is because increasing the Fe content can make the growth of platelet β type Fe compound occur at higher temperature. The longer growth time and high temperature itself lead to the formation of larger size platelet β type Fe compound, which will damage the tensile properties of cast Al-Si alloys significantly. Hence, the Fe content in cast Al alloys should be carefully controlled as low as possible.

2. Mn addition can make the Chinese script Fe compound nucleate based on the crystal structure of $Al_{15}Mn_3Si_2$ (cubic) compound. And this kind of Chinese script Fe compound is more stable and easily to grow at higher temperature than platelet Fe compound. Hence, the growth of Chinese script Fe compound happened accompanied by the transformation from platelet compound to Chinese script compound with the solidification proceeding. More Mn addition can make the nucleation of this kind of Chinese script Fe compound happen at higher temperature.

3. The high cooling rate can refine the size of Fe compounds by shortening the growth period of Fe compounds during solidification. In addition, increasing the cooling rate apparently can restrict the transformation process from platelet β type Fe compound to Chinese script α type Fe compound.

References

[1] L. Backerud, G. Chai and J. Tamminen: *Solidification Characteristics of Aluminium Alloys*, AFS/Skanaluminum, Foundry Alloys Vol. 2 (1990), 71-84.

[2] G. Effenberg and S. Ilyenko: *Landolt-Börnstein, Ternary Alloy Systems Phase Diagrams, Crystallographic and Thermodynamic Data, Subvol. D, Part 1, Springer-Verlag Berlin, Heidelberg*, (2008) pp.53-54.

[3] L.F. Mondolfo: *Aluminum Alloys: Structure and Properties*, Butterworths, London, 1976.

[4] PDF card: 04-007-2118.

Table 5.1 Nominal compositions of the Al-7.0wt.%Si-0.35wt.%Mg based alloys with different Mn contents. The samples are named as x Mn, where the x represents the Mn content (in mass %).

Alloys	Elements (mass %)				
	Al	Si	Mg	Fe	Mn
0.5 Mn	Bal.	7.00	0.35	0	0.5
1.0 Mn	Bal.	7.00	0.35	0	1.0
1.5 Mn	Bal.	7.00	0.35	0	1.5

Table 5.2 Summary of main Fe compounds in the alloys with different levels of Fe content by different levels of Mn/Fe ratio at different levels of cooling rate. Two kinds of compounds at most are listed when the alloys contained all of three kinds of Fe compounds depending on their amounts and the main Fe compound between them is highlighted.

		Low Mn/Fe ratio	Moderate Mn/Fe ratio	High Mn/Fe ratio
Low cooling rate	Low Fe content	Platelet	Platelet Chinese script	Chinese script
	High Fe content	Platelet Chinese script	Chinese script polyhedral	Polyhedral shape Chinese script
High cooling rate	Low Fe content	Platelet	Platelet	Platelet Chinese script
	High Fe contnet	Platelet	Chinese script platelet	Chinese script Polyhedral shape

Table 5.3 WDS quantitative analysis of Mn compounds in the alloy Al-7.0wt.% Si-0.35wt.% Mg-1.5wt.% Mn at the cooling rate of 3.6˚C/s.

Compounds	Al	Si	Fe	Mn	Mg	(Fe+Mn)/Si
	at. %	at. %	at. %	at. %	at. %	atomic ratio
①	72.58	15.39	0.53	11.35	0.15	1/1.30
②	72.26	13.39	0.66	13.57	0.12	1/0.94
③	69.12	15.96	0.43	14.45	0.04	1/1.07

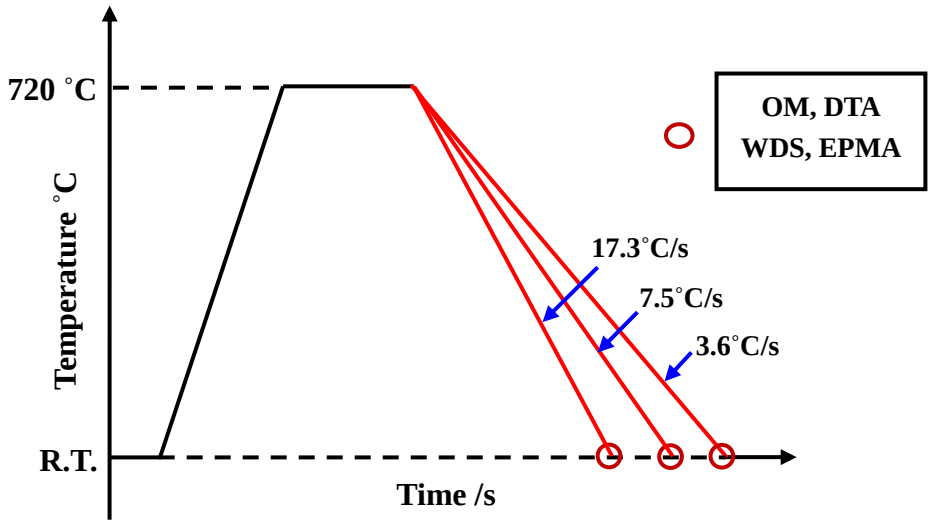

Fig. 5.1 Schematic illustration of the casting process. Three different cooling rates used in this chapter are indicated in the drawing.

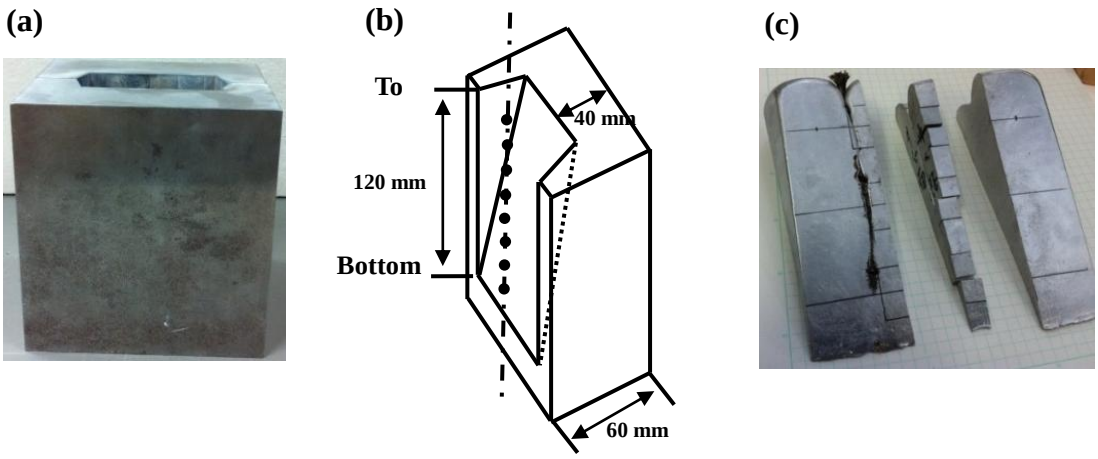

Fig. 5.2 The stainless steel mold for casting (a) and its half schematic drawing (b). The locations of the thermocouples during casting were marked by the close rounds.

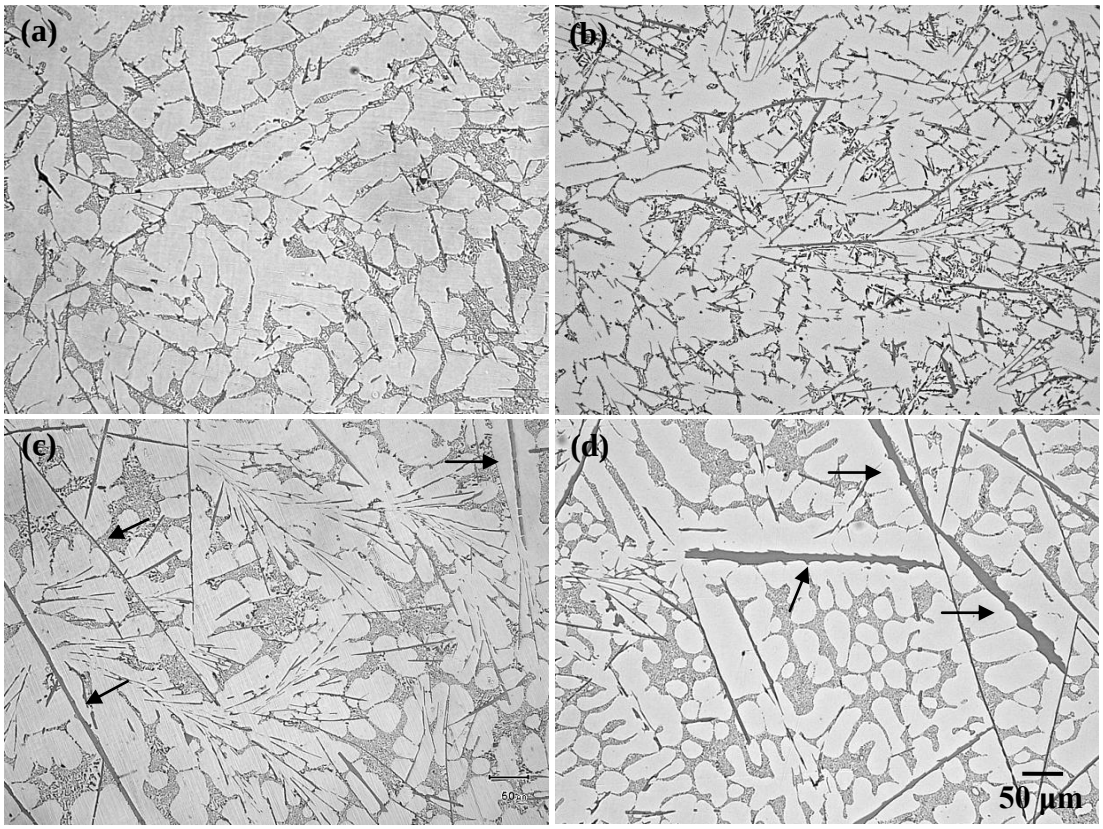

Fig. 5.3 Microstructures of the alloys with different Fe contents under the cooling rate of 3.6^{o}C/s: (a) 1.0 Fe, (b) 1.5 Fe, (c) 2.0 Fe, (d) 2.5 Fe. The large size platelet β type Fe compound particles are indicated by the arrows.

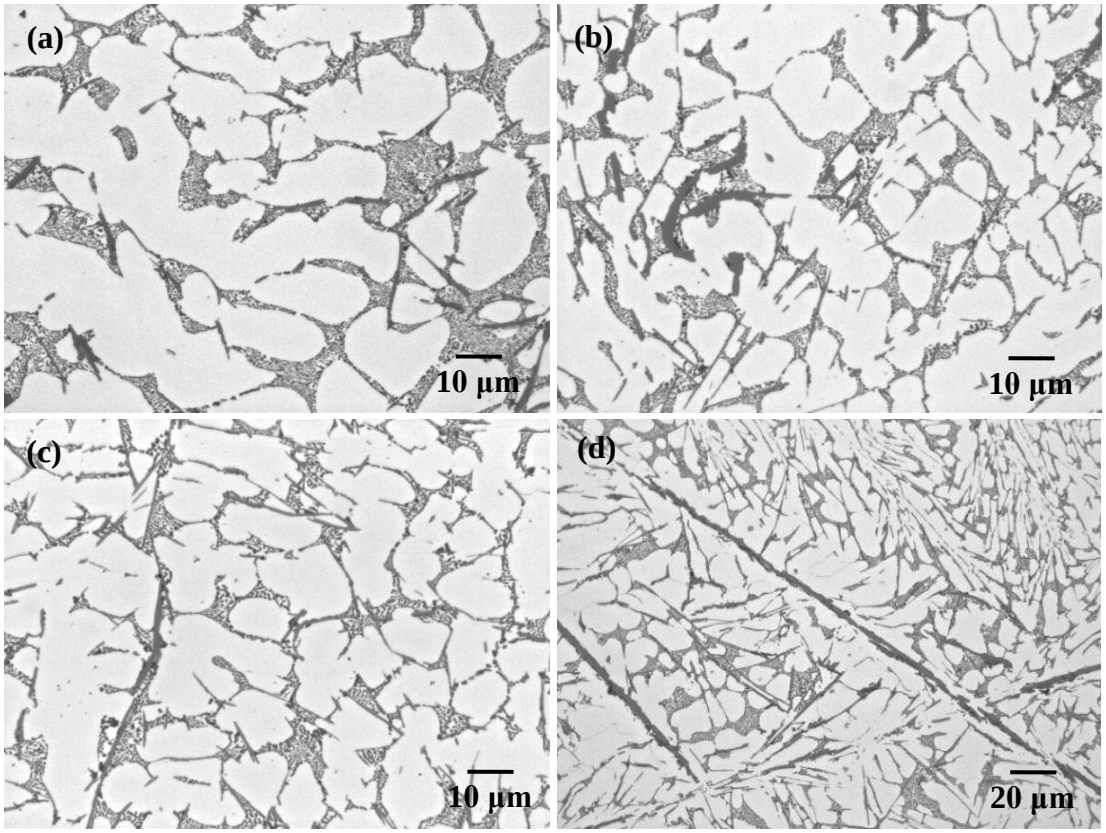

Fig. 5.4 Microstructures of the alloys with different Fe contents water-quenched at different temperature: (a) 1.0 Fe, 620^{o}C (b) 1.5 Fe, 620^{o}C (c) 2.5 Fe, 660^{o}C (d) 2.5 Fe, 620^{o}C.

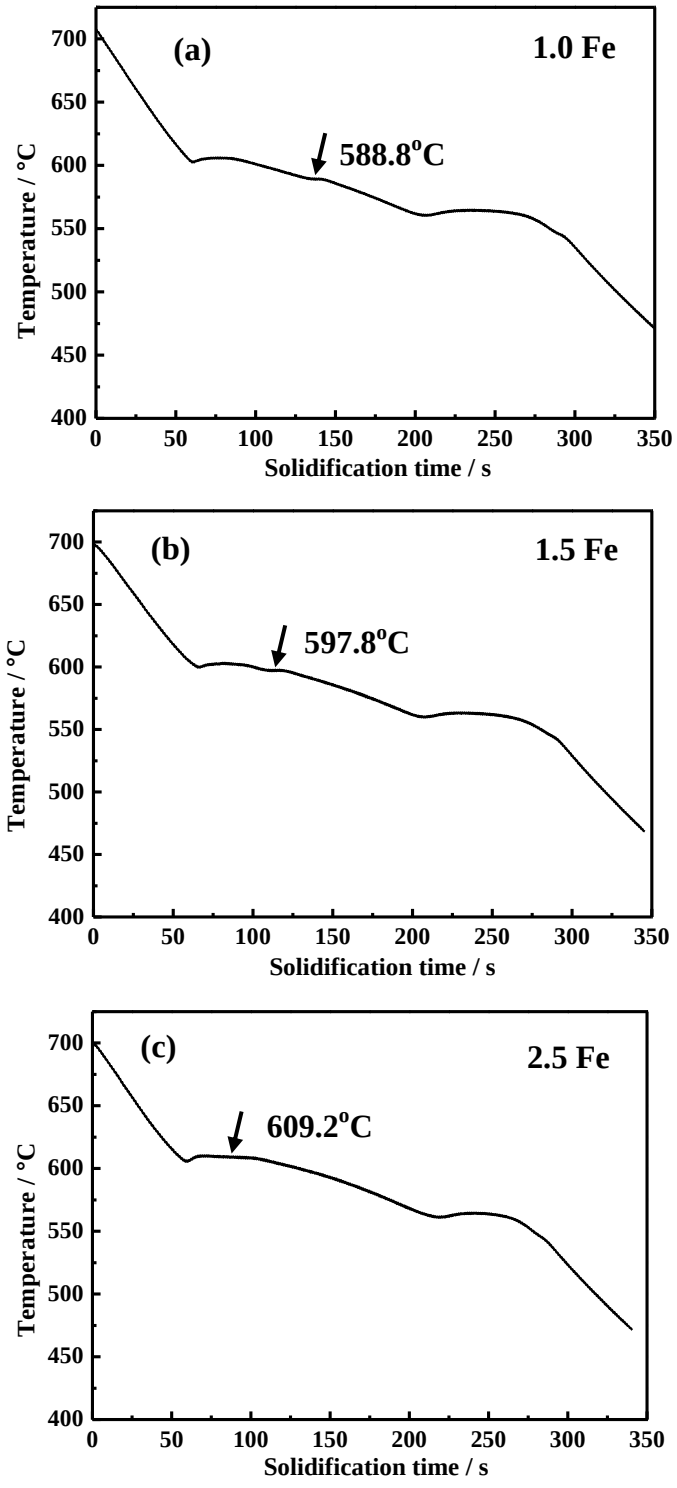

Fig. 5.5 Cooling curves of the alloys with different Fe contents in the cup mold. The stage indicated the growth of β compound marked by arrows.

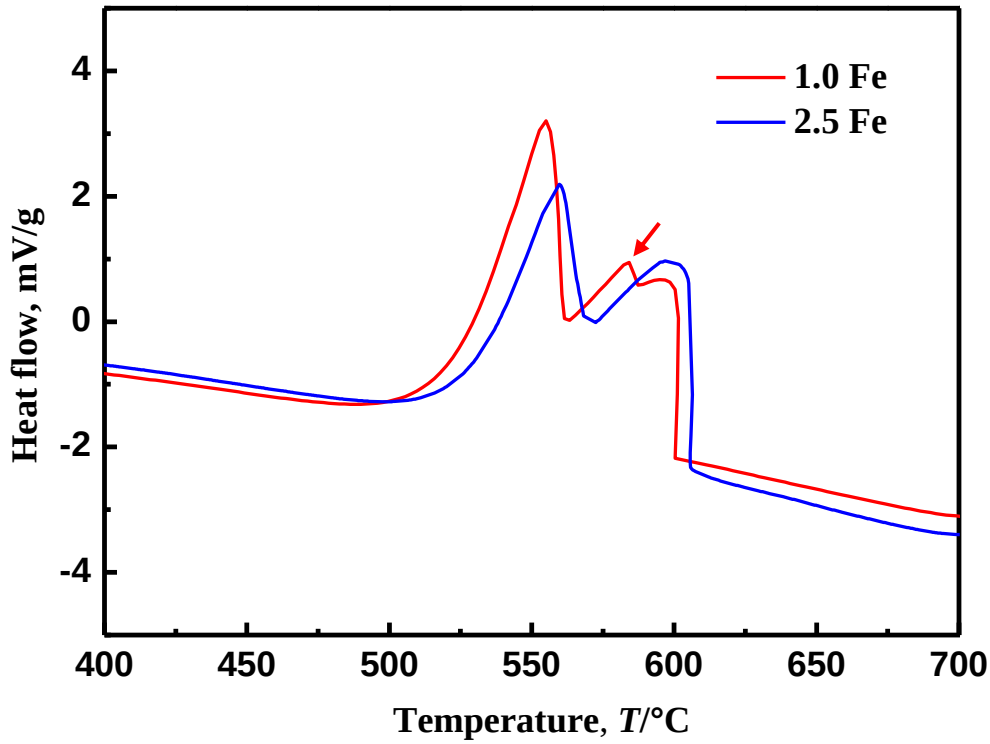

Fig. 5.6 DTA analysis of the alloys 1.0 Fe and 2.5 Fe cooled at 0.5°C/s. The peak of the platelet β type Fe compound crystallization is highlighted by arrow.

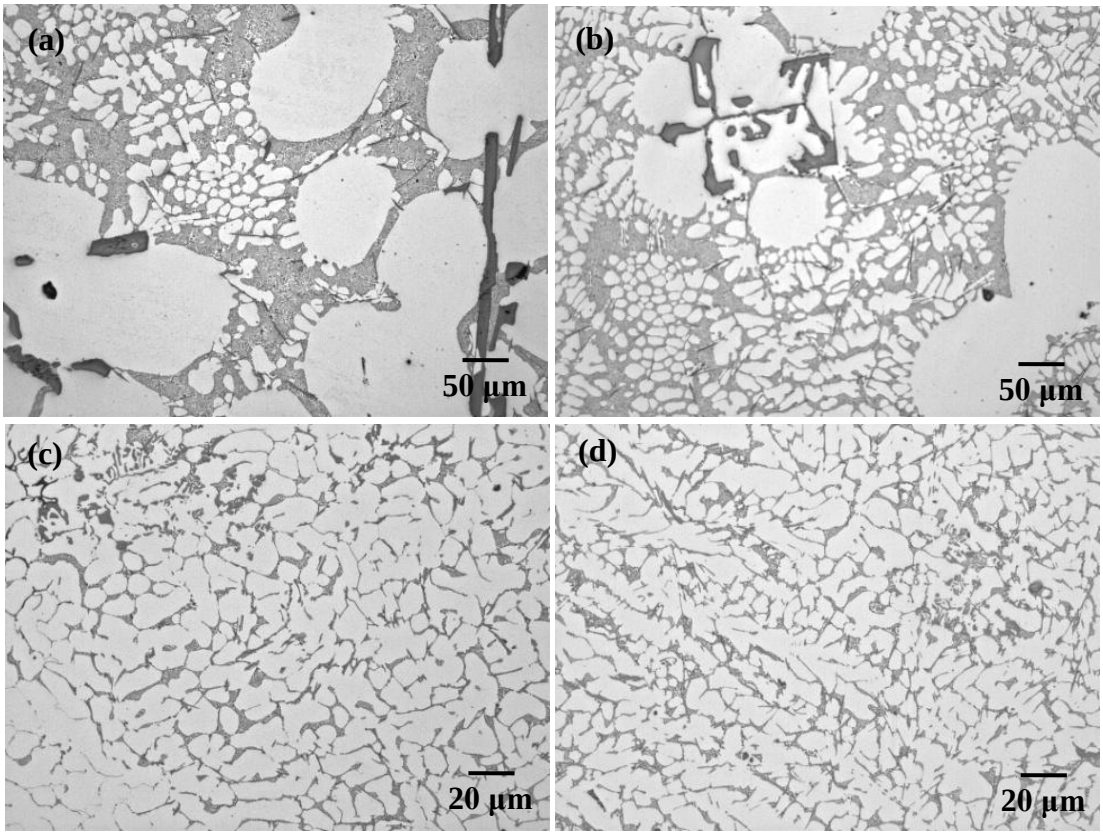

Fig. 5.7 Microstructures of the alloys with 1.0wt.% Fe and different Mn/Fe ratio water-quenched at different temperature after holding 60 minutes: (a) 1.0 Fe, α-Al phase crystallization temperature, (b) 1.0 Fe +0.35, α-Al phase crystallization temperature, (c) 1.0 Fe + 0.65, 660^{o}C, (d) 2.5 Fe + 0.35, 660^{o}C.

(a)

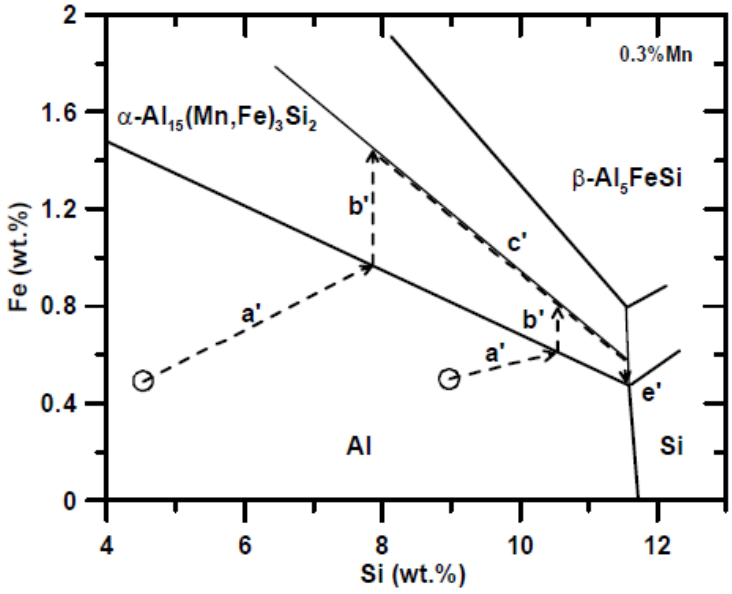

(b)

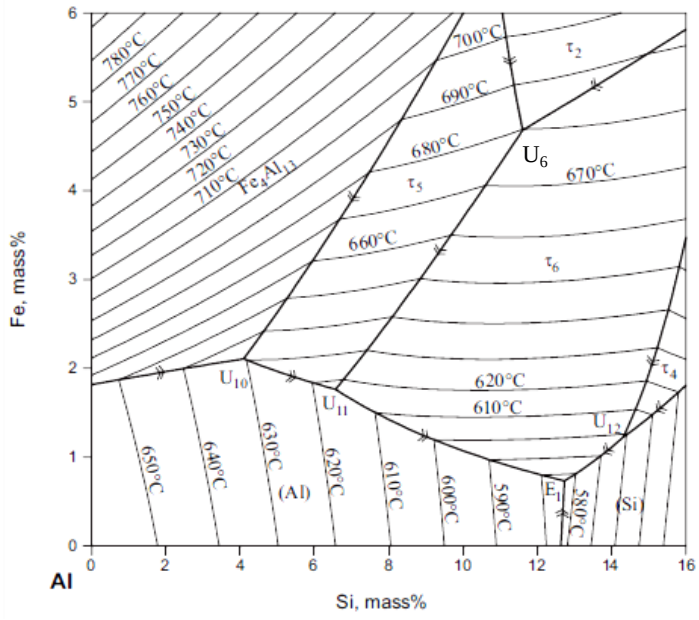

Fig. 5.8 (a) Al-Si-Fe phase diagram for alloys with 0.3 wt.% Mn. Sequences of arrowed dashed lines are the suggested solidification paths for the two alloys containing 0.5 wt.% Fe with 4.5 wt.% and 9.0 wt.% Si, respectively [1]; [b]Calculated liquidus surface of the Al-Fe-Si ternary phase diagram, where τ4 represents δ–Al_3FeSi_2, τ5 represents α-Al_8Fe_2Si and τ6 represents β–Al_5FeSi, respectively. Fe_4Al_3 also was confusedly named as θ–Al_3Fe [2].

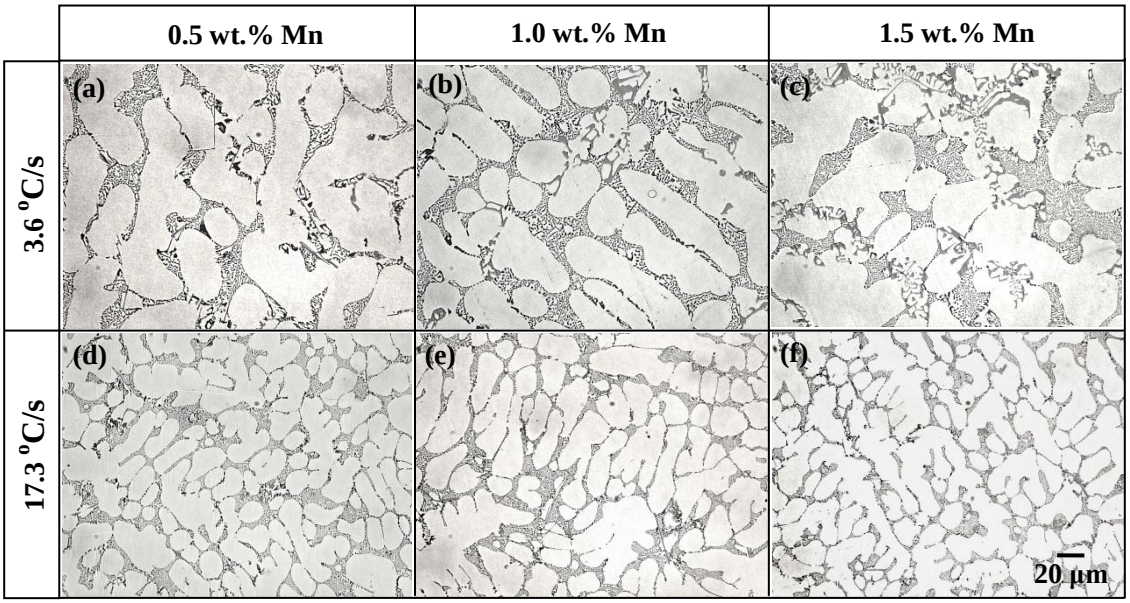

Fig. 5.9 Microstructures of Al-7.0wt.% Si-0.35wt.% Mg based alloys with different Mn contents at the different cooling rates: (a) 0.5wt.% Mn, 3.6˚C/s; (b) 1.0wt.% Mn, 3.6˚C/s; (c) 1.5 wt.%, 3.6˚C/s; (d) 0.5wt.% Mn, 17.3˚C/s; (e) 1.0wt.% Mn, 17.3˚C/s; (f) 1.5wt.% Mn, 17.3˚C/s.

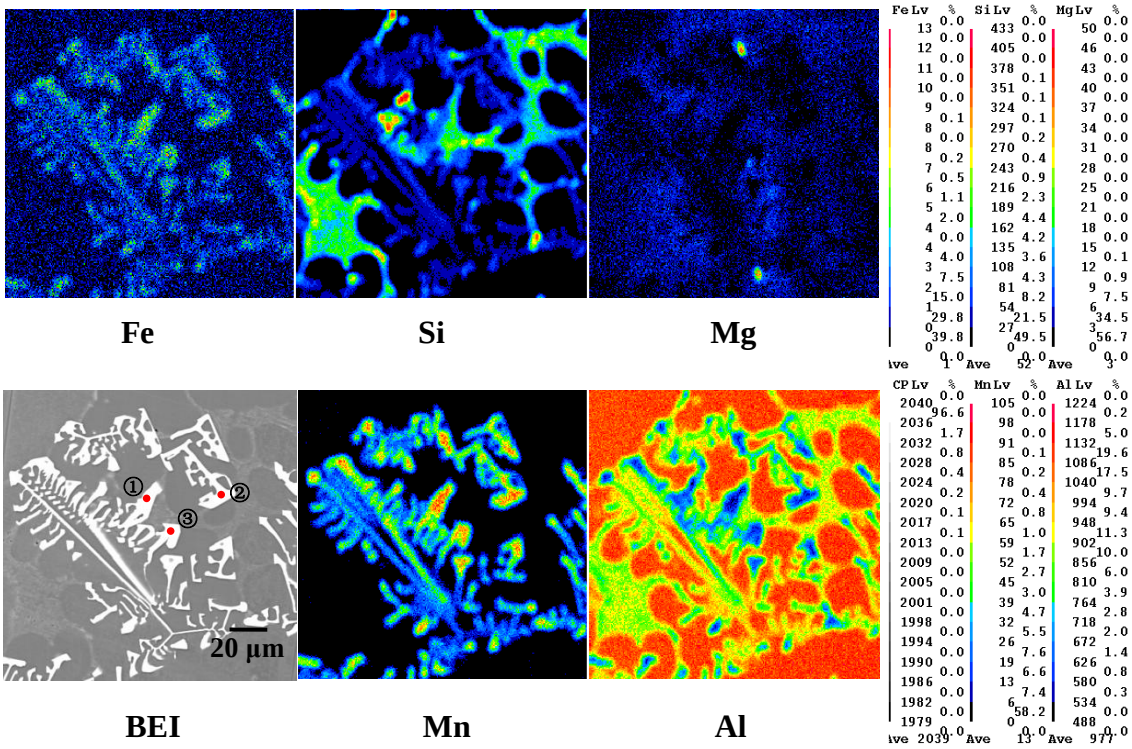

Fig. 5.10 Chemical composition analysis by EPMA color mapping of the Chinese script Mn compound in the alloy Al-7.0wt.% Si-0.35wt.% Mg-1.5wt.% Mn cast at the cooling rate of 3.6˚C/s. The locations to make the WDS analysis were marked by different numbers in the BEI images.

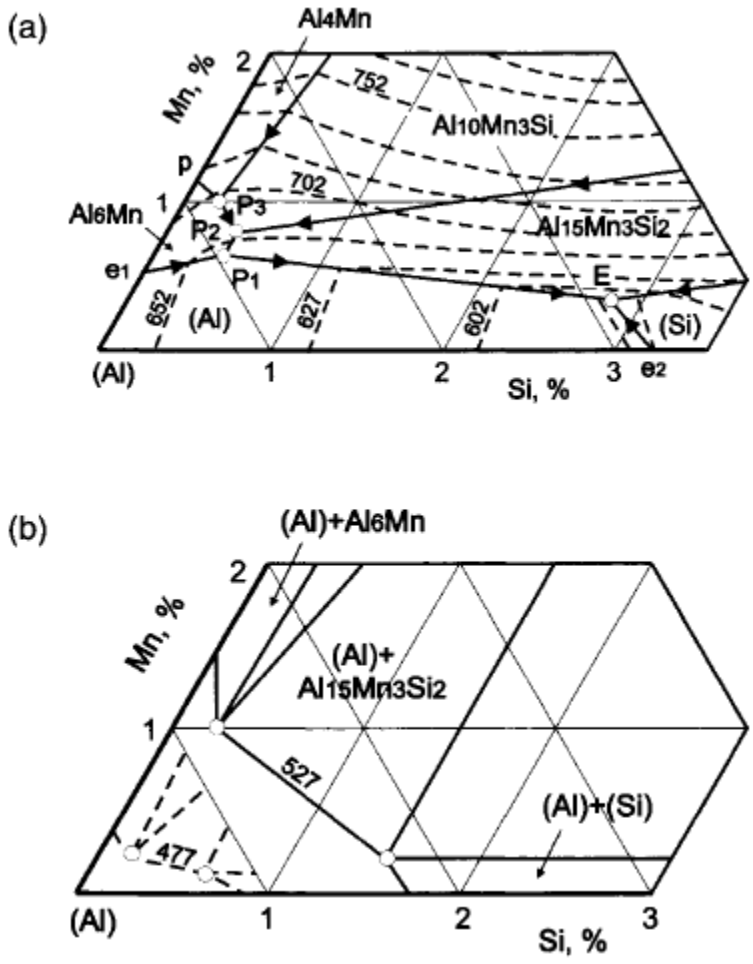

Fig. 5.11 Phase diagram of Al-Mn-Si system: (a) liquidus, (b) isothermal sections at 527˚C and 477˚C [3].

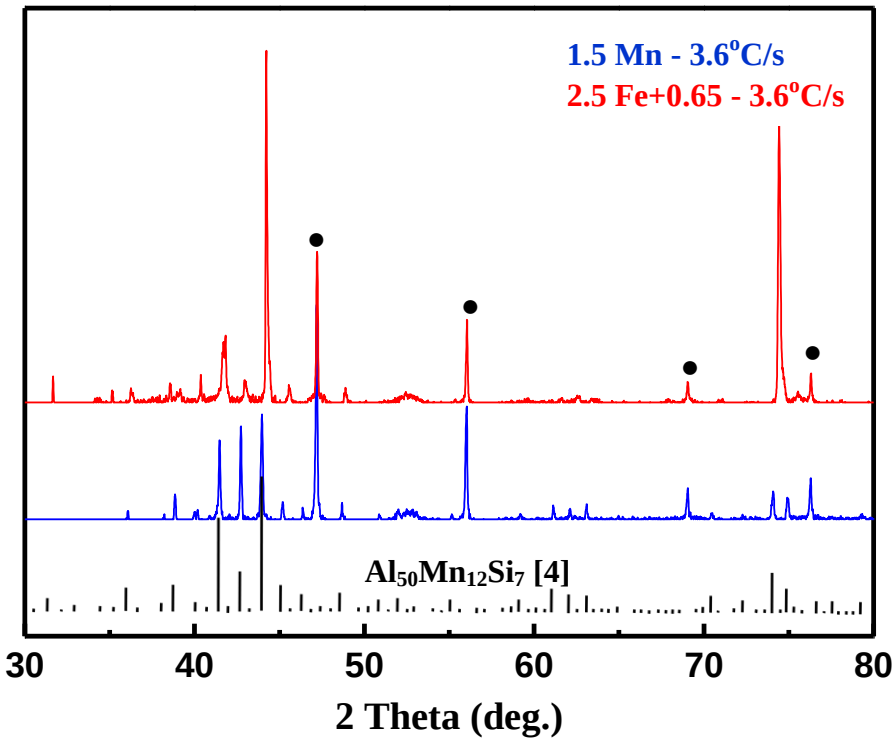

Fig. 5.12 XRD pattern of alloy 1.5 Mn and 2.5 Fe + 0.65 at the cooling rate of 3.6°C/s. The peaks matched well with the Mn compound $Al_{50}Mn_{12}Si_7$ from the database [4]. The peaks indicated the Fe compounds shifted to the higher degree comparing to the peaks of Mn compounds.

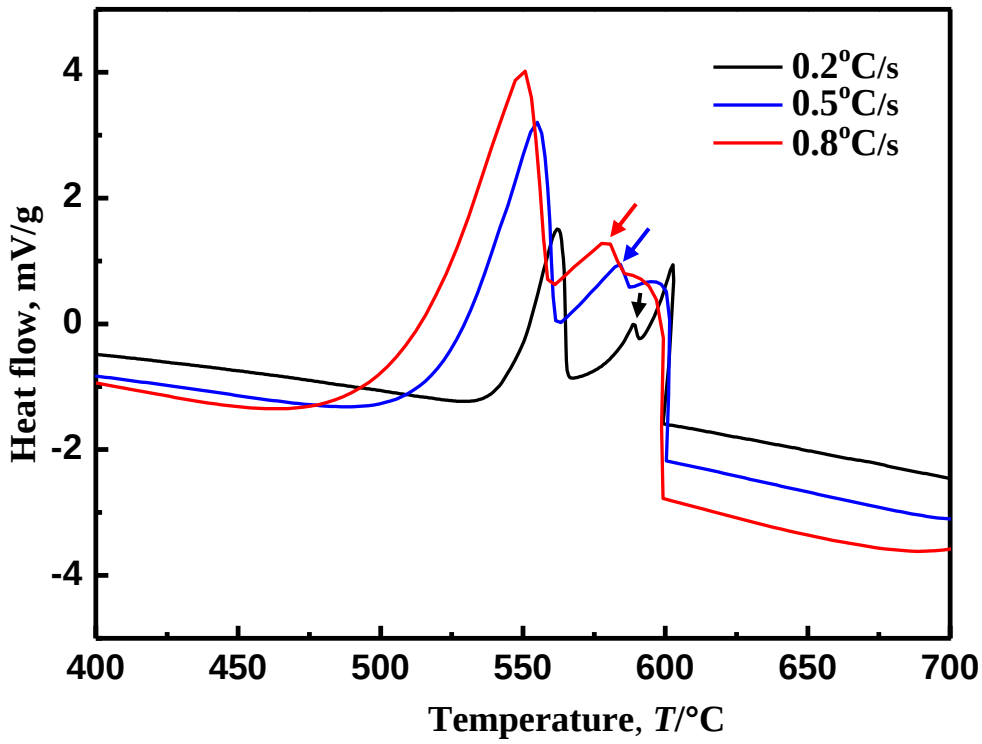

Fig. 5.13 DTA analysis of the alloys 1.0 Fe and 2.5 Fe cooled at 0.5°C/s. The peak of the platelet β type Fe compound crystallization is highlighted by arrow.

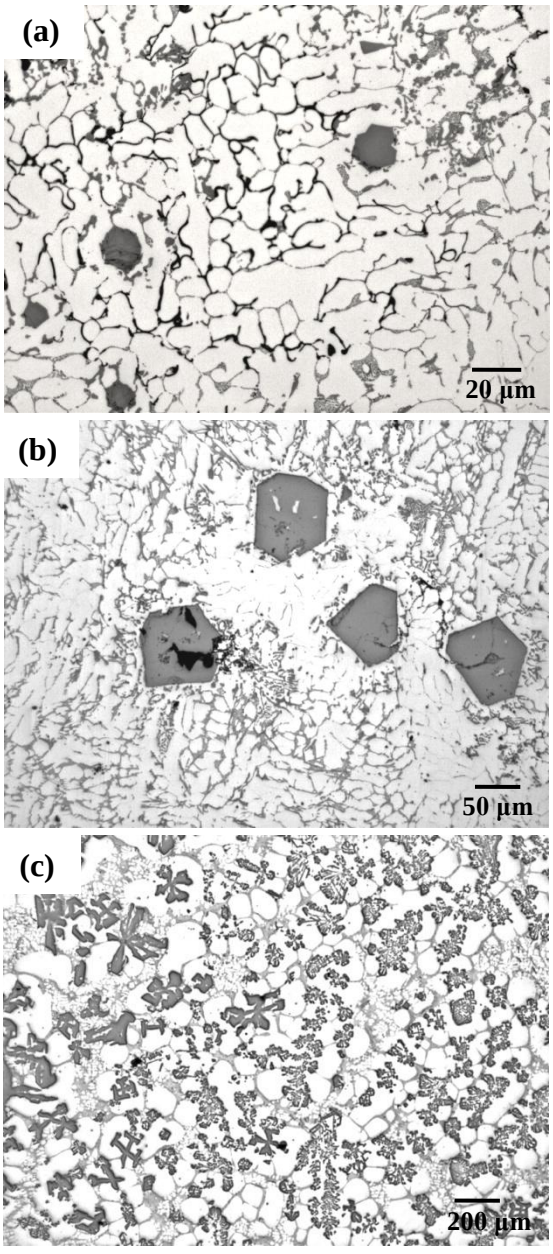

Fig. 5.14 Microstructures of the alloys water-quenched at different temperature (with holding 60 minutes before quenching): (a) 1Fe + 0.65, 660^{o}C; (b) 2.5 Fe + 0.35, 660^{o}C; (c) 2.5 Fe + 0.35, α-Al phase crystallization temperature.

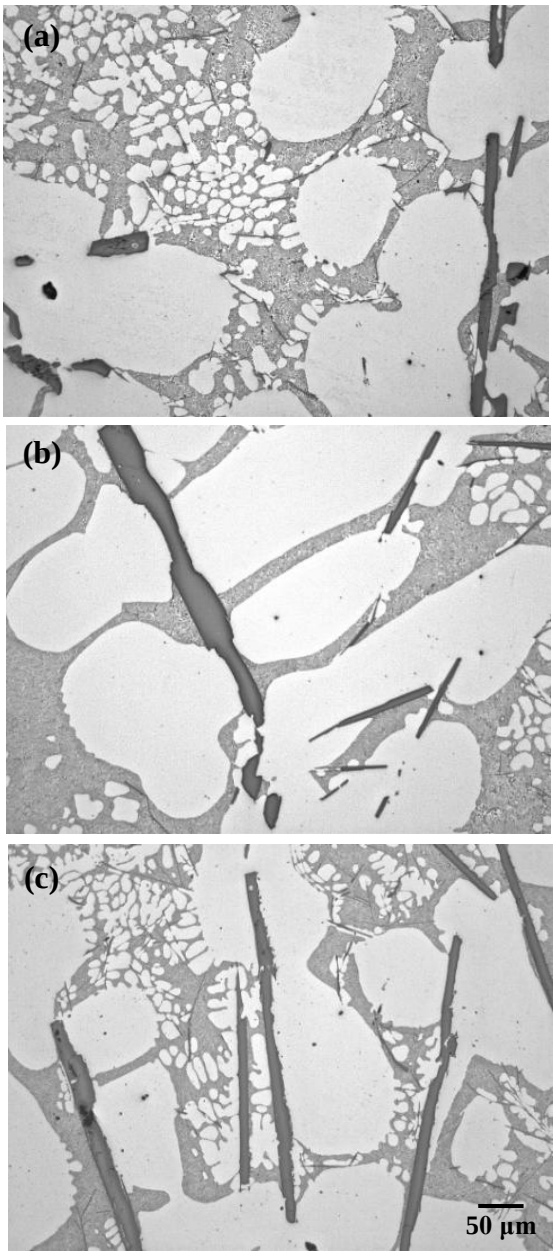

Fig. 5.15 Microstructures of the alloys water-quenched at α-Al crystallization temperature at different air cooling time (with holding 60 minutes before quenching): (a) 1.0 Fe, (b) 1.5 Fe, (c) 2.5 Fe.

Chapter 6

General conclusions

In Chapter 1 "General introduction", the source of Fe impurity in primary and recycled aluminum alloys and its influence of the application of cast Al-Si alloys are described. The characteristics of different Fe compounds and methods of Fe compounds modification to decrease their detrimental influence are introduced. Then the objective and the outlet of the present thesis are presented.

In Chapter 2 "Influence of Fe content, Mn/Fe ratio and cooling rate on mechanical properties of cast AA356 based alloys", effects of the modification of Fe compounds on mechanical properties of cast Al-Si alloys with high Fe content are evaluated. Fe content is the main factor which can determine the final tensile properties of alloys. The high Fe content can lead to the formation of large size platelet β type Fe compound, which can easily be a crack initiation region and result in the decrease of the elongation and UTS. Mn addition can convert platelet β type Fe compound to Chinese script α type Fe compound and/or polyhedral shape α type Fe compound, which was expected to enhance the tensile properties of alloys. However, in the alloy with low Fe content (1.0 wt.%), the increase of elongation of alloys by converting the Fe compound is not obvious in the present work. The branches of large size Chinese script can easily be a crack initiation region and result in the decrease of the tensile properties as well. The large size polyhedral shape Fe compound shows very detrimental influence on the tensile properties of alloys as that of large size

platelet shape Fe compound. Both of them can easily act as the nucleation sites for cracks under loading. In addition, the formation of large size polyhedral shape Fe compound usually accompanies by the formation of pores. High cooling rate can refine the size of all phases in the alloys. The refined small size Fe compound is beneficial to the tensile properties of alloys. Simultaneously, the cooling rate influences the modification process from platelet β type Fe compound to Chinese script α type Fe compound (over-modified to polyhedral shape α type Fe compound). Hence, the influence of cooling rate on the tensile properties of alloys with Mn as a modifier should be considered carefully in both the type of Fe compound as well as the size of Fe compounds.

In Chapter 3 "Influence of Fe content, Mn/Fe ratio and cooling rate on morphology of Fe intermetallic compounds in cast AA356 based alloys", influences of Fe content, Mn/Fe ratio and cooling rate on the modification of Fe intermetallic compounds in cast AA356 based alloys were investigated systematically. Fe content greatly influences the size of platelet β type Fe compound in the alloys without Mn addition. The size of β type Fe compound increases significantly with increasing the Fe content. Mn addition is effective to modify platelet β type Fe compound to more compact compounds, Chinese script and/or polyhedral shape α type Fe compound. The amount of these different Fe compounds is greatly affected by the Mn/Fe ratio and the cooling rate at a given Fe content. At high cooling rate, in the alloy with low Fe content and high Mn/Fe ratio and high Fe content and high Mn/Fe ratio, Fe compounds mainly appear as platelet shape and Chinese script separately. It is considered that the platelet β type Fe compound can solidify earlier than Chinese script α type Fe compound. The formation of the polyhedral shape Fe compound mainly came from the growth of the Chinese script Fe compound.

In Chapter 4 "Evolution of Fe intermetallic compounds during solidification in cast

AA356 based alloys with different Fe content and Mn/Fe ratio”, evolution of Fe intermetallic compounds during solidification in based AA356 cast alloys was investigated by water-quenched experiment. Two factors, Fe content and Mn/Fe ratio were alerted individually and combined in the modification process during solidification to reveal their influence on the evolution of Fe compounds. Additionally, the solidification sequence of the alloys was discussed based on the quenching experiments and microstructural analysis. Fe content is the main factor which can influence the solidification sequence and the evolution of Fe compounds. In the alloy without Mn addition, only platelet Fe compound appears. With increasing the Fe content, the growth of the platelet Fe compound occurs earlier (at higher temperature). More growth time make the final size of platelet Fe compound much bigger. Mn addition is very effective to modify the platelet β type Fe compound to the less harmful Chinese script α type Fe compound. In the alloys with low Fe content and low Mn addition, the Fe compound crystallizes as the platelet β type Fe compound at the beginning of the solidification. With the solidification proceeding, the Chinese script α type Fe compound becomes the dominant one. The growth of the Chinese script Fe compound during solidification accompanied by the decrease of the platelet β Fe compound. More Mn addition in the alloys with both the low and high Fe contents, at the beginning of the solidification, part of the Fe compound crystallized as the Chinese script and/or polyhedral shape. With the solidification proceeding, the growth of the Chinese script Fe compound accompanied by the decrease of the platelet β Fe compound as well. In the alloy with high content Fe and high Mn addition, Fe compounds appear as polyhedral shape. The formation of polyhedral shape α type Fe compound mainly comes from two aspects, crystallizes as the primary phase and the growth of Chinese script α type Fe compound. The ratio of these two parts of compounds mainly depends on the composition and cooling rate.

In Chapter 5 "Mechanisms of modification of Fe intermetallic compounds by different factors: Mn addition, Fe content and cooling rate in cast AA356 based alloys", mechanisms of the refinement and morphologies change of Fe compounds by three factors, Mn addition, Fe content and cooling rate were investigated. Increasing Fe content can increase the size of platelet Fe compounds significantly. This is because increasing the Fe content can make the growth of platelet β type Fe compound happen at higher temperature. The longer growth time leads to the formation of larger size platelet β type Fe compound. Hence, the Fe content in cast Al alloys should be carefully controlled as low as possible. Mn addition can make the Chinese script Fe compound nucleate based on the crystal structure of $Al_{15}Mn_3Si_2$ (cubic) compound. And this kind of Chinese script Fe compound is more stable and easily to grow at higher temperature than platelet Fe compound. Hence, the growth of Chinese script Fe compound occurs accompanied by the transformation from platelet compound to Chinese script compound with the solidification proceeding. More Mn addition can make the nucleation of this kind of Chinese script Fe compound happen at higher temperature. High cooling rate can refine the size of Fe compounds by shortening the growth period of Fe compounds during solidification. In addition, increasing the cooling rate apparently can restrict the transformation process from platelet β type Fe compound to Chinese script α type Fe compound.

Acknowledgements

This thesis is based on my research work during the past three years in Japan as a doctoral student. It would never have been finished without the help and support of many people.

Firstly, I would like to express my sincere gratitude to Professor Tatsuo Sato, my vice supervisor during the study in Tokyo Institute of Technology. His comments on my research work and my ideas always made me think further and deeper. Always try to open mind is one of very important points I learned from him, which makes me benefit in my whole lifetime. Nothing would be possible without his support.

I am profoundly grateful to my supervisor Associate Professor Equo Kobayashi. It is my great honor to be his first doctoral student. His suggestions, comments and help made my research work and my life easily in Japan. I learned a lot of things from him, how to be a good researcher, how to be a good husband and how to be a good man. I deeply appreciate his encouragement forever ‘Yes, you can’.

I would like to thank Assistant Professor Hiroyasu Tezuka for his support and help in both my experiments as well as my daily life. Without these, I can’t finish my research topic on time. His kindness to others is very valuable for me to learn in the rest of my life. I deeply hope this great man can enjoy his retirement life.

I am very grateful to Professor Ji Shi for his comments on my research and his help on my daily life in Japan. Also I am very thankful to Associate Professor Yoshisato Kimura. He kindly gave me a very great one-to-one lecture about my research work, which helped me open a new world.

I would also like to thank Professor Yi Tan from Dalian University of Technology. He gave me this great opportunity and encouraged me to study at Tokyo Institute of Technology. As Associate Professor Equo Kobayashi always said ‘everything starts from him’.

It is my great honor to do the doctoral research work in Sato-Kobayashi laboratory. I have been very lucky to meet and work with so many wonderful persons during these three years. It is a very big family and of course it will stay in my heart forever. Also my thanks are extended to all of my friends I met in Japan during these past three years. I deeply cherish the friendship with these good guys.

I am grateful for financial support from the China Scholarship Council (CSC) and the Japan Foundry Engineering Society for the award of a scholarship to me for my research in Japan as a doctoral student.

Finally, I would like to express my deep love to my family, especially to my parents and parents in law. They always gave me endless support, understanding and love. Please be healthy forever. I would like to share all of my achievements with my wife, Jing Han. Everything is meaningless without she and her love.

Zhang Zhijun

张志军

Tokyo, Japan

August 12, 2013